Kinematics and Locomotion Analysis for the Six Legged Walking Robots Using the Theory of Screws, Reciprocal Screws and the Graph Theory

Eyad Al Masri

Submitted to the
Institute of Graduate Studies and Research
in partial fulfillment of the requirements for the degree of

Master of Science
in
Electrical and Electronic Engineering

Eastern Mediterranean University
July 2017
Gazimağusa, North Cyprus

Approval of the Institute of Graduate Studies and Research

Prof. Dr. Mustafa Tümer
Director

I certify that this thesis satisfies the requirements as a thesis for the degree of Master of Science in Electrical and Electronic Engineering.

Prof. Dr. Hasan Demirel
Chair, Department of Electrical and Electronic Engineering

We certify that we have read this thesis and that in our opinion it is fully adequate, in scope and quality, as a thesis for the degree of Master of Science in Electrical and Electronic Engineering.

Prof. Dr. Mustafa Kemal Uyguroğlu
Supervisor

Examining Committee

1. Prof. Dr. Hasan Demirel
2. Prof. Dr. Osman Kükrer
3. Prof. Dr. Mustafa Kemal Uyguroğlu

ABSTRACT

Not long time ago, legged walking robot, especially the robot that uses six legs to walk has received a great attention from researchers due to its extreme importance in several domains. Legged robots are suitable to function in an erratic, alarming and unsympathetic environments such as space habitat, mine territory, and benthos. Moreover, legged walking robots are satisfactory in some critical tasks like rescue applications and examine nuclear facilities. Generally, the legged robot divided in terms of the number of the legs into the two-legged, four-legged, six-legged and eight-legged robot. However, the six legs robot has asset over the first and the second one since the six-legged robot is much faster and stable. Furthermore, it has proven that increasing the legs of the robot will not give better results.

In this dissertation, an endeavor has exerted in order to handle the kinematic analysis of the walking robot that has six legs. A serial chain consists of three revolute joints (RRR) are chosen to form the leg of the robot due to reproducing the architecture of the insect’s leg. First, a brief summary of Denavit-Hartenberg (D-H) convention and the theory of screws, two of an essential technique used in the kinematic analysis of the robot manipulators, is provided. Then, the configurations of the walking robot’s leg studied in details for the sake of building a comprehensive representation of the six-legged walking robot. Third, the problem of finding the position and orientation of the center of gravity of the walking robot is solved using the closing circuit technique. In contrast, depending on knowing the pose of the center of mass of the robot, Inverse kinematics is achieved geometrically. Furthermore, screw theory approach has been beneficial to find the linear and angular velocity. However, the reciprocity theorem could deeply simplify the direct velocity analysis. Since the locomotion analysis is one of the most important aspects of walking robot, a review presented for the purpose of highlight on some fundamental locomotion approach. Finally, the mechanical configuration of the six-legged robot structures is to be represented using the theory of graph.

Keywords: Hexapod, Legged-Robot, Kinematics, D-H Convention, Screw Theory, Reciprocal Screws, Locomotion, Graph Theory.

ÖZ

Yakın zamanda, ayaklı yürüyen robotlar, özellikle yürümek için altı ayak kullanan robotlar, bazı alanlardaki önemlerinden dolayı araştırmacı, uzman ve üniversite profesörlerinin büyük ilgisini çekmiştir. Ayaklı robotlar, uzay ortamı, mayın bölgeleri ve deniz dibi gibi değişken, panik yaratıcı ve aynı zamanda sevimsiz ortamlarda görev yapma uygunluğuna sahiptirler. Tüm bunlara ek olarak, ayaklı robotlar, kurtarma uygulamaları ve nükleer tesislerin incelenmesi gibi bazı kritik görevleri yerine getirme yeterliliğine de sahiptirler. Genel olarak, ayaklı robotlar ayak sayısına göre iki ayaklı, dört ayaklı, altı ayaklı ve sekiz ayaklı robot olmak üzere gruplandırılırlar. Bununla birlikte, altı ayaklı robotlar daha hızlı ve tutarlı olmalarından dolayı ilk ikisine göre daha fazla değer taşımaktadırlar. Tüm bunlara ek olarak, robot ayak sayısının artırılmasının daha iyi sonuçlar vereceği çeşitli araştırmalarla kanıtlanmıştır.

Sözkonusu tez çalışması, altı ayaklı yürüyen robotun kinematik analizini yapma amacı taşımaktadır. Böcek ayağı mimarisine benzer bir yapı oluşturma amacı ile, sözkonusu robotun ayağını oluşturmak için üç adet mafsallı ek yerinden (RRR) oluşan bir zincir dizisi seçilmiştir. İlk olarak, robot işleticilerinin kinematik analizinde kullanılan iki gerekli teknik olarak kabul edilen Denavit-Hartenberg (D-H) konvensiyonu ve vida teorisinin kısa bir özeti sunulmuş ve daha sonra ise temsili bir altı ayaklı yürüyen bir robot oluşturmak için yürüyen robotun ayak konfigürasyonu detaylı olarak incelenmiştir. Üçüncü olarak, kapalı devre tekniği kullanılarak yürüyen robotun çekim merkezinin pozisyonu ve yönü bulunmuştur. Buna zıt olarak, robotun kütle merkezinin duruşunu belirleyerek, geometrik olarak ters kinematik elde edilmiştir. Her ne kadar, lineer ve açısal hızı bulmak için vida teorisi yararlı bir teori olsa da karşılıklılık teoremi direk hız analizini oldukça basitleştirebilmektedir. Bir yerden diğerine gitme analizinin yürüyen robotun en önemli özelliklerinden birisi olmasından dolayı, temel hareket yaklaşımına ışık tutma amacı ile bir değerlendirme sunulmuştur. En son olarak da grafik teorisi kullanılarak altı ayaklı robot yapısının mekanik konfigürasyonu sunulmuştur.

Anahtar kelimeler: Hexapod, Ayaklı-Robot, Kinematik, D-H Konvensiyonu, Vida, Karşılıklı Vidalar, hareket yaklaşımına, Grafik Teorisi.

DEDICATION

A special feeling of gratitude to my loving parents,

brothers and friends

ACKNOWLEDGMENT

I would love to record my sincere gratitude to Prof. Dr. Mustafa Kemal Uyguroğlu for his endless support of my Master study. His supervision, patience, and inspiration helped me in all the time of research and writing of this dissertation. All the results described in this thesis accomplished with the help and support of him.

I would also like to extend my sincere thanks to all professors and faculty members of the Electrical and Electronic Department for their care, help, and dedication.

TABLE OF CONTENTS

LIST OF TABLES

LIST OF FIGURES

Chapter 1

INTRODUCTION

1.1 Introduction

Thousands of years ago, the nature was the main origin of inspiration for humankind. Birds, mammalian, reptiles and marine creatures weren't far from the imagination of humans in an attempt to mimic them and take advantage of their unique characteristics. In the Contemporary era, experts and academics have made a significant leap technology in the field of manufacturing various types of robots, especially those relating to emulation of humans and animals [1-3]. Generally, these sorts of robots are called locomotive manipulators.

The terrestrial manipulators that able to change their absolute position to achieve its duty could be separated into 3 main categories; robots capable of varying its locations using characteristics of the trundles, robots that use crawler motion system depends on the persistent track and multi limbs robots. The locomotive robots that use trundles or track are characterized by inexpensive, being easy to build, and solidity in ordinary environment. However, in case of capricious environment, especially rocky or arenaceous territory, mobile robots that use the legs for locomotion are preferred [4].

Several reasons are behind the priority of the multi-terminals walking robot, the place where the leg touch the ground is extremely tiny, and consequently, extra stability arises because of the robot able to select a suitable spot to support. Since the leg contains sundry actuators and separated limbs, the robot capable of adjusting itself to handle the harsh surrounding environment [5].

Multi-limbs peripatetic robots can be sectioned into four main classes; dual-legged robots, quad-legged robots, sixfold-legged robots and octal-legged robots. Designing and implementation of the traveling robots that standing on two lists was and still is one of the most complicated engineering issues since single limb should be touching the terrain and carries out stability process so that the center of gravity still supports the stabilization[6]. Quad-legged robot considered lower complexity compared to humanoid. Moreover, the Most scientific studies assume that the presence of two legs supporting the body of the Quad-legged robot [2]. Realizing the fact that say, the most Invertebrate creatures contain six legs, may lead us to investigate its special characteristics [7]. Two of indispensable issues to be considered during the design of the multi-limbs walking machine are quickness and the constancy. It is appropriate to say that, walking manipulator that uses 6 limbs to move shows better performance in terms of constancy since sixfold-legged robots have further backing limbs [8]. Furthermore, in comparison with dual-legged robots and quad-legged robots concerning the quickness, the robots with six legs show improved results [9]. The possibility of failing decreases strongly by using six legs mobile robot since 5 legs are enough to perform all functionalities of the robot, as a result, the fidelity getting better [10]. With regard to the 2 additional legs in octal-legged machines, robot researchers have confirmed that utilize supplementary legs will not award extra enhancement [11]. For all these faced reasons, hexapod traveling robot will receive a great solicitude through this thesis.

The prototypes of the sixfold peripatetic robots relied on manual operation of mechanical or hydraulic actuators to move, away from any control systems. It was the first technical advance in the field of auto six legged mobile robot in the early 1970s [12]. In 1973 *Okhotsimski* and *Plantov* produced the first hexapod mobile robot capable of overcoming obstacles using complicated artificial intelligence algorithm [13]. In [14] presented a new technique to make the robot capable of maneuvering using perimeter sensors. Moreover, Prof. *Robert B. McGhee* designed a six-legged robot not only to avoid obstacles but to walk on them [15]. The innovation of the *Odex* had a great impact in using the six-legged peripatetic robots in abroad applications [16]. The robot used internal electrical system controlled from afar. Latterly, as in all technical areas, Robot science has seen great progress. Several attempts have succeeded in extracting biological advantages from nature. One such attempt was cockroach-like hexapod robot [17]. Stick insects were not far from the observation of the robot scientists. Different versions of the *LAURON* designed based on the structure of this insect [18]. In [19] another example of six-legged robot insect-inspired in which the robot mimic the ant's walking style.

As sixfold peripatetic robots have multiple shapes, types, and sizes, they also have numerous applications in different fields. In [20] a six-legged robot named Rise skillfully designed to perform steep ascending tasks, thanks to the talons at the end of its limbs. Several hexapod walking robot produced to suit the tasks in a space environment. However, one of the most interesting six-legged robots specialized to duty in space conditions was *Athlete* [21]. This robot holds the characterized of both legged and trundle robot. *Athlete* performs its duties in normal conditions using locomotive trundle. In contrast, during uncomfortable territory, the robot turns off the rotation and uses the techniques of the legged robot, where the locked wheel serves the end terminal of the robot’s leg. The sixfold robot called *LAURON V* considered as the most improved version of the series *LAURON*. This robot has a strong structure of reinforced aluminum designed with inspiration from stick insect. *LAURON V* holds advanced techniques in sensing and assessing the surrounding reality, for these reasons *LAURON V* suitable for work in very complicated and difficult circumstances as space conditions. Another important application takes its place in this concept, operations that depend on dive. A hybrid robot called *CR 200* [22] is one of the six-legged robots working in this field. This robot capable of walking on sturdy land easily and can plunge until 200 meters under water. *CR 200* designed to withstand pressure under water to perform precise tasks such as examination and investigation of the deep sea environment, search for sea-soaked pieces and preparing of some inquiry that relate to marine creatures. Moreover, several commercial models of the hexapod robot have recently been launched for educational or recreational purposes.

In terms of the central frame shape, six-legged robots can be organized into two basic forms quadrilateral style and orbicular style. Typically, Hexapod robot that holds the former style includes six legs dispensed into two directions in which three on each side. Since the most of the ancient versions were built on this basis, this style of hexapod has been studied well especially in balancing and ability to maneuver [23]. The six-legged robot that has the later design possesses six limbs assigned harmonically about the shape. Recently, varied surveys have been made to contrast between these two forms [24]. The orbicular hexapod robot may hike in all lines and has advantages over quadrilateral in terms of stability edge, this is what Preumont et al explained in [25]. Takahashi et al confirmed what Preumont et al had put forward and he provided several additional evidence [26]. Although the quadrilateral hexapod is in need to a special locomotion to change its direction line unlike Orbicular which has the ability to hike in all lines, quadrilateral one achieves better results in terms of walking forward a fixed channel.

As we mentioned earlier, there are many applications that the robot hexapod are designed to perform. However, the six-legged hexapod robot which are constructed to achieve some tasks in unearthly environment considered as one of the most crucial topic among robot researchers and experts due to its enormous priority in the field of scientific research. Recently, a new six-legged robot attracts special attention in the field of space robots called NOROS derived from the expression “novel robot for space exploration”. This robot was a result of cooperation between Chinese and Italian robot scientists for the purpose of exploring in space environments away from the earth [46-48].

The survey in this dissertation takes into consideration architecture, criterions, guidelines, and limitations of the *NOROS* Hexapod robot in all subsequent investigations and experiments.

1.2 Thesis Overview

Chapter 1 (Introduction), is preparatory to understanding the definition of the Hexapod robots. It includes the chronological evolution, types, and the advantages of the legged robots. Moreover, this chapter gives a description of the Hexapod structure in addition to an explanation of its classifications, applications, and preference of use it.

Chapter 2 (Kinematics Review), provides a comprehensive overview of the kinematic science involved mainly the position and the velocity analysis. Several techniques concerns in analyzing the location of a considered frame system. These techniques include the D-H convention, conventional screw theory and the product of exponential method. All of them, have been studied in details. Moreover, the problem of finding the velocity of the center of moving platform of a closed chains manipulator solved in this chapter through the theory of the screws and the reciprocity technique. Studying of the mobility of the robot has been mentioned in this chapter through the Kutzbach–Grubler formula besides to the reciprocity-based technique.

Chapter 3 (Kinematics analysis of the Hexapod), addresses several kinematic issues taking into account the structure and the configuration of the NOROS Hexapod robot, including the kinematic of the swinging and assistant Hexapod's leg, the direct and inverse location analysis that handles a coordinate system located in the center of gravity of the robot, velocity analysis based on the theory of reciprocal screws and the mobility analysis based on the conventional and reciprocity based approach.

Chapter 4 (Locomotion Analysis), discusses the stability edge and provides the definition of the gait study according to the Hexapod's configuration. Also, two essential triple system locomotion types called mammal gait and insect gait are studied kinematically through this chapter.

Chapter 5 (Kinematics Representation) gives an extensive review of the theory of graph representation. Moreover, the kinematic configuration of the Hexapod robot in this chapter is represented using the network model approach [48].

Chapter 6 (Conclusion and Future work) discusses the works done through this dissertation in addition to a comprehensive review of the experiences and results presented in Appendix A and B. Furthermore, an ambitious future plan to work towards building an integrated Hexapod model is presented.

Chapter 2

KINEMATICS REVIEW

2.1 Introduction

By definition, kinematics study is a specific domain in the conventional mechanical analysis that cares about the movement of the solid particle without taking the cluster weight and strengths that inspire the changes in consideration [27-28]. Accordingly, this field just related with the characteristics of the mechanical shape and timing of displacement occurrence. It is known that there is a tight relevance between the properties of the joint and the positioning of the impact point in any robotics mechanism determined by some restrictions on joints movement. However, finding this relation considered as a cornerstone in kinematics study. Essentially, kinematics survey separated into positioning study, velocity analysis, and superior order analysis. In each case, there is a schism into frontal and reverse analysis. Firstly, the issue of kinematics positioning analysis refers to detect the linkage between the characteristics of the mechanical joints and the effective point at the end of robotics chain in serial mechanisms or the mass center of gravity in closed loops mechanisms. In this sense, frontal analysis aims to find the impact point's place with regard to the angles of the joints, the opposite concept represents the study of the reverse positioning analysis. The purpose of velocity analysis is to find the equation that relates the rapidity of the joints and velocity parameters of the effector point in open chain mechanism or gravity center of the closed chains manipulator. Hence, the linear analysis considers the parameters of the joints as an input in its equation. In contrast, reversal analysis takes the velocity of the effector as input parameters. Precisely, on the same principle of positioning or velocity, superior order analysis such acceleration or higher derivative of time aims to generate an equalization between the high order derivatives of time for both of joints angles and effector parameters.

Two of the most crucial techniques used in kinematics studies are Denavit-Hartenberg procedure and the theory of the screws [29]. In the following two sections, these two methodologies will be dealt with in details.

2.2 Kinematics Modeling Based on (D-H) Representation

Denavit and Hartenberg (D-H) representation technique has been invented by the scientists *Jacques Denavit* and *Richard S. Hartenberg* in the middle of the last century [30], since then it turned out to be the typical way to model the kinematics structure in compact and harmonious characterization. Denavit-Hartenberg methodology is a fluent path that can build a robust representation of any collection of links and joints which shape the robot disposition.

As the kinematics paradigm of a robot structures depicts the linkage of the joints and the effector, Denavit-Hartenberg allocates a system of coordinate to all the joints that exist in the robot. The next target is to identify a diversion that relates any sequential coordinate systems. Finally, the definitive relationship between all coordinates is accomplished by integrating all diversions in the robot system forming ultimate transport movement pattern of the robot.

The kinematics structure in Figure 2.1 has two joints namely the joint s and the joint $s+1$, these joints are bonded by the link s. The Joint's type could be any manner such as rotating pin or translation slider.

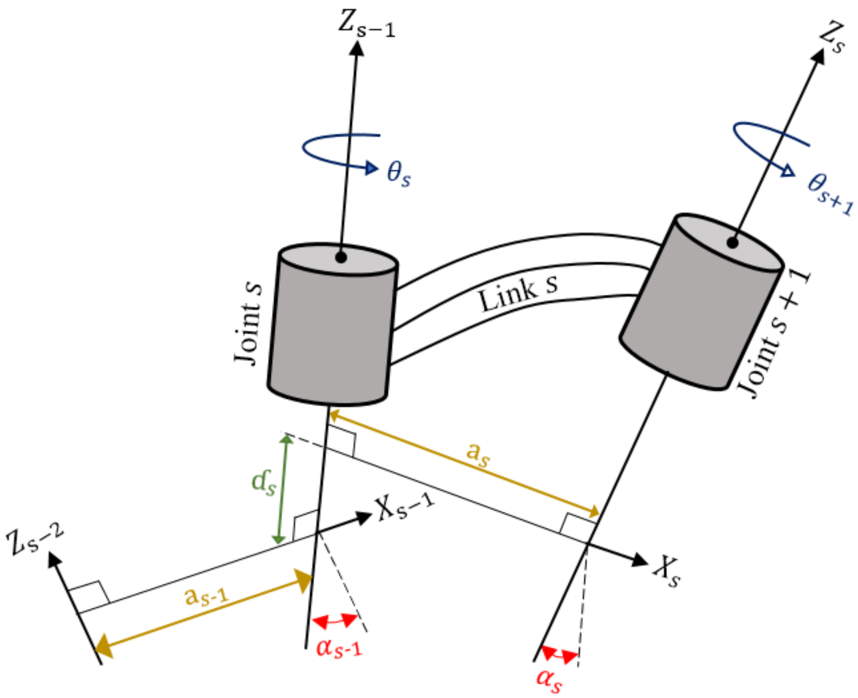

Figure 2.1: The Specifications of the Denavit-Hartenberg Method

Assigning the domestic coordinate systems for the two joints will be the first interest in order to handle the structure shown in Figure 2.1 using the Denavit-Hartenberg method. However, Y-axis is discarded since Y-axis is orthogonal to the plane that specified by X-axis and Z-axis. If the joint has rotating motion, the trend of rotation will be around the Z-axis according to the rule of the right hand. While the Z-axis will take the direction of sliding in the case of the joint is prismatic. For the sake of simplifying the process of assigning the Z-axes, Z_{s-1} will indicate to the Z-axis of the joint s. The next step is to identify the X-axes. The vector of X-axis sets based on the relation between the two sequential Z-axes. There are 3 main cases specify the relationship between any two lines; the parallelism, the intersecting and the skew case. In the case of the two Z-axes are analogous, there is a countless number of alternately vertical to the both Z-axes and consequently, X-axis will be the alternately vertical that go over the system of coordinate. When the successive Z-axes are intersecting, in this situation X-axis allocates in the direction orthogonal to the plan that specified by the two successive Z-axes. If the Z-axes are skew lines, in this situation there is only one mutually normal and the X-axis holds the same normal direction.

After allocating the domestic system of coordinates, the following phase is to uniquely specify the Denavit-Hartenberg variables. Mainly, there are 4 essential variables that form the backbone of Denavit-Hartenberg technique. The first variables is theta, overwhelmingly recalled as θ so that θ_s symbolizes the rotational angle about the joint axis Z_{s-1}. The second variables ɗ$_s$ indicates to the proportion of the joint axis Z_{s-1} that specified by two sequential common perpendiculars. The following parameter refers to lengths of mutually vertical lines, generally symbolized as a, in this case a_s is the length of common normal of Z_s and Z_{s-1} .The fourth parameter α indicates to the angle between the two sequential joint axes.

Once the joint systems of coordinates become ready, finding the relation between these coordinates will be the top priority, knowing that 4×4 matrix can relate any two Cartesian coordinates. Several steps should be accomplished in order to transform the coordinate system from one local frame to another, fusion these steps will give us, in the end, general transformation matrix.

The following steps aim to find the matrix that represents the relation between any two sequential local systems of coordinate s-1th and sth. The strides are clarified as follow. Firstly, Rotation process by the angle θ_s around the Z_{s-1} in which X_{s-1} and X_s will become parallel. Then, sliding movement straight Z_{s-1} axis by the magnitude of ɗ$_s$ so that the axes X_s and X_{s-1} become collinear. Moreover, another sliding motion happen, this time along the direction of the axes X_{s-1} and X_s by a distance a_s. This will make the centroid of the local systems of coordinates s-1th and sth at the same point. Lastly, revolute motion about the axis X_s by the alpha parameter, α_s in which the axes Z_s and Z_{s-1} become coincident.

The above four steps could be represented by the following matrix equation in order to build a homogeneous matrix that expresses the transformation from the coordinate system s-1th to another coordinate system sth.

$$T_{s^{th}}^{s-1^{th}} = \begin{bmatrix} \cos\theta_s & -\sin\theta_s \cdot \cos\alpha_s & \sin\theta_s \cdot \sin\alpha_s & a_s \cdot \cos\theta_s \\ \sin\theta_s & \cos\theta_s \cdot \cos\alpha_s & -\cos\theta_s \cdot \sin\alpha_s & a_s \cdot \sin\theta_s \\ 0 & \sin\alpha_s & \cos\alpha_s & d_s \\ 0 & 0 & 0 & 1 \end{bmatrix} \tag{2.1}$$

In order to obtain the transformation matrix for any serial robot starting from the base coordinate frame Bth ending in the hand reference frame Hth , a total reference frames transformation should be accomplished. This idea could be clarified by the equation (2.2)

$$T_{H^{th}}^{B^{th}} = T_{1^{th}}^{B^{th}} . T_{2^{th}}^{1^{th}} \ldots T_{H^{th}}^{H-1^{th}} \tag{2.2}$$

2.3 Kinematics Modeling Based on the Theory of the Screws

In the beginning of the nineteenth century, the French mathematician, *Michel Chasles* proves that, it is always possible to characterize the movement of the solid body in 3D space, by divide this movement into two components, the first is rotation around a shaft called *Mozzi* line, attributed to the mathematician *Assi De Mozzi*, who the first scientist talk about this theorem, and the second is translation over that shaft. Later, the *Mozzi* line named as screw axis because of the similarity between this movement and the screw displacement. Chasles's theorem could be a cornerstone in an attempt to derive a general relation describe the rigid body displacement [31-33]. In order to characterize this displacement, three main steps will do this task [27]. First, an attempt will be made to model a rotatory movement around an axis passing through the center of coordinate system. Second, generalize the displacement in first so that the rotation axis is not coincident with the origin of coordinate. Besides, a line movement along that axis. Finally, extend this displacements to represent sequential screw lines describe several consecutive joints.

2.3.1 Pure Rotational Modeling Using Coincident Screw Line

Initially, considering that position vector V belongs to the 3D space R3, represents the movement of a rigid body B around a fixed shaft called screw axis. Assuming that this axis passes through the center of the fixed reference frame O. this analysis aims to describe the rotational movement of a rigid body B from the first position M till the second position N about the screw axis S, where S represents the unit vector in the rotational direction. This rotary motion of the solid body B around the axis creates a circle shape plane R so that the axis S passes through its center. Furthermore, the plane R and the axis S are columnar. Figure 2.2 illustrates this rotation displacement.

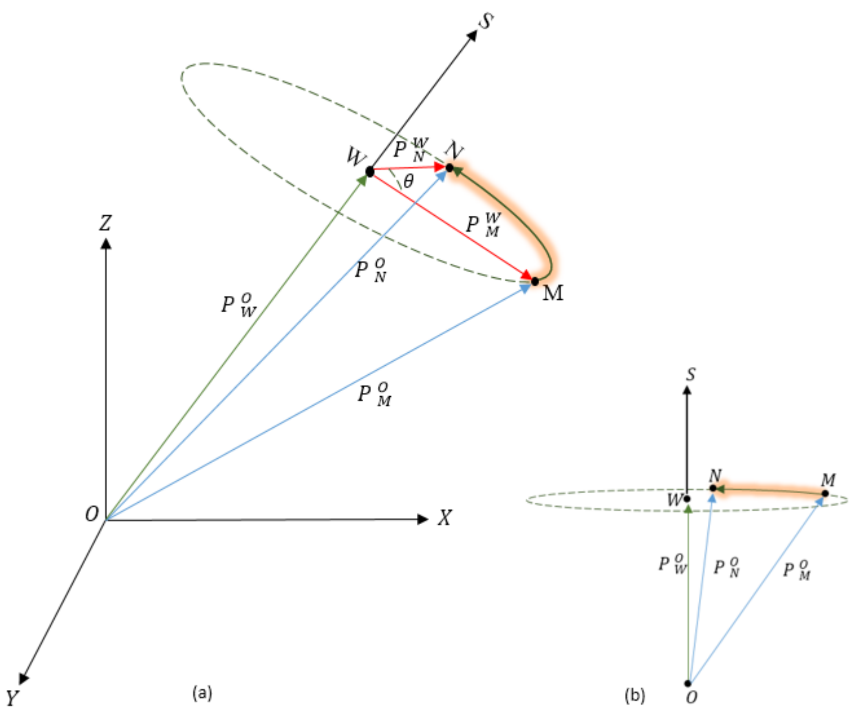

Figure 2.2: (a) Illustration of the Rotation about Coincident Screw Line (b) Another Visual Angle Taken to Clarify the Modeling

The following vectorial equations are derived from the Figure 2.2

$$P^{O}_{M} = P^{O}_{W} + P^{W}_{M} \tag{2.3}$$

$$P^{O}_{N} = P^{O}_{W} + P^{W}_{N} \tag{2.4}$$

The vector P^{O}_{W} is the projection of the positions of M and N on the screw axis, the following equation clarifies this fact.

$$P^{O}_{W} = (P^{O}_{M}.\mathrm{S})\,\mathrm{S} = (P^{O}_{N}.\mathrm{S})\,\mathrm{S} \tag{2.5}$$

The equations (2.3) and (2.4) could be reconstructed according to equation (2.5)

$$P^{O}_{M} = (P^{O}_{M}.\,\mathrm{S})\,\mathrm{S} + P^{W}_{M} \tag{2.6}$$

$$P^{O}_{N} = (P^{O}_{M}.S)\,S + P^{W}_{N} \tag{2.7}$$

Equations (2.6) and (2.7) crystallize the subsequent fact, through the rotary movement of a solid body, only the level portion of the vector position will change while the columnar part doesn't change. Figure 2.3 gives a look from the top on the orbicular plane R that contain the points M and N.

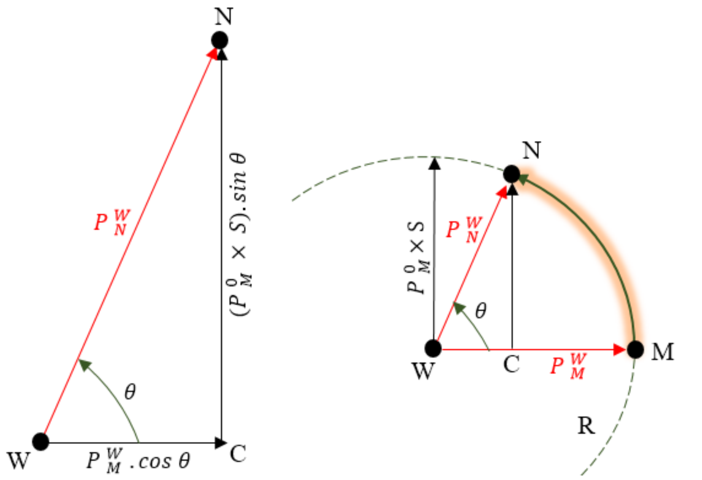

Figure 2.3: Scene from Top on the Rotating Plane R which Illustrates the Path of the Body

Figure 2.3 illuminates that the level portion of the positions of points M and N will change in direction only, whereas the magnitude value is preserved. The following equation (2.8) is derived from the Figure 2.3.

$$P_{N}^{W} = (P_{M}^{O} \times S) \sin\theta + P_{M}^{W} \cos\theta \tag{2.8}$$

The vectors P_{N}^{W} and P_{M}^{W} could be easily isolated from the equations (2.6) and (2.7) in order to simplify the equation (2.8), so that P_{N}^{W} and P_{M}^{W} are to be replaced.

$$P_{N}^{O} - (P_{M}^{O}.S)\,S = (P_{M}^{O} \times S) \sin\theta + (P_{M}^{O} - (P_{M}^{O}.S)\,S) \cos\theta \tag{2.9}$$

By reordering the equation (2.9) in order to obtain the position of the point N in terms of the position of the point M, the rotatory angle θ and the screw axis S. The following Equation (2.10) famous as Rodrigues's equation [34].

$$P_{N}^{O} = P_{M}^{O} \cos\theta + (P_{M}^{O}.S)\,S\,(1 - \cos\theta) + (P_{M}^{O} \times S) \sin\theta \tag{2.10}$$

2.3.2 General Displacement Modeling Using Arbitrary Screw Line

The assumption of *Michel Chasles* states that; general displacement of a solid body can be detached to turning movement and linear displacement. However, in the previous section, the analysis was about getting a relation that expresses the rotational displacement about an axis coincident with the center of the reference coordinate system. In order to generalize the displacement, the axis should be taken arbitrarily. Figure 2.4 explains the comprehensive displacement of a solid body when it displaces from one position M to another position K passing through the point N. This movement expresses as at first turning motion concerning the axis of screw S by magnitude θ, then linear displacement by distance ḑ over that axis. The following vectorial equations (2.11) and (2.12) derived from the Figure 2.4 geometrically.

$$P_{M}^{\emptyset} = P_{O}^{\emptyset} + P_{M}^{O} \tag{2.11}$$

$$P_{K}^{\emptyset} = P_{O}^{\emptyset} + P_{N}^{O} + \text{d}.S \tag{2.12}$$

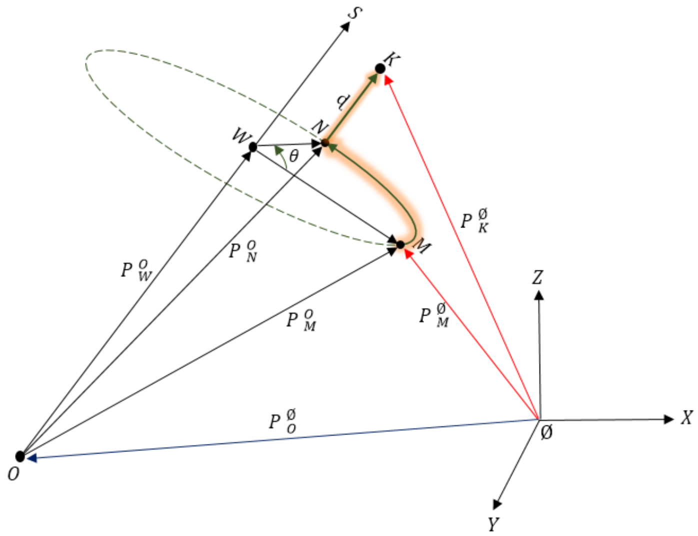

Figure 2.4: Comprehensive Displacement of a Solid Body Displaces from one Position to Another

The following step aims to generalize Rodrigues's equation so that expresses a comprehensive movement of a solid body. For this purpose, the position vectors P_{M}^{O} and P_{N}^{O} are to be isolated in the equations (2.11) and (2.12), then by substituting these vectors in equation (2.10), we will obtain the equation (2.13)

$$\begin{aligned} &P_{K}^{\emptyset} - P_{O}^{\emptyset} - \text{d}\,S \\ &= \left(P_{M}^{\emptyset} - P_{O}^{\emptyset}\right)\cos\theta + \left(\left(P_{M}^{\emptyset} - P_{O}^{\emptyset}\right).S\right)S\,(1 \\ &- \cos\theta) + \left(\left(P_{M}^{\emptyset} - P_{O}^{\emptyset}\right) \times S\right)\sin\theta \end{aligned} \tag{2.13}$$

Equation (2.13) can be extremely simplified by using expanding technique so that the new position K can be explained by two components. This process explained in the following equations

$$P_{K}^{\emptyset} = E1 + E2 \tag{2.14}$$

The portions E1 and E2 in (2.13) given in the following equation

$$E1 = P^{\emptyset}_{M} \cos\theta + \left(P^{\emptyset}_{M}.S\right) S\,(1 - \cos\theta) + \left(P^{\emptyset}_{M} \times S\right) \sin\theta \qquad (2.15)$$
$$E2 = P^{\emptyset}_{O} + ɖS - P^{\emptyset}_{O} \cos\theta - \left(P^{\emptyset}_{O} \times S\right) \sin\theta - (P^{\emptyset}_{O}.S)\, S\,(1 - \cos\theta)$$

The portion E1 in the equation (2.15) is identical to the Rodrigues's equation and refers to perspicuous rotatory movement. In order to derive a matrix expresses this movement, there is a possibility to expand E1 into 3 combinations each of them indicates to one of the global reference frame components.

$$\begin{aligned}
E1_X &= \left(((S_X)^2 - 1)(1 - \cos\theta) + 1\right)(P^{\emptyset}_{M})_X \\
&+ \left((S_X S_Y)(1 - \cos\theta) - (S_Z \sin\theta)\right)(P^{\emptyset}_{M})_Y \\
&+ \left((S_X S_Z)(1 - \cos\theta) + (S_Y \sin\theta)\right)(P^{\emptyset}_{M})_Z \\
E1_Y &= \left((S_Y S_X)(1 - \cos\theta) + (S_Z \sin\theta)\right)(P^{\emptyset}_{M})_X \\
&+ \left(((S_Y)^2 - 1)(1 - \cos\theta) + 1\right)(P^{\emptyset}_{M})_Y \\
&+ \left((S_Y S_Z)(1 - \cos\theta) - (S_X \sin\Theta)\right)(P^{\emptyset}_{M})_Z \\
E1_Z &= \left((S_Z S_X)(1 - \cos\theta) - (S_Y \sin\theta)\right)(P^{\emptyset}_{M})_X \\
&+ \left((S_Z S_Y)(1 - \cos\Theta) + (S_X \sin\theta)\right)(P^{\emptyset}_{M})_Y \\
&+ \left(((S_Z)^2 - 1)(1 - \cos\theta) + 1\right)(P^{\emptyset}_{M})_Z
\end{aligned} \qquad (2.16)$$

The equations (2.16), which represents the rotatory movement, could be rearranged using the matrix $T1$ so that this equation will be rewritten in matrix format.

$$\begin{bmatrix} \mathrm{E1_X} \\ \mathrm{E1_Y} \\ \mathrm{E1_Z} \end{bmatrix} = \begin{bmatrix} T1(1,1) & T1(1,2) & T1(1,3) \\ T1(2,1) & T1(2,2) & T1(2,3) \\ T1(3,1) & T1(3,2) & T1(3,3) \end{bmatrix} . \begin{bmatrix} (P^{\emptyset}_{M})_\mathrm{X} \\ (P^{\emptyset}_{M})_\mathrm{Y} \\ (P^{\emptyset}_{M})_\mathrm{Z} \end{bmatrix} \qquad (2.17)$$

The components of the Matrix $T1$ can be specified in the following equation

$$\begin{aligned}
T1(1,1) &= ((S_X)^2 - 1)(1 - \cos\theta) + 1 \\
T1(1,2) &= (S_X S_Y)(1 - \cos\theta) - (S_Z \sin\theta) \\
T1(1,3) &= (S_X S_Z)(1 - \cos\theta) + (S_Y \sin\Theta) \\
T1(2,1) &= (S_Y S_X)(1 - \cos\theta) + (S_Z \sin\theta) \\
T1(2,2) &= ((S_Y)^2 - 1)(1 - \cos\theta) + 1 \\
T1(2,3) &= (S_Y S_Z)(1 - \cos\theta) - (S_X \sin\theta) \\
T1(3,1) &= (S_Z S_X)(1 - \cos\theta) - (S_Y \sin\theta) \\
T1(3,2) &= (S_Z S_Y)(1 - \cos\theta) + (S_X \sin\theta) \\
T1(3,3) &= ((S_z)^2 - 1)(1 - \cos\theta) + 1
\end{aligned} \qquad (2.18)$$

The portion E2 in the equation (2.18) refers to the second movement of the solid body B, where the direction of the displacement identical to the direction of the screw line S. In order to derive a matrix expresses this movement, there is a possibility to expand E2 into 3 combinations each of them indicates to one of the global reference frame components.

$$\begin{aligned}
E2_X = {} & (P\,^{\emptyset}_{O})_X + \text{ɖ}\, S_X + (P\,^{\emptyset}_{O})_X \cos\theta \\
& - \left(((P\,^{\emptyset}_{O})_Y\, S_Z) - ((P\,^{\emptyset}_{O})_Z\, S_Y)\right) \sin\theta \\
& - \left(\left((P\,^{\emptyset}_{O})_X\, S_X + (P\,^{\emptyset}_{O})_Y\, S_Y + (P\,^{\emptyset}_{O})_Z\, S_Z\right) S_X\right)(1-\cos\theta) \\
E2_Y = {} & (P\,^{\emptyset}_{O})_Y + \text{ɖ}\, S_Y + (P\,^{\emptyset}_{O})_Y \cos\theta \\
& - \left(((P\,^{\emptyset}_{O})_Z\, S_X) - ((P\,^{\emptyset}_{O})_X\, S_Z)\right) \sin\theta \\
& - \left(\left((P\,^{\emptyset}_{O})_X\, S_X + (P\,^{\emptyset}_{O})_Y\, S_Y + (P\,^{\emptyset}_{O})_Z\, S_Z\right) S_Y\right)(1-\cos\theta) \\
E2_Z = {} & (P\,^{\emptyset}_{O})_Z + \text{ɖ}\, S_Z + (P\,^{\emptyset}_{O})_Z \cos\theta \\
& - \left(((P\,^{\emptyset}_{O})_X\, S_Y) - ((P\,^{\emptyset}_{O})_Y\, S_X)\right) \sin\theta \\
& - \left(\left((P\,^{\emptyset}_{O})_X\, S_X + (P\,^{\emptyset}_{O})_Y\, S_Y + (P\,^{\emptyset}_{O})_Z\, S_Z\right) S_Z\right)(1-\cos\theta)
\end{aligned} \tag{2.19}$$

The groups of Lie, admits to represent any rotatory displacement in three dimensional space by using a 3by3 matrix such as the matrix T1, usually referred as “SO (3)”. Furthermore, any combinations of rotational and linear displacement in space has 3 dimensions could be represented in the groups of Lie by 4by4 matrix, generally pointed out as “SE (3)”.

Now, it is possible to derive a comprehensive transformation expresses the displacements from the first position M to the final position K. Suppose that, the (4×4) matrices M_{Mat} and K_{Mat} indicate to the two systems of coordinates attached to the points M and K in universal coordinate frame configuration. The matrix M_{Mat} illustrates the location and the orientations of the solid body B in the elementary position M and K_{Mat} indicates to the location and the orientations of the solid body B in the eventual position K. Through this section, the general displacement separated into two movements, rotatory and linear, due to Chasles's theorem. These two movements represent the relation between the first configuration M_{Mat} and the second configuration K_{Mat}. The theory of Lie algebra defines the thorough displacement as 4by4 matrix includes two section. The first section has the form of a 3by3 matrix and represents the rotational movement. The second part has the form 3by1 matrix and illustrates the linear motion.

$$K_{Mat} = \begin{bmatrix} \mathrm{T1}(1,1) & \mathrm{T1}(1,2) & \mathrm{T1}(1,3) & \mathrm{E2_X} \\ \mathrm{T1}(2,1) & \mathrm{T1}(2,2) & \mathrm{T1}(2,3) & \mathrm{E2_Y} \\ \mathrm{T1}(3,1) & \mathrm{T1}(3,2) & \mathrm{T1}(3,3) & \mathrm{E2_Z} \\ 0 & 0 & 0 & 1 \end{bmatrix} . M_{Mat} \tag{2.20}$$

Equation (2.20) represents the general displacement modeling using the theory of screws. In the next section, equation (2.20) will be generalized in order to handle with successive movements as existing in open loop chains. The matrix transformation that expresses the comprehensive motion will be referred as R in the next section.

2.3.3 Sequential Screw Axes Technique

In an open loop kinematics, the manipulator consists of several links connected by joints in a consecutive manner. In order to analyze such robot based on the screw axis method, the screw which represents the combination of all screw axes in the robot is to be found. The scientists Tsai and Roth, publicize a paper in 1972 [35], through it, they explain and prove that finding the solution to the problem of existence two screw axes allow the rigid body to rotate around and translate along depending on identifying another screw axis as a fusion of these two screw axes. This fusion is done by considering the displacement of the rigid body around and along the second screw axis, then the displacement of the rigid body around and along the first screw axis. This discussion is illustrated in the following figure.

Let the 4×4 matrix $R1$ expresses the comprehensive displacement of the solid body over the first screw axis $S1$ and $R2$ represent the general motion through the second screw axis $S2$. Then, the combination of these two transformations given in equation (2.21).

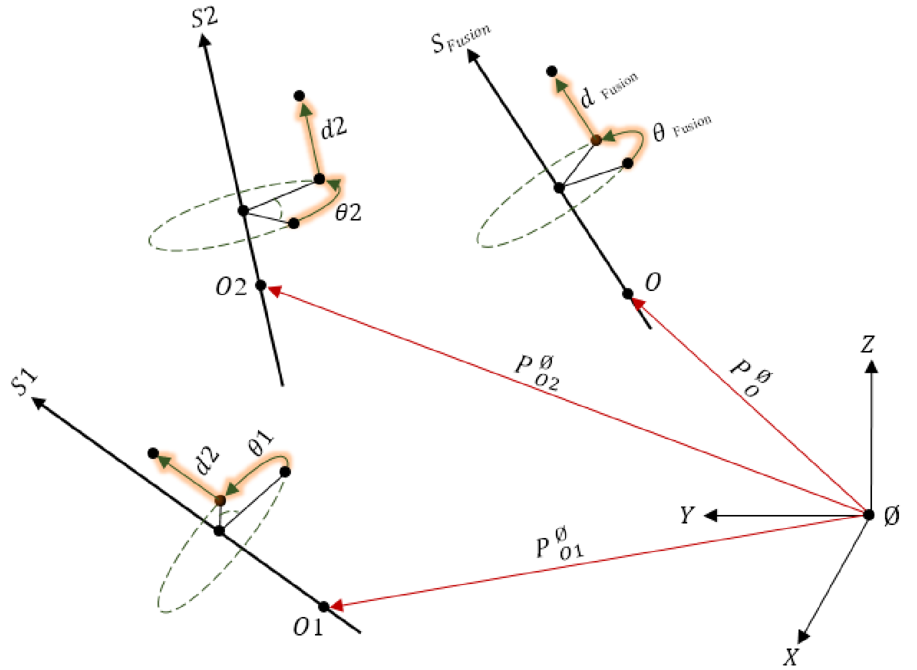

Figure 2.5: Clarifying the Consecutive Screw Axes Method

$$R_{Fusion} = R1.R2 \tag{2.21}$$

Equation (2.21) can be generalized to be suitable for serial link combination has rank equal to n as follow.

$$R_{Fusion} = R1.R2.R3.\ldots Rn-1.Rn \tag{2.22}$$

2.4 Kinematic Modeling Using the Product of Exponential Method

In the science of kinematics, The "Product of Exponential" technique, sometimes called as "POE", is another method that has been used in the most recent kinematic analysis. Many factors have made this method classified as the most efficient, quality and easy to use. In addition to the essential priority that provided by the kinematics analysis using the conventional screw theory representation over D-H modeling which is the significant reduction in the number of the coordinates systems. However, the computational complexity in the classic screws theory method is remarkably minimized in this kinematic modeling.

As seen in the previous section, any solid body proceed in the triple space could be characterized as a particular motion regarding exclusive vector. For this reason, it is essential to realize how this arbitrary vector can be represented in space. Different notation has been written to this end. However, plùcker representation [36] and screw assortment are the most widely used in the kinematic science. In this section, an attempt has been made in order to model of the kinematic structure according to the product of exponential configuration.

2.4.1 Line Formalization Using *Plùcker* Assortment

Two centuries ago, the mathematician *Julius plùcker* provides an efficient method to represent any vector or line in space using six specifications, later these six components are called plùcker parameters. Essentially, this method based on identify the direction of the line and specify an arbitrary point located on that line. It's known that any direction in space could be recognized by 3 variables, these 3 variables occupy the first three parameters. Furthermore, the vectorial product of the direction vector and the positioning vector symbolizes the second group of the parameters. This process is cleared in the figure 2.6.

As seen in the Figure 2.6, giving an arbitrary line L in three-dimensional space, let the unit vector $\hat{\imath}$ indicates to the direction of the line L, and let n be an arbitrary dot on the line L. Then, the components of the vectors $\hat{\imath}$ and $P{}_{n}^{o} \times \hat{\imath}$ could define the line L due to the plücker assortment.

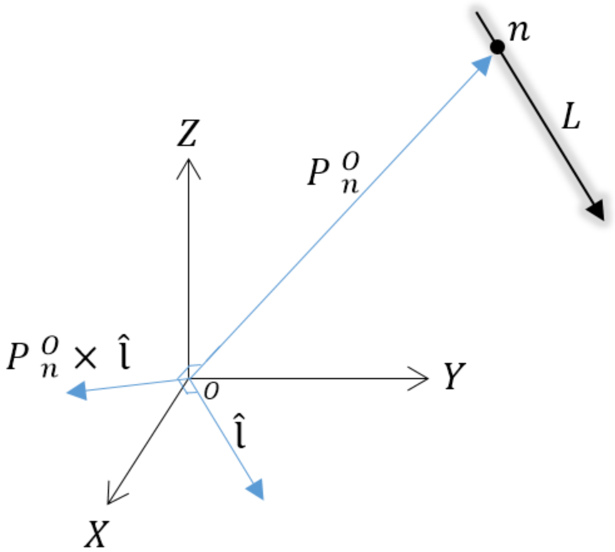

Figure 2.6: Vector Representation Using Plücker Assortment

2.4.2 The Representation of the Screws

Recalling the Chasles's statement, the mutual locomotion of the solid body, which described in the theory, is pretty much compatible with the trace of the screw. Based on this observation, the astrophysicist, *Robert Stawell Ball* in the middle of the 19th century, established one of the most important theorems in the solid body mechanics [37], the theory of the screws.

In the mechanics of the solid body, screw defined as a vector composed of six elements detached equally into two groups. The theorem content of the screw representation states that these separation subgroup are either associated with kinetic or dynamic knowledge. However, in the science of kinematics, the term screw may change into more specialized expression, which is twist. Hence, the phrase twist indicates to the collective motion of the body whatever it expresses a fusion of a rotary and longitudinal or a couple of velocities. Mathematically, two matters are needed in order to specify a screw. The first is a line called a screw axis defined as a rotational shaft of the screw, located in the middle of the spiral trace. Thanks to the plùcker assortment which makes us able to represent any line easily. The second portion is a constant represents the length of the single screw turning cycle taken along the screw shaft, usually referred as ɧ.

For the sake of describing the locomotion of the solid body in 3-dimensional space using the definition of the twist, there is a need to represent the motion using the specification of a uniform matrix. Suppose that, the dot n refers to a solid body displaces in the space of three dimensional. This displacement could be characterized using the uniform of 4×4 matrix representation E, which is composed of rotating and translation sections as seen in the equation (2.23).

$$n = [E].n0 \tag{2.23}$$

Where

$$[E] = \begin{bmatrix} m(1,1) & m(1,2) & m(1,3) & k(1,1) \\ m(2,1) & m(2,2) & m(2,3) & k(2,1) \\ m(3,1) & m(3,2) & m(3,3) & k(3,1) \\ 0 & 0 & 0 & 1 \end{bmatrix} \tag{2.24}$$

$$n = \begin{bmatrix} n(1,1) \\ n(2,1) \\ n(3,1) \\ 1 \end{bmatrix}, \qquad n0 = \begin{bmatrix} n0(1,1) \\ n0(2,1) \\ n0(3,1) \\ 1 \end{bmatrix}$$

In equation (2.24) the vector n refers to the position of the moving body n. In the other hand, the vector $n0$ indicates the position of the point n before the movement began. The equation (2.24) can be written as follow

$$n \; = \; [M].n0 + k \tag{2.25}$$

By applying the derivation of the both sides of the equation (2.25)

$$\frac{dn}{dt} = \frac{d[M]}{dt} . n0 \ + \frac{dk}{dt} \tag{2.26}$$

Since the matrix M represents (3×3) orthogonal matrix, the inverse of the matrix M is always equal to the transpose. By substitute $n0$ into the equation (2.26)

$$\frac{dn}{dt} = \frac{d[M]}{dt} . (n \ - \ k). [M]^T \ + \frac{dk}{dt} \tag{2.27}$$

Then, by expanding the equation (2.27)

$$\frac{dn}{dt} = \ \left(\frac{d[M]}{dt} . [M]^T\right) n \ + \left(\frac{dk}{dt} \ - \ k . \frac{d[M]}{dt} . [M]^T\right) \tag{2.28}$$

Where

$$\begin{gathered} \frac{d[M]}{dt} . [M]^T \ = [\omega] \\ \frac{dk}{dt} \ - \ k . \frac{d[M]}{dt} . [M]^T = v \end{gathered} \tag{2.29}$$

Equation (2.29), clearly shows that the velocity of the movable solid body may be separated into two portions, the first part indicated to the rapidity of the angle ω, guided straight the axis of rotation. As seen in the equation, $[\omega]$ refers to the velocity matrix exemplification of the angular part, could be calculated using skew-symmetric matrix. On the other hand, the second ν refers to linear velocity part taken in the parameters of the global frame. In the sake of simplicity, we can separate the linear portion in two components, analogous to the screw axis and columnar to the axis. We can reformulate the linear velocity ν as in the equation (2.30)

$$\nu = \text{ƥ} \times \omega \ + \ \text{ɧ} . \omega \tag{2.30}$$

In the equation (2.30), the vector ƥ refers to the pose of the rigid body in the fixed coordinate guideline and the constant ɧ related to the parameters of the screws usually referred as pitch. The twist, screw axis, pitch and the velocities are illustrated in the following figure

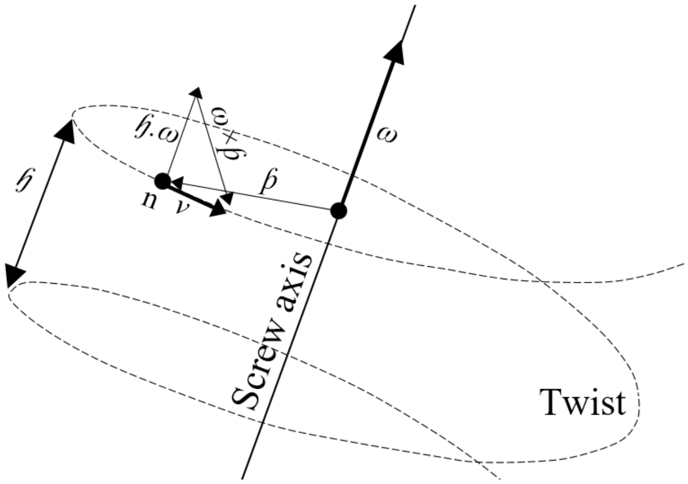

Figure 2.7: The Representation of the Screw Assortment

Now, we can rewrite the equation (2.28) regarding the angular and linear velocity of the solid body as a vectorial equation

$$\begin{bmatrix} \omega \\ \nu \end{bmatrix} = \begin{bmatrix} \omega \\ ƥ \times \omega + ɧ.\omega \end{bmatrix} \tag{2.31}$$

The angular velocity ω may be written as direction û and magnitude c, then the equation (2.31) can be rewritten as in equation (2.32)

$$\begin{bmatrix} \omega \\ \nu \end{bmatrix} = c.\begin{bmatrix} \hat{u} \\ ƥ \times \hat{u} + ɧ.\hat{u} \end{bmatrix} \tag{2.32}$$

As mentioned in the beginning of this section, the three-dimensional displacements of the movable solid body may be regarded as a screw movement around its shaft. In this direction, the equation (2.32) also refers to the representation of the twist using six-dimensional vector. In equation (2.33), the six-dimensional vector Ŝ refers to the unit screw or unit twist.

$$\hat{S} = \begin{bmatrix} \hat{u} \\ \text{þ} \times \hat{u} \; + \; \text{ђ}.\hat{u} \end{bmatrix} \tag{2.33}$$

As known in robotic science, the most used joints are the revolute joints and the prismatic joints. However, the other classical joints such as the spherical and the universal joints may be regarded as a combination of a revolute and prismatic joint. The equation (2.33) can be rearranged due to the revolute and prismatic. Supposing a solid body moving in a rotation trace, then the pitch of the twist should be eliminated from the equation (2.33). Whereas, in the case of the body moving linearly, and subsequently the angular velocity turn to zero, and the pitch will be infinity [38]. These two specific situations are described in the following equations.

$$\hat{S}_R = \begin{bmatrix} \hat{u} \\ \text{þ} \times \hat{u} \end{bmatrix} \tag{2.34}$$

$$\hat{S}_P = \begin{bmatrix} 0 \\ \hat{u} \end{bmatrix} \tag{2.35}$$

We can observe that the equation (2.34) is identical to the line representation using plücker assortment so that the plücker representation is a particular case of the representation of the screws.

The same principle as in sequential screw axes technique, the equation (2.32) can be generalized to fit several consecutive screws aiming to determine an eventual twist as in subsequent equation

$$\$_n = \sum_{i=1}^{n} c_i . \begin{bmatrix} \hat{u}_i \\ \text{þ}_i \times \hat{u}_i + \; \text{ђ}_i . \hat{u}_i \end{bmatrix} = \sum_{i=1}^{n} c_i . \hat{\$}_i \tag{2.36}$$

2.4.3 The Product of Exponential Formulation

We've found in the last section that there is a possibility to represent the moving body traveling in space using the definition of the screw. Based on this verity, a kinematic structure modeling can be assembled.

Equation (2.33) might be rebuilt to form 4×4 matrix representation of the velocities by using the matrix model of the angular velocity

$$\begin{bmatrix} [\omega] & \nu \\ 0 & 0 \end{bmatrix} = \begin{bmatrix} [\omega] & \text{ƥ} \times \omega + \text{ɧ}.\omega \\ 0 & 0 \end{bmatrix} \tag{2.37}$$

Equation (2.37) is identical to the definition of the twist matrix representation [S]. Hence, we become able to subedit the following derivative statement (2.38) depending on the fact that states the screw matrix possesses the full knowledge about the angular and linear velocities of the mobile solid body [38].

$$\frac{d\,E(\varphi)}{d\,\varphi} = [S]\,.E(\varphi) \tag{2.38}$$

In equation (2.38), $E(\varphi)$ indicates to the 4×4 matrix representation of the movements of the solid body in 3 dimensional space. In the mathematic science, this equation has to untie using matrix exponential technique. The next equation (2.39) represents an acceptable solution to the former equation

$$E(\varphi) = e^{\varphi.[S]}\,.E(0) \tag{2.39}$$

Equation (2.39) composes a relation between the matrix representation of the final position of the moving solid body and the initial configuration of the body before the displacement using exponential portion. However, this equation considered as one of the most substantial statement in kinematic chains modeling. The inconstant φ defines the style of the movement whether it is rotating or translate.

Identically to the previous section that illustrates the case of existence series of the screws that represent the kinematic chains [39]. The equation (2.39) can be generalized as stated in the subsequent equation

$$E(\varphi) \;=\; e^{\varphi 1.[S1]} \,.\, e^{\varphi 2.[S2]} \,.\, e^{\varphi 3.[S3]} \,.\ldots.\, e^{\varphi n.[Sn]} \;E(0) \qquad (2.40)$$

2.5 Jacobian Analysis Techniques

In the science of kinematics, the jacobian analysis defined as a representative transformation function relates the velocities or differential movements of the robotic joints with the velocity or differential motion of the Robot's hand frame. The learning of the differential movement analysis enables the robotic specialists to proceed the hand frame of the robot on required trace together with a particular quickness. The fundamental aspect of this inquiry is based on establishing a linkage between the actuator parameter variations that take place during the robot movement and the both velocity combinations of the effective point of the robot.

2.5.1 The Mathematical Definition of the Jacobian Model

Mathematically, the Jacobian representation indicates to the favorable method of derivative characterization of a multidimensional-based function [40]. Assuming that, the multidimensional function $\mathfrak{f}$ possesses i variables as an input and j variables as an output according to the following mapping

$$\mathfrak{f}\colon Ri \;\rightarrow Rj \;:\; y_m = \;\mathfrak{f}_m(\varphi_1 , \varphi_2 ,\; \varphi_3 , \ldots\; \varphi_i\,)\;, m = 1,2,3, \ldots j \qquad (2.41)$$

By taking the rate of change of the function $\mathfrak{f}$ in equation (2.41) regarding the time. This step is shown in the subsequent equation.

$$\frac{d\,y_m}{dt} = \frac{d\,y_m}{d\varphi_1} \cdot \frac{d\varphi_1}{dt} + \frac{d\,y_m}{d\varphi_2} \cdot \frac{d\varphi_2}{dt} + \dots + \frac{d\,y_m}{d\varphi_i} \cdot \frac{d\varphi_i}{dt} \tag{2.42}$$

Equation (2.42) can be reformulated as a matrix model as follow

$$\begin{bmatrix} \frac{d\,y_1}{dt} \\ \frac{d\,y_2}{dt} \\ \vdots \\ \frac{d\,y_{j-1}}{dt} \\ \frac{d\,y_j}{dt} \end{bmatrix} = \begin{bmatrix} \frac{d\,y_1}{d\varphi_1} & \frac{d\,y_1}{d\varphi_2} & \cdots & \frac{d\,y_1}{d\varphi_{i-1}} & \frac{d\,y_1}{d\varphi_i} \\ \frac{d\,y_2}{d\varphi_1} & \frac{d\,y_2}{d\varphi_2} & \cdots & \frac{d\,y_2}{d\varphi_{i-1}} & \frac{d\,y_2}{d\varphi_i} \\ \vdots & \vdots & \ddots & \vdots & \vdots \\ \frac{d\,y_{j-1}}{d\varphi_1} & \frac{d\,y_{j-1}}{d\varphi_2} & \cdots & \frac{d\,y_{j-1}}{d\varphi_{i-1}} & \frac{d\,y_{j-1}}{d\varphi_i} \\ \frac{d\,y_j}{d\varphi_1} & \frac{d\,y_j}{d\varphi_2} & \cdots & \frac{d\,y_j}{d\varphi_{i-1}} & \frac{d\,y_j}{d\varphi_i} \end{bmatrix} \cdot \begin{bmatrix} \frac{d\varphi_1}{dt} \\ \frac{d\varphi_2}{dt} \\ \vdots \\ \frac{d\varphi_{i-1}}{dt} \\ \frac{d\varphi_i}{dt} \end{bmatrix} \tag{2.43}$$

In the previous equation, the $(j \times i)$-dimensional matrix forms a linkage between two vectors of velocity. This matrix is generally recognized as Jacobian

2.5.2 The Kinematic Definition of the Jacobian Model

In the robot science, the Jacobian structure is used to relate the amount of change of the robot's joints regarding the time with the combinations of the velocity of the impact point coordinate frame. Recalling the equation (2.42), the inconstant φ represents the turning degree or linear displacement amount. The velocity coordinate of the action point can be found by different techniques. However, the traditional Jacobian and the Jacobian using the theory of the screws are among the most famous methods [27].

The method that depends on the differential equations to find the velocity of the hand coordinate frame considered as one of the most simple and widespread techniques regarding the open loop chain manipulators. Sometimes this method called conventional or traditional Jacobian. However, traditional Jacobian procedure becomes more stiffness in the case of the closed loops chain robots. According to this method, the hand velocity is described as a pair of three-dimensional vectors as follow

$$\frac{d\,y_m}{dt} = [\nu \quad \omega]^T \quad , m = 1,2,3,\dots 6 \tag{2.44}$$

In equation (2.44), the three-dimensional vector ν represents the linear velocity of the impact point of the hand In terms of the specific point located on the hand, while the vector ω defines the angular velocity of the hand frame.

The Jacobian modeling that builds on the theory of the screws is one of the most crucial issues in kinematics due to its benefit in the velocity analysis problem of the parallel manipulator. Using this technique, the velocity model of the hand has a uniform as follows

$$\frac{d\,y_m}{dt} = [\omega \quad \nu]^T \tag{2.45}$$

We can observe clearly that there are two essential differences between the two previous equations (2.44) and (2.45). Firstly, the pair vectors that combined the velocity are ordered in an opposite way. Secondly, the technique that established on the theory of the screws included calculating the linear and angular velocities of the hand coordinate in terms of the global coordinate frame in contrast to the traditional method.

2.5.2.1 Jacobian of the Open Chain Manipulator Based on the Theory of Screws

Open chain manipulators considered among the extremely well-known robot due to its straightening in work, the principle of uncomplicated designing and easy to guide. These robots consisting mainly of solid compounds called links gathered by other elements known as joints. Ordinarily, electric or hydraulic motors are installed on the joints so that these joint named actuated joint. In the case of the joint is left free, then the joint called passive [27]. As long as the global frame is utilized as a reference of the manipulator, the successive twists might constitute the Jacobian. Equation (2.36) could be reformulated as follows

$$\begin{bmatrix}\omega \\ \nu\end{bmatrix} = \begin{bmatrix}\hat{\$}_1 & \hat{\$}_2 & \cdots & \hat{\$}_{n-1} & \hat{\$}_n\end{bmatrix}.\begin{bmatrix}c_1 & c_2 & \cdots & c_{n-1} & c_n\end{bmatrix}^T \tag{2.46}$$

In equation (2.46), ω and ν symbolize the angular and linear velocity of an arbitrary dot taken on the hand of the serial manipulator parameterized in world reference frame. The quantity c in the equation represents the changes in rotation angle or translation distance with regard to the time. The unit screw in equation consists of a couple of three- dimensional vectors as known, then it is clear that the matrix $\begin{bmatrix}\hat{\$}_1 & \hat{\$}_2 & \cdots & \hat{\$}_{n-1} & \hat{\$}_n\end{bmatrix}$ that has (6×n)-dimensional demonstrates the Jacobian matrix of an open chain manipulator has n joints.

2.5.2.2 Jacobian of the Closed Chains Based on the Theory of the Screws

Generally, closed chain robot or parallel manipulator refers to the kinematic structure made up of single or several closed loops. Stalks, moving body, and the fixed platform are the major pieces that make up the parallel robot. Basically, the limbs or stalks of the robot are portioned sequentially into different linkages united by joints so that each limb composes an open chain from the fixed platform to the moving body. Commonly, the limbs of the parallel manipulator contain the both active and passive joints which make the kinematic analysis a problematic task. In order to derive the velocity matrix specialized for the parallel manipulator using the theory of screws, suppose that the number of the limbs is λ each has n joints whether passive or active. Hence, the twists that related to each joint could be symbolized by $\$_{(i,j)}$, where the first subscript refers to the order of the joint, and the second subscript indicates the number of the limb. Subsequently, equation (2.46) may generalized aiming to suit the parallel manipulator.

$$\$_c = \begin{bmatrix}\hat{\$}_{(1,j)} & \dots & \hat{\$}_{(n,j)}\end{bmatrix}.\begin{bmatrix}c_{(1,j)} & \cdots & c_{(n,j)}\end{bmatrix}^T, j = 1,2, \dots \lambda \tag{2.47}$$

In equation (2.47), $\$_c$ defines the velocity of the center of mass of the moving body of the closed chain robot. The intensity $c_{(i,j)}$ represents the changing of the rotation angle or translation distance related to the joint i of the leg j regarding the time. Consequently, the equation (2.47) represents the velocity equation, so that the matrix $[\hat{\$}_{(1,j)} \quad \dots \quad \hat{\$}_{(n,j)}]$ defines the Jacobian matrix of the robot [41].

2.6 The Advantages of the Reciprocity in Kinematics

In the previous section, the discussion was about defining the motion of the solid body kinematically in space so that this movement may be represented by six combinations separated into a couple of three-dimensional vectors named as a twist. In dynamics, the forces that affect the solid body also might be defined as influential force straight some line and couple exist around this line. Similarly, this force and couple could be represented by helical trace comparable to the screw. Hence, the screw that represents dynamics forces will be named as a wrench [27, 32].

In spite of the fact that twist and wrench possess diverse concept physically, the theory of screws managed to exemplify them mathematically in the same approach. One of the first scientists who submitted a research on the reciprocity was *Sir Robert Stawell Ball* [38]. Later, several papers were presented for this purpose [27, 43].

The physical meaning of the reciprocity is summarized as follow, considering a solid body move in 3-dimensional space, then in the case of the body affected by forces that don't cause any action. Subsequently, we can say that the screws that define the motion and the forces are reciprocal one another. Mathematically, we can easily determine whether two screws are reciprocal or not through apply *Klein* formula. If the *Klein* equation gives zero then, the two input screws are reciprocal.

Suppose that, two screws $\$_1$ and $\$_2$ are given, each has a couple of 3 element vector. Then, the *Klein* formula is given as follows

$$\{\$_1; \$_2\} = \{[s_1 \quad s_{o1}]^T; [s_2 \quad s_{o2}]^T\} = s_1.s_{o2} + s_2.s_{o1} = 0 \qquad (2.48)$$

2.6.1 Screw and Reciprocal Screw System

The system of the screw may be defined as a linear span made up of a single screw or multiple screws that are independent of each other. Mainly, the number of the linearly independent screws that consists the system symbolized as q so that q are less than the space parameter, i.e. $q \leq 6$. On the other hand, the system of the reciprocal screw with regard to a particular screw system can be determined as a $6 - q$ system so that each screw in this system is reciprocal with all others.

The most researchers in the domain of the kinematics depend on the particular procedure to identify the reciprocal system mathematically [44]. This multiple steps method named as Plùcker technique which organized as follow

- Set up a suitable fixed coordinate system.
- Determine the coordinate representation of the screw.
- An examination is needed to verify the independence state between the screws in order to form a screw system.
- Via the reciprocity rules, a set of solvable equations can be generated, resolving these equations will grant us the reciprocal system.

However, in the robot science, the comprehensive displacement of the solid body specialized to two particular situations, rotational motion as in revolute joints or linear movement as in prismatic joints. Consequently, another kinematic joint that used in robots such as spherical and universal can be represented by separate its motion into several simple movements.

As discussed in the screw representation section, especially the equations (2.34) and (2.35), the screw that possesses ignored pitch represents the screw that model the revolute motion. This is also true when talking about the net force. Consequently, the screw may be titled as a line screw [44], because the helical form turns into a line may be defined using Plücker assortment [36]. On the other hand, when addressing the prismatic motion or the momentum, we can observe that the pitch of the screw will possess an infinite value. In this case, it is possible to realize that the representation screw vector possesses freedom of movement in space. Sometimes, this screw vector called moment vector.

[44] Involves valuable perceptions taken from the understanding the equation (2.48). These notes could make the process of finding the reciprocal system much easier.

- Any two screw vectors that model whether rotational motion or pure force are reciprocal if they belong to the same plane.
- Any two screws that represent prismatic motion or momentum are reciprocal permanently.
- Two screw vectors that one of them possess zero value in its pitch whereas, the other has infinite pitch, are said to be reciprocal if they are orthogonal to each other.

The process of finding the system of the reciprocal screw can become better understood through an example. Suppose a system of 3 linearly independent screw vector, shown in Figure 2.8, represents a kinematic structure consisting of three revolute kinematic joints. In this case, we can regard these screw vectors as a line vector representable via plùcker assortment.

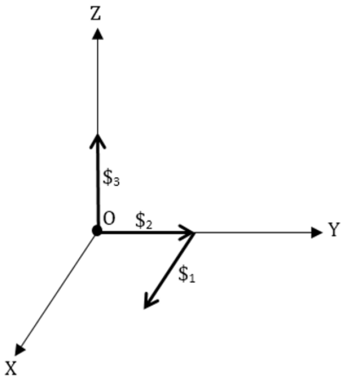

Figure 2.8: Illustration of a Screw System Hold 3 Linearly Independent Screw Vectors

In order to identify the reciprocal system for the kinematic chain stated in Figure 2.8. First, we need to define the line vectors using plùcker coordinate.

$$\begin{cases} \$_1 = [1 \quad 0 \quad 0 \quad 0 \quad 0 \quad -1]^T \\ \$_2 = [0 \quad 1 \quad 0 \quad 0 \quad 0 \quad 0]^T \\ \$_3 = [0 \quad 0 \quad 1 \quad 0 \quad 0 \quad 0]^T \end{cases} \tag{2.49}$$

For each vector, we can find an associate reciprocal five-system. Subsequently, a linear equation related to each reciprocal system can be generated to form a system of three linear equations each of them is linked to one of the reciprocal 5-system. Assuming that the plùcker assortment of the reciprocal vectors has the form $\$_r = [\, p_1 \; p_2 \; p_3 \; p_4 \; p_5 \; p_6 \,]^T$. Thereafter, using this notation the linear equation can be generated as following

$$\begin{cases} p_3 \;\; - p_4 \;\; = 0 \\ \quad p_5 \;\; = 0 \\ \quad p_4 \; = 0 \end{cases} \tag{2.50}$$

Each vector succeeds in achieving the equation (2.49) will be a reciprocal to entire screws that represented in the example. We can find a basis demonstrate the system of reciprocity as follows

$$\begin{cases} \$_{r1} = [\,1 \quad 0 \quad 0 \quad 0 \quad 0 \quad 0\,]^T \\ \$_{r2} = [\,0 \quad 1 \quad 0 \quad 0 \quad 0 \quad 0]^T \\ \$_{r3} = [\,0 \quad 0 \quad 1 \quad 1 \quad 0 \quad 0]^T \end{cases} \tag{2.51}$$

2.6.2 Specify the Precise Degree of Freedom for Parallel Manipulator

Knowing the degree of freedom of a robot manipulator especially parallel one considered one of the critical aspect in kinematics. Although, the *Kutzbach–Grubler* formularization [45] could give an accurate number of degree of freedom of parallel manipulators, it doesn't provide any information about the motion type. However, the reciprocity analysis may lead to formalize a procedure grant to give the both of degree of freedom and some information about the robot's activities.

In [44], an ingenious method may help to give a precise degree of freedom for parallel manipulator based on the theory of reciprocal screws system. This technique assumes four mains steps to accomplish the purpose. Firstly, starting from each limb individually, according to the definition of the screw system, there is a need to recognize the screw system associated with each leg of the robot. Secondly, depending on the system of the screws for each leg, we can find the system of reciprocity separately based on the reciprocity analysis. Subsequently, the system of reciprocity of the mobile body that is a combination of all the legs reciprocal systems is to be placed. Finally, by applying the reciprocity analysis, the system of the screw of the movable body can be obtained after resolving the system of reciprocity of the body. The basis of the mentioned system explains the degree of freedom of the robot. This technique is to be applied to the Hexapod robot in the next chapter.

2.6.3 The Functionality of Reciprocal Screws in the Velocity Analysis

Recalling the equation that demonstrates the velocity of the moving platform of the closed loops manipulator based on the screws theory (2.47). It is observable that the equation is not applicable when passive joints exist. However, the theory of reciprocal screws can make the equation succeed in achieving the analysis. Moreover, in the sake of address, the problem of existence some passive joints, the velocity associated with these joints should be canceled from the equation. Subsequently, detecting screws that are reciprocal to the only passive joints is needed. Then, through stratifying Klein formula to the equation and the reciprocal screws mentioned earlier, performs the canceling target will be possible. An example is an optimal way to clarify the concept of canceling the velocity of the passive joints. The Figure 2.9 illustrates a structure of a parallel Manipulator's limb, where finding the cancellation screw is required.

The example in Figure 2.9 aims to find a screw that is reciprocal to only the passive joint so that the velocity of its joint is to be canceled.

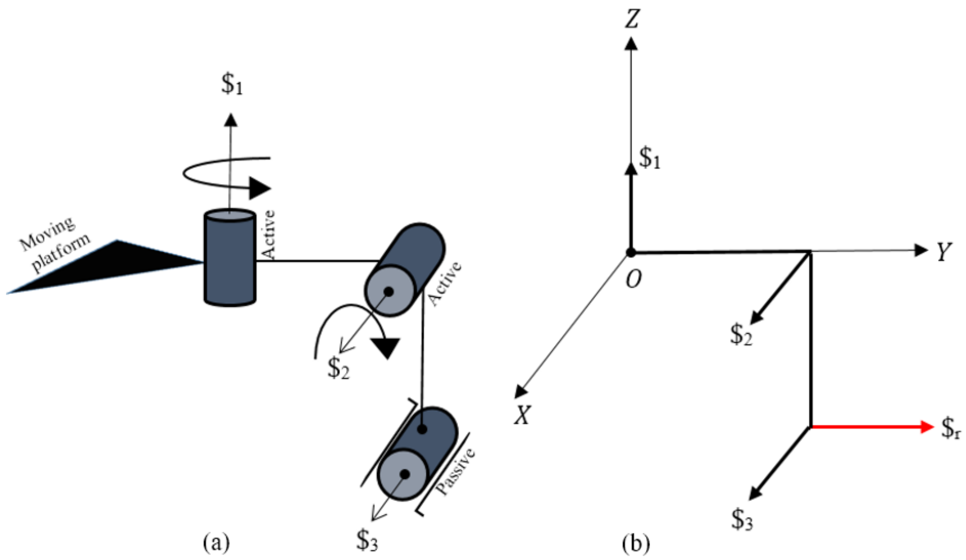

Figure 2.9: Illustration of the Cancellation Technique (a) The Structure of an Assumed Parallel Manipulator's Limb (b) Clarify the Fixed Reference Frame of the Limb, the Screws of the Joints and the Cancellation Reciprocal Screw.

Firstly, there is a need to close the active joints. Moreover the five-system of reciprocal screws for the passive joint is as follow

$$\begin{cases} \$_{r1} = [1 \quad 0 \quad 0 \quad 0 \quad 0 \quad 0]^T \\ \$_{r2} = [0 \quad 1 \quad 0 \quad -1 \quad 0 \quad 0]^T \\ \$_{r3} = [0 \quad 0 \quad 1 \quad 1 \quad 0 \quad 0]^T \\ \$_{r4} = [0 \quad 0 \quad 0 \quad 1 \quad 0 \quad 0]^T \\ \$_{r5} = [0 \quad 0 \quad 0 \quad 0 \quad 0 \quad 1]^T \end{cases} \tag{2.52}$$

We can notice that only the reciprocal screw $\$_{r2}$ is reciprocal only to the passive joint. Whereas the others are reciprocal to some of the active joints. Consequently, the screw $\$_r = [0 \quad 1 \quad 0 \quad -1 \quad 0 \quad 0]^T$ successes to form a cancellation screw.

Chapter 3

KINEMATICS ANALYSIS OF THE HEXAPOD

3.1 Introduction

As mentioned previously in Chapter 1, hexapod robots occupy an increasing importance among the robot analysts. However, one of the hexapod models that proved its ability and effectiveness among the others was the NOROS [46]. In this chapter, a general explanation of the *NOROS* robot's structure will be explained, as well as, several topics related to the kinematic analysis of the hexapod robot including position, velocity, and mobility study are to be presented in terms of the properties, structure, and parameters of the *NOROS* robot.

3.2 Designing of the *NOROS* Hexapod Robot

It's well known that, the territory in such space environment is something terribly complex. Frequently, the land in space setting composed of a collection of soft moving sand dunes or contains so many rocky difficulties making the use of trundles impractical way, while there is an urgent need to use the trundles with the aim of moving more distance in a short time when the terrain is suitable. Thanks to the dual estate of this robot that allows using both properties of trundle and leg making it fully suitable in such coarse environment.

The architecture of the robot is in the following format, the torso of the robot is located in the middle shaped like a dome, where the base consists of double layer. In this case, the balance center of gravity designed to be in the torso base center. The processing unit, telecommunication circuits, batteries and another equipment placed inside the dome cavity in order to provide acceptable protection from external factors. In addition, there are six stalks or leg assigned in a regular manner concerning the torso [47]. The 3D structure of the NOROS robot is clarified in Figure 3.1.

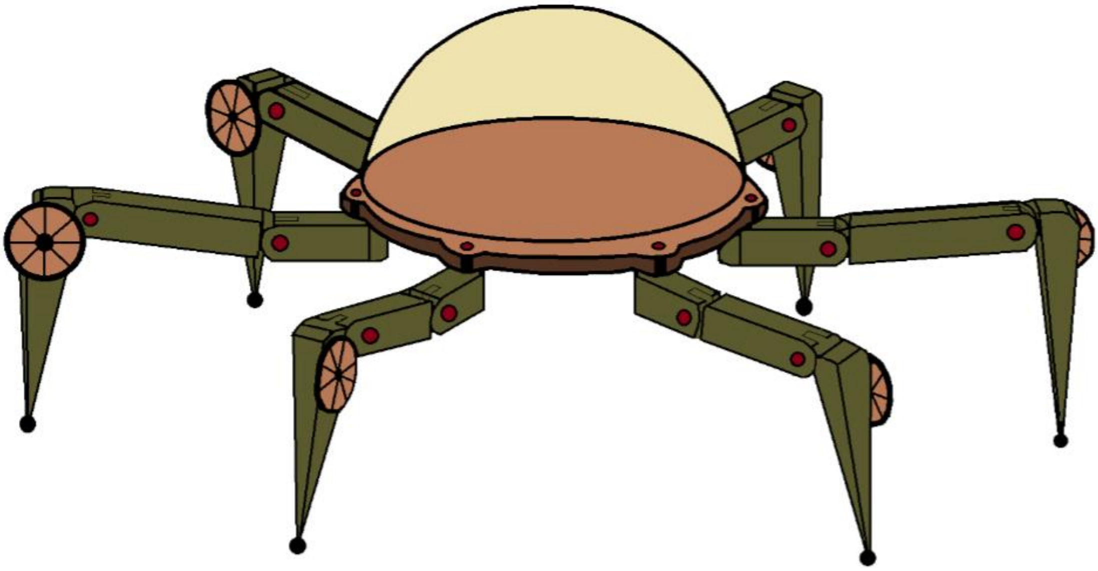

Figure 3.1: The Architecture of the NOROS in 3-Dimensional Space

The leg supposed structure of the *NOROS* hexapod robot mainly composed of five segments: Hip part, Thigh part, Foot part, trundle, and terminal. The segments that make up the robot's leg are attached using three connections that are respectively, head, trochanter, and lap joint. The first joint works on bind the leg with the torso of the robot so that the rotational axis is always vertical to the torso base, on the other hand, trochanter and lap joints are parallel to each other in which they combine Hip, Thigh and Foot sections appropriately. The architecture and the specifications of the robot's leg [48-49] explained in Figure 3.2 and Table 3.1.

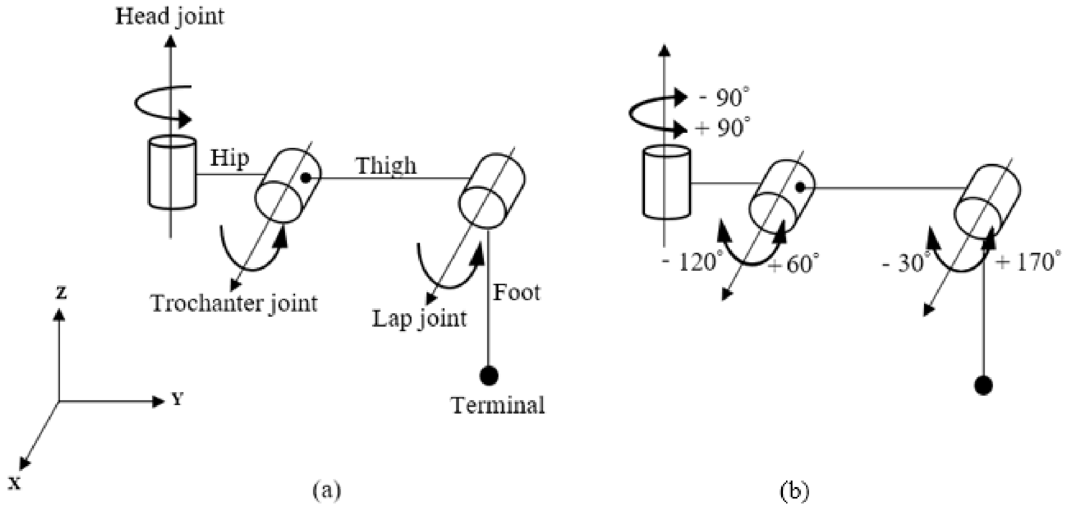

Figure 3.2: (a) The Structure of the NOROS Hexapod's leg (b) The Configuration of the NOROS Hexapod's Leg

Table 3.1: The Parameters of the Individual Leg of the NOROS

parameter	Hip	Thigh	Foot
longitude	9 cm	30 cm	30 cm
mass	800 g	2000 g	2000g

3.3 Kinematics of the Individual Leg of the *NOROS* Robot

Studying the kinematic structure of the single leg of the mobile robot considered as basic substrate for any subsequent analysis. In this section, several issues will be handled regarding the supposed hexapod's leg which are the direct and inverse kinematics for the NOROS leg whether the foot's function is supporting or moving. Distinct techniques will be used for this survey such as D-H method, the theory of screws and geometric approach.

3.3.1 The Kinematic Study of the Separate Leg of the Robot via the Geometry

Using the geometry, the forward and inverse kinematics could be found accurately as following in subsections.

3.3.1.1 Inverse Kinematics Study of the Hexapod's Leg via the Geometry

In the kinematics analysis, the survey that defines the angles of the actuators that gives the effector a specific location called inverse kinematics. In Figure 3.3 a comprehensive geometry of the individual leg is given.

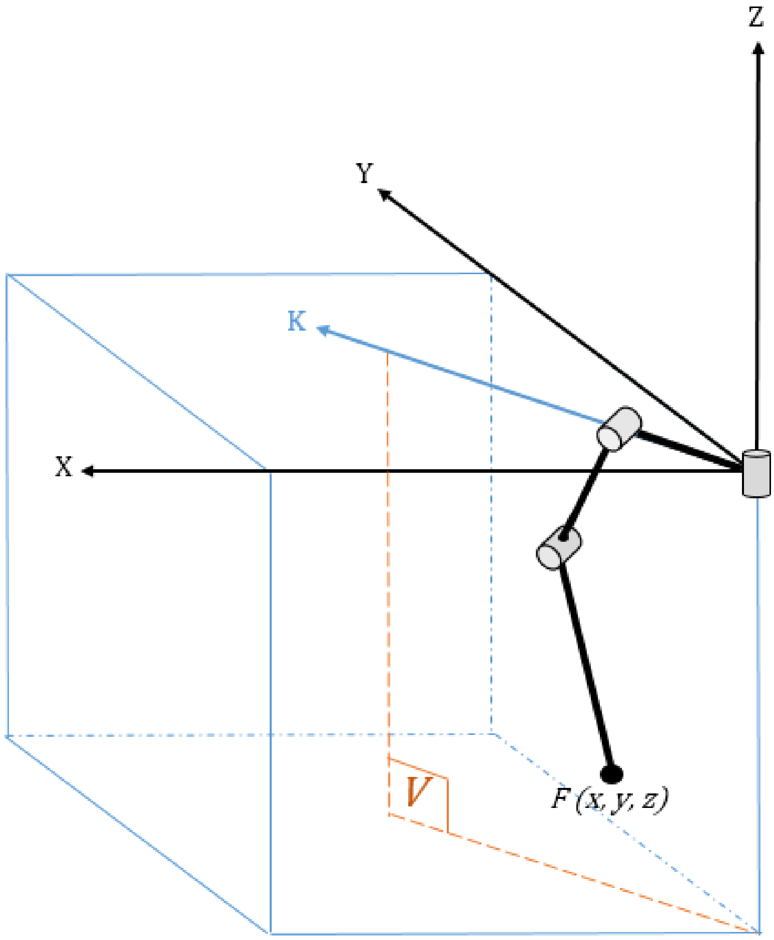

Figure 3.3: General Geometry of the Supposed Hexapod's Leg

In this survey, the lengths of the leg are specified. Presuming that the $t1$, $t2$ and $t3$ indicate to the longitudes of the Hip, Thigh and Foot respectively. Moreover, the placement of the leg's terminal $F(x, y, z)$ is also known. What required is to calculate the joints parameters $\theta 1$, $\theta 2$ and $\theta 3$ in terms of the given information. In Figure 3.4 the level that includes the structure of the leg is demonstrated with all required variables, besides the upper scene of the leg is also shown.

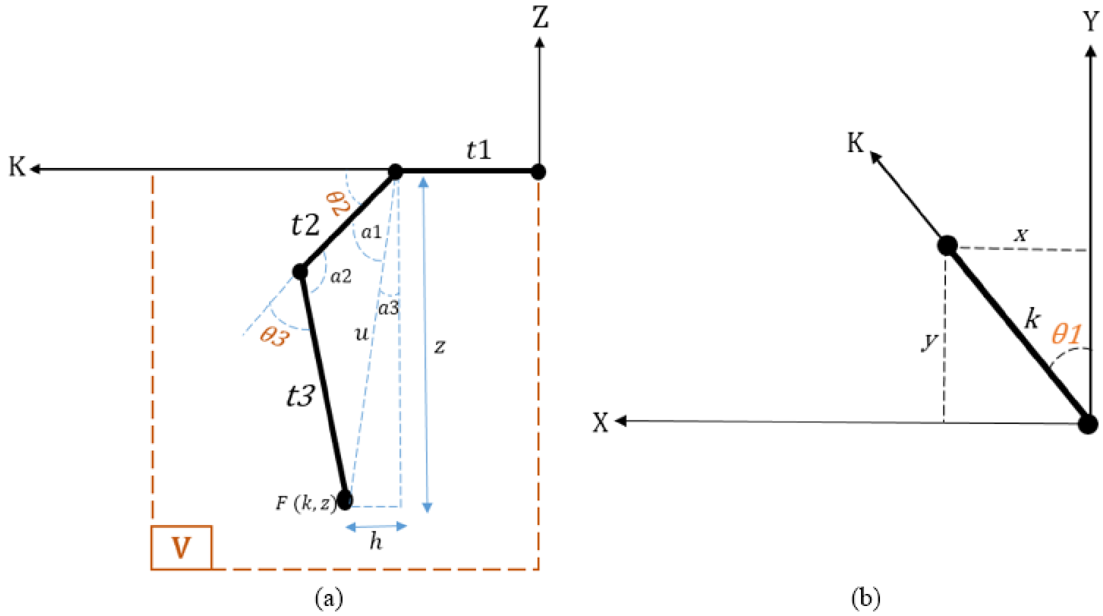

Figure 3.4: (a) The Plane that Contains the Structure of the Hexapod's Leg (b) An Upper Scene of the Hexapod's Leg

It's observable that in figure 3.4, the vector K belongs to the XY plane. In this case, we can calculate the variables k and $\theta 1$ that shown in Figure 3.4 (b) via the following equations. Moreover, due to the configuration shown in Figure 3.2, y is always positive.

$$k = \sqrt{y^2 + x^2} \tag{3.1}$$

$$\theta 1 = \tan^{-1}\frac{x}{y} \tag{3.2}$$

The second and third joints parameters $\theta 2$ and $\theta 3$ could be found using the Figure 3.4 (a) by using the subsequent equations.

$$\theta 2 = 90° - a1 - a3 \tag{3.3}$$

$$\theta 3 = 180° - a2 \tag{3.4}$$

In equations (3.3) and (3.4) the angles $a1$, $a2$ and $a3$ can be defined using the low of cosines [47] as follows

$$a1 = \cos^{-1}\frac{-t3^2 + t2^2 + z^2 + (k - t1)^2}{2.t2.\sqrt{z^2 + (k - t1)^2}} \tag{3.5}$$

$$a2 = \cos^{-1}\frac{-z^2 - (k - t1)^2 + t2^2 + t3^2}{2.t2.t3} \tag{3.6}$$

$$a3 = \tan^{-1}\frac{k - t1}{z} \tag{3.7}$$

3.3.1.2 Direct kinematics study of the Hexapod's leg via the geometry

This survey aims to locate the position of the leg's terminal $F(x, y, z)$ based on knowing the Joint's parameter and the longitudes of the links. By utilizing the geometric figure 3.4 (a), the point $F(k, z)$ that belongs to the plane V could be positioned through following equations

$$k = t1 + t2.\cos(\theta 2) + t3.\cos(\theta 2 + \theta 3) \tag{3.8}$$

$$z = -t2.\sin(\theta t2) - t3.\sin(\theta t2 + \theta t3) \tag{3.9}$$

Once the point $F(k, z)$ calculated, finding the projection of the position terminal on the plane XY become an easy task through the subsequent two equations

$$x = k.\cos(\theta 1) \tag{3.10}$$

$$y = k.\sin(\theta 1) \tag{3.11}$$

The equations (3.10), (3.11) and (3.9) represent the projection of the leg's terminal on the vectors X, Y and Z respectively.

3.3.2 The Kinematics of the Individual Leg via D-H Method

Recalling the Denavit-Hertenberg methodology, one of the ultimate crucial technique in kinematic chain representation, in the previous chapter. In this subsection, an endeavor to build a kinematic system for the single leg of the hexapod using the D-H parameters. The subsequent Figure 3.5 illustrates the architecture of the hexapod's leg and the internal systems of coordinates associated with each joint considering the requirements of this method.

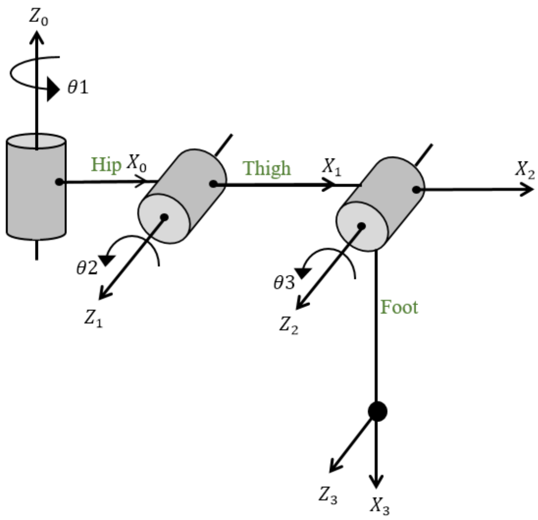

Figure 3.5: Kinematic Representation of the Single Leg via the Parameter of the D-H Convention

The coordinate frame system (X_0, Y_0, Z_0) which is placed on the Head joint will be considered as a fixed frame. It is noticeable that the Y axes in Figure 3.5 have been neglected since these axes could be defined by right hand rule easily. The objective of the subsequent study is to establish a linkage between the fixed frame and the frame associated with the terminal of the hexapod's leg. The parameters related to the D-H convention due to the leg's structure are given below inline in a table. Moreover, assuming that the lengths of the leg's links Hip, Thigh and Foot are awarded as $t1$, $t2$ and $t3$ respectively.

Table 3.2: D-H Parameters of the Single Leg of the Hexapod

Leg's links	θ	a	ɗ	α
Hip	$\theta 1$	$t1$	0	90°
Thigh	$\theta 2$	$t2$	0	0
Foot	$\theta 3$-90°	$t3$	0	0

Using the equations (2.1) and (2.2), we can locate the position of the leg's terminal in fixed reference frame parameters. This step is explained via the following equation

$$\mathrm{T}_{3}^{0} = \mathrm{T}_{1}^{0} . \mathrm{T}_{2}^{1} . \mathrm{T}_{3}^{2} \tag{3.12}$$

$$\mathrm{T}_{1}^{0} = \begin{bmatrix} \cos\theta 1 & 0 & \sin\theta 1 & t1.\cos\theta 1 \\ \sin\theta 1 & 0 & -\cos\theta 1 & t1.\sin\theta 1 \\ 0 & 1 & 0 & 0 \\ 0 & 0 & 0 & 1 \end{bmatrix} \tag{3.13}$$

$$\mathrm{T}_{2}^{1} = \begin{bmatrix} \cos\theta 2 & -\sin\theta 2 & 0 & t2.\cos\theta 2 \\ \sin\theta 2 & \cos\theta 2 & 0 & t2.\sin\theta 2 \\ 0 & 0 & 1 & 0 \\ 0 & 0 & 0 & 1 \end{bmatrix} \tag{3.14}$$

$$\mathrm{T}_{3}^{2} = \begin{bmatrix} \cos(\theta 3 - 90°) & -\sin(\theta 3 - 90°) & 0 & t3.\cos(\theta 3 - 90°) \\ \sin(\theta 3 - 90°) & \cos(\theta 3 - 90°) & 0 & t3.\sin(\theta 3 - 90°) \\ 0 & 0 & 1 & 0 \\ 0 & 0 & 0 & 1 \end{bmatrix} \tag{3.15}$$

$$\mathrm{T}_{3}^{0} = \begin{bmatrix} S\theta_{23}.C\theta_1 & C\theta_{23}.C\theta_1 & S\theta_1 & C\theta_1.(t1 + t3.S\theta_{23} + t2.C\theta_2) \\ S\theta_{23}.S\theta_1 & C\theta_{23}.S\theta_1 & -C\theta_1 & S\theta_1.(t1 + t3.S\theta_{23} + t2.C\theta_2) \\ -C\theta_{23} & -S\theta_{23} & 0 & t2.S\theta_2 - t3.C\theta_{23} \\ 0 & 0 & 0 & 1 \end{bmatrix} \tag{3.16}$$

Equation (3.16) describes the comprehensive transference of the leg's terminal frames that associated with the leg reference system. In order to shorten the general equation, C and S used instead of cos and sin respectively. Moreover, the variable θ_{23} defines as $\theta 2 + \theta 3$.

3.3.3 The Kinematics of the Single Leg Using the Theory of Screws

Remembering the modeling of comprehensive displacement using the screws in the previous chapter. It is possible to build a general kinematic representation of hexapod's leg using the theory of screws simpler than in the D-H parameters. Recalling the equation (2.20) which enables us to construct a homogeneous transformation that links two positions with each other. Moreover, the equation (2.21) and (2.22) can award a transformation matrix between any two systems of coordinate based on the process of finding a particular screw that represents the successive movement of the kinematic structure. The architecture of the robot's leg, as well as the fixing and terminal coordinates and the positions of the screws, are shown below in the figure 3.6. This survey aims to find the resultant screw that associated with the three revolute joints of the hexapod's leg. Before beginning to apply the equations, we have to locate the screw lines associated with each joint besides the relation associated with fixing and moving frames before the movement begins should be accomplished. The parameters $t1$, $t2$ and $t3$ refer to the longitudes of the *NOROS* leg Hip, Thigh and Foot appropriately.

Table 3.3: The Parameters of the Screws Associated with the Hexapod's Leg

Joints	Screws direction	Point located on the screws
head	$[0 \quad 0 \quad 1]^T$	$[0 \quad 0 \quad 0]^T$
Trochanter	$[1 \quad 0 \quad 0]^T$	$[0 \quad t1 \quad 0]^T$
Lap	$[1 \quad 0 \quad 0]^T$	$[0 \quad t1 + t2 \quad 0]^T$

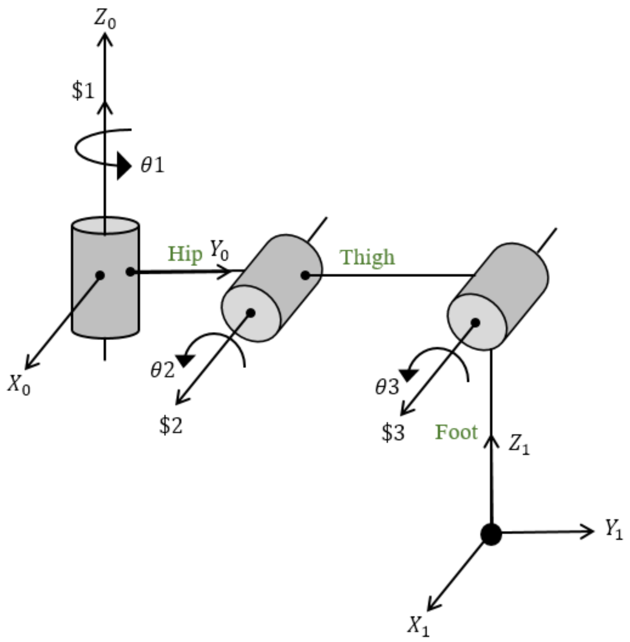

Figure 3.6: Kinematic Modeling of the Hexapod's Leg Using the Parameters of the Screw Theory

The initial configuration of the terminal frame in fixed coordinate parameters can readily obtained from the figure 3.6 through the next equation.

$$\mathrm{T}\,^{0}_{1}(0) = \begin{bmatrix} 1 & 0 & 0 & 0 \\ 0 & 1 & 0 & t1+t2 \\ 0 & 0 & 1 & -t3 \\ 0 & 0 & 0 & 1 \end{bmatrix} \tag{3.17}$$

Equation (2.22) that expresses the general displacement representation may be specialized to represent the revolute joints [27] as in the case of the hexapod's leg.

$$\mathrm{A} = \begin{bmatrix} \mathrm{A1} & \mathrm{A2} \\ 0 & 1 \end{bmatrix} \tag{3.18}$$

Matrix A in equation (3.18) defines as a homogeneous matrix that represents a screw associated with the revolute joint. The combinations of the matrix A are given in the subsequent equation.

$$\mathrm{A1} = \begin{bmatrix} (s_x^2-1).(1-\mathrm{C}\theta)+1 & s_x.s_y.(1-\mathrm{C}\theta)-s_z.\mathrm{S}\theta & s_x.s_z.(1-\mathrm{C}\theta)+s_y.\mathrm{S}\theta \\ s_y.s_x.(1-\mathrm{C}\theta)+s_z.\mathrm{S}\theta & (s_y^2-1).(1-\mathrm{C}\theta)+1 & s_y.s_z.(1-\mathrm{C}\theta)-s_x.\mathrm{S}\theta \\ s_z.s_x.(1-\mathrm{C}\theta)-s_y.\mathrm{S}\theta & s_z.s_y.(1-\mathrm{C}\theta)+s_x.\mathrm{S}\theta & (s_z^2-1).(1-\mathrm{C}\theta)+1 \end{bmatrix} \tag{3.19}$$

$$\mathrm{A2} = \begin{bmatrix} -s_{ox}.\left(\mathrm{A1}_{(1,1)}-1\right)-s_{oy}.\mathrm{A1}_{(1,2)}-s_{oz}.\mathrm{A1}_{(1,3)} \\ -s_{ox}.\mathrm{A1}_{(2,1)}-s_{oy}.\left(\mathrm{A1}_{(2,2)}-1\right)-s_{oz}.\mathrm{A1}_{(2,3)} \\ -s_{ox}.\mathrm{A1}_{(3,1)}-s_{oy}.\mathrm{A1}_{(3,2)}-s_{oz}.\left(\mathrm{A1}_{(3,3)}-1\right) \end{bmatrix} \tag{3.20}$$

The six parameters of the screw line that represent the revolute motion symbolized as follow $\$ = [s_x \quad s_y \quad s_z \quad s_{ox} \quad s_{oy} \quad s_{oz}]^T$. Now it is possible to represent the produced motions of the three revolute joints which compose the structure of the *NOROS* leg.

$$\mathrm{R1} = \begin{bmatrix} \mathrm{C}\theta_1 & -\mathrm{S}\theta_1 & 0 & 0 \\ \mathrm{S}\theta_1 & \mathrm{C}\theta_1 & 0 & 0 \\ 0 & 0 & 1 & 0 \\ 0 & 0 & 0 & 1 \end{bmatrix} \tag{3.21}$$

$$R2 = \begin{bmatrix} 1 & 0 & 0 & 0 \\ 0 & C\theta_2 & -S\theta_2 & -t1.(C\theta_2 - 1) \\ 0 & S\theta_2 & C\theta_2 & -t1.S\theta_2 \\ 0 & 0 & 0 & 1 \end{bmatrix} \tag{3.22}$$

$$R3 = \begin{bmatrix} 1 & 0 & 0 & 0 \\ 0 & C\theta_3 & -S\theta_3 & -(t1 + t2).(C\theta_3 - 1) \\ 0 & S\theta_3 & C\theta_3 & -(t1 + t2).S\theta_2 \\ 0 & 0 & 0 & 1 \end{bmatrix} \tag{3.23}$$

Equations (3.21), (3.22), (3.23) have a resultant given as in equation (2.22). Moreover, this resultant $R = R1.R2.R3$ represents a homogeneous matrix that linkages between the head fixed coordinate frame and terminal coordinate of the hexapod's leg.

$$T\,{}^{0}_{1}(\theta) = R\,.\,T\,{}^{0}_{1}(0) \tag{3.24}$$

$$R = \begin{bmatrix} B1 & B2 \\ 0 & 1 \end{bmatrix} \tag{3.25}$$

$$B1 = \begin{bmatrix} C\theta_1 & -C\theta_{23}.S\theta_1 & S\theta_{23}.S\theta_1 \\ S\theta_1 & C\theta_{23}.C\theta_1 & -S\theta_{23}.C\theta_1 \\ 0 & S\theta_{23} & C\theta_{23} \end{bmatrix} \tag{3.26}$$

$$B2 = \begin{bmatrix} t1.S\theta_1.(C\theta_2 - 1) - S\theta_1 S\theta_2 S\theta_3.(t1 + t2) + C\theta_2 S\theta_1.(C\theta_3 - 1).(t1 + t2) \\ C\theta_1 S\theta_2 S\theta_3.(t1 + t2) - t1.C\theta_1.(C\theta_2 - 1) - C\theta_1 C\theta_2.(C\theta_3 - 1).(t1 + t2) \\ -t1.S\theta_2 - C\theta_2 S\theta_3.(t1 + t2) - S\theta_2.(C\theta_3 - 1).(t1 + t2) \end{bmatrix} \tag{3.27}$$

3.3.4 The Kinematics of the Single Leg Using the (POF) Technique

The product of exponential representation is relatively considered more widespread than any other method as a result of its simplicity and ease to use. As explained previously in Chapter 2, this method based on the theory of screws and built on the line representation due to the *plücker* coordinate, so that any helical trace could be modeled by a line and a constant ratio called pitch. In *NOROS* hexapod robots, all the leg's chains consist of revolute joints, in this case the screws that represent the motion are essentially lines may be modeled via the *plücker* representation [36].

$$[\hat{\$}] = \begin{bmatrix} [s] & s_o \times s \\ 0 & 0 \end{bmatrix} \tag{3.28}$$

The matrix representation of the unit screw associated with the revolute joints given in equation (3.28), where the 3×3 matrix $[s]$ is a skew symmetric of the screw line direction, in addition, the vector $s \times s_o$ given as the cross product of the line direction with an arbitrary point vector taken on the line. To be clear, in some notation, the angular and linear velocity also may be used to represent the motion as in equation (2.32). Considering the figure 3.6 and the table 3.3, then the unit screws easily obtained via the subsequent equations

$$[\hat{\$}1] = \begin{bmatrix} 0 & -1 & 0 & 0 \\ 1 & 0 & 0 & 0 \\ 0 & 0 & 0 & 0 \\ 0 & 0 & 0 & 0 \end{bmatrix} \tag{3.29}$$

$$[\hat{\$}2] = \begin{bmatrix} 0 & 0 & 0 & 0 \\ 0 & 0 & -1 & 0 \\ 0 & 1 & 0 & -t1 \\ 0 & 0 & 0 & 0 \end{bmatrix} \tag{3.30}$$

$$[\hat{\$}3] = \begin{bmatrix} 0 & 0 & 0 & 0 \\ 0 & 0 & -1 & 0 \\ 0 & 1 & 0 & -(t1 + t2) \\ 0 & 0 & 0 & 0 \end{bmatrix} \tag{3.31}$$

Now, it is possible to apply the equation (2.40) that gives a comprehensive displacement using the product of exponential. The initial configuration $\mathrm{T}\,{}^{0}_{1}(0)$ is given in equation (3.17)

$$\mathrm{T}\,{}^{0}_{1}(\theta) = e^{[\hat{\$}1].\theta_1}\,.\,e^{[\hat{\$}2].\theta_2}.\,e^{[\hat{\$}3].\theta_3}\mathrm{T}\,{}^{0}_{1}(0) \tag{3.32}$$

In order to simplify, it is possible to define a resultant screw representation instead of using consecutive screws due to the equation (2.36)

$$\mathrm{T}\,{}^{0}_{1}(\theta) = e^{[\$_n]}\,.\,\mathrm{T}\,{}^{0}_{1}(0) \tag{3.33}$$

The consequent screw in equation $[\$_n]$ given in following equation

$$[\$_n] = \begin{bmatrix} 0 & -\theta_1 & 0 & 0 \\ \theta_1 & 0 & -\theta_{23} & 0 \\ 0 & \theta_{23} & 0 & -\theta_3.(t1+t2) - t1.\theta_1 \\ 0 & 0 & 0 & 0 \end{bmatrix} \tag{3.34}$$

3.3.5 The Kinematics of the Hexapod's Leg in the Case of Supporting

Once the *NOROS* starts to move, the balance situation must be guaranteed. The static stabilization for the hexapod will be defined in the next chapter. However, this stability needs at least three legs link the ground and assist the Robot's body in staying standing [49]. In this subsection, the kinematics of the supporting leg is to be studied using the product of exponential method. There are several analyses about the modeling of the linkage between the leg's terminal and the terrain due to factors, such as the characteristics of the leg and the technique that used by the researcher. Since the terminal that connects with the territory is a point, the most rational way to represent this linkage is by utilizing the spherical joint. Moreover, as mentioned earlier, the spherical joint may be represented simply as three columnar revolute joints. The following Figure 3.7 illustrates the architecture of the hexapod's leg in assisting situation. Now, it is possible to construct a kinematic modeling of the supporting leg that shown in the Figure 3.7 using the product of exponential method. The parameters that define the screws associated with the supporting leg shown in Table 3.4.

The kinematic study in the case of the leg supports the body, aims to find the head coordinate in order to the fixed frame which located at the point contact. This analysis would be more understanding when the entire part of the hexapod responsible for supporting the robot is taken as a parallel manipulator. That is what will be seen in subsequent sections.

Table 3.4: The Parameters of the Screws Associated with the Supporting Leg

Joints	Screws direction	Point located on the screws
Spherical	$[0 \quad 1 \quad 0]^T$	$[0 \quad 0 \quad 0]^T$
Spherical	$[0 \quad 0 \quad 1]^T$	$[0 \quad 0 \quad 0]^T$
Spherical	$[1 \quad 0 \quad 0]^T$	$[0 \quad 0 \quad 0]^T$
Lap	$[1 \quad 0 \quad 0]^T$	$[0 \quad 0 \quad t1]^T$
Trochanter	$[1 \quad 0 \quad 0]^T$	$[0 \quad -t2 \quad t1]^T$
Head	$[0 \quad 0 \quad 1]^T$	$[0 \quad -(t2+t3) \quad t1]^T$

Due to the theory of screws notation, the comprehensive equation that models the displacement of the supporting leg is given in equation (3.33). However, the initial configuration is written in the following equation

$$\mathrm{T}\,{}^{0}_{1}(0) = \begin{bmatrix} 1 & 0 & 0 & 0 \\ 0 & 1 & 0 & -(t1+t2) \\ 0 & 0 & 1 & t3 \\ 0 & 0 & 0 & 1 \end{bmatrix} \tag{3.35}$$

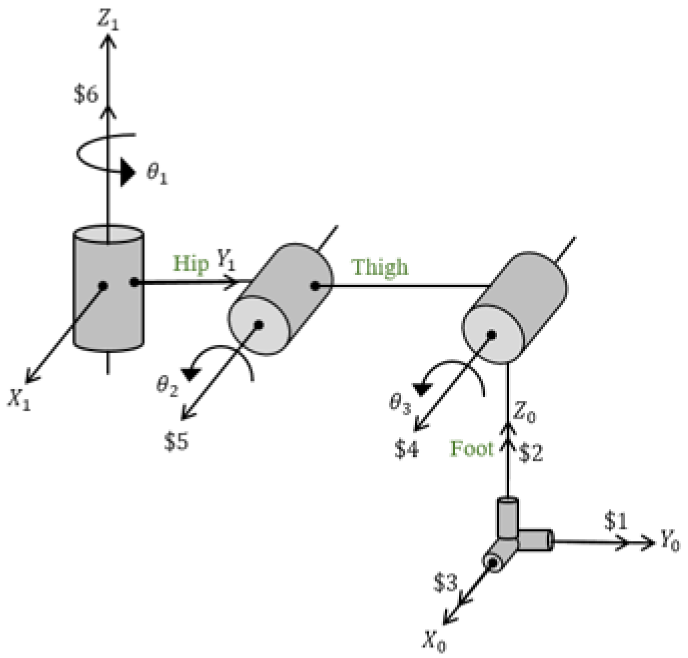

Figure 3.7: The kinematic modeling of the hexapod's leg during assistance phase

Similarly to the analysis in the previous subsection, the unit screws of the joints associated with the structure of the supporting leg regarding to the fixed coordinate are to be found.

Then, the resultant screw $[\$_n]$ will be given in the following equation.

$$[\$_n] = \begin{bmatrix} 0 & -(\theta_2+\theta_5+\theta_6) & \theta_1 & -\theta_6.(t1+t2+t3) \\ (\theta_2+\theta_5+\theta_6) & 0 & -(\theta_3+\theta_4) & t1.(\theta_4+\theta_5) \\ \theta_1 & \theta_3+\theta_4 & 0 & t2.\theta_5 \\ 0 & 0 & 0 & 0 \end{bmatrix} \quad (3.36)$$

Now, applying the equation that give the general displacement of the hexapod's supporting leg is possible through the following equation

$$\mathrm{T}\,{}^0_1(\theta) = e^{\begin{bmatrix} 0 & -(\theta_2+\theta_5+\theta_6) & \theta_1 & -\theta_6.(t1+t2+t3) \\ (\theta_2+\theta_5+\theta_6) & 0 & -(\theta_3+\theta_4) & t1.(\theta_4+\theta_5) \\ \theta_1 & \theta_3+\theta_4 & 0 & t2.\theta_5 \\ 0 & 0 & 0 & 0 \end{bmatrix}}.\mathrm{T}\,{}^0_1(0) \quad (3.37)$$

3.4 Position kinematics analysis for the Hexapod

In general, the position kinematics problem involves knowing the relation between the joints angles and the location of the end-effector. Moreover, this mentioned relationship may be directly or counterproductive. In this survey, an effort will be made to address the problem of position kinematics for the NOROS hexapod robot in both cases direct and indirect. However, before proceeding to handle this issue, we need to identify appropriate and sufficient systems of coordinates that associated with the robot. Also, there are several presumptions related to the hexapod's motion analysis [47] will be taken into account in any subsequent analysis in this thesis.

3.4.1 Theoretical Constraints Associated with the Modeling of the *NOROS*

In order to avoid some problematic confrontations in kinetic analysis and make the modeling more realistic and straightforward, four substantial restrictions are taken into consideration in this study. These limitations are as follows

- Although in some cases sliding movements occur between the leg's terminal and the territory while the hexapod walk, however, this slippery motion will be considered as non-exist.
- Constantly, the locations of the supporting leg's terminals, the touch points between the hexapod's leg and the terrain, are recognized.
- For some considerations regarding keeping the robot in the symmetric case, this issue will be discussed in details in mobility analysis, parallel state between the hexapod's framework and the ground should be preserved.
- During the locomotions of the hexapod, the static stabilization factors are always ensured.

3.4.2 Definition of the Hexapod Coordination Systems

Four coordinate systems can be recognized in order to study the kinematics of the *NOROS* robot. The first Cartesian system $\mathrm{W}(x_W, y_W, z_W)$ located outside the body so that it constitutes an external observer of the movement. The second frame referred as $\mathrm{C}(x_C, y_C, z_C)$, placed at the center of gravity. *NOROS* robot designed so that the center of mass is fully positioned at the center of the circular polygon of the body. Moreover, the remaining reference system $\mathrm{H}_n(xn_H, yn_H, zn_H)$ and $\mathrm{F}_n(xn_F, yn_F, zn_F)$ are established at the Head joints and the endpoint of the links Foot respectively. In the figure 3.8, the relation between these systems is well illustrated.

It is noticeable that the relation between the center of gravity coordinate system and the Head coordinate system are always steady, as shown in Figure 3.9. It is possible to formulate an equation that explains this relationship.

$$\mathrm{T}_{\mathrm{H}_n}^{\mathrm{C}} = \begin{bmatrix} \cos((n-1).pi/3) & \sin((n-1).pi/3) & 0 & \mathrm{r}.\sin((n-1).pi/3) \\ -\sin((n-1).pi/3) & \cos((n-1).pi/3) & 0 & \mathrm{r}.\cos((n-1).pi/3) \\ 0 & 0 & 1 & 0 \\ 0 & 0 & 0 & 1 \end{bmatrix} \quad (3.38)$$

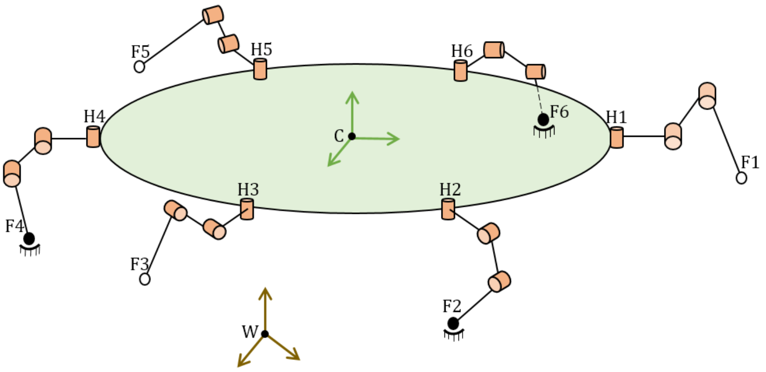

Figure 3.8: Kinematics Scheme of the Hexapod Showing the Locations of the Coordinate Systems

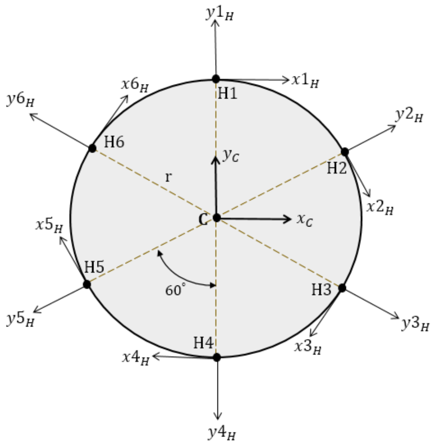

Figure 3.9: The Relation between the Center of Gravity Coordinate and the Head Coordinate Systems

3.4.3 Inverse Kinematics Study for the NOROS

Generally speaking, inverse kinematics study of any parallel manipulator given as finding the parameters of the joints that associated with each limbs in the robot so that the coordinate frame that represents the center of gravity point is known. Mainly, the studies that handle indirect kinematics relies on the geometric techniques due to its simplicity and flexibility. Although the hexapod robot considered as a semi-parallel manipulator, recognizing the angles of the joints by utilizing the geometry is an easy duty [47]. Moreover, according to the inverse kinematics assumption, the location of the hand frame, in our case called leg's terminal, is also known. The figure 3.10 shows the structure of the Hexapod's leg n in three-dimensional space which used to define the inverse kinematics of the hexapod.

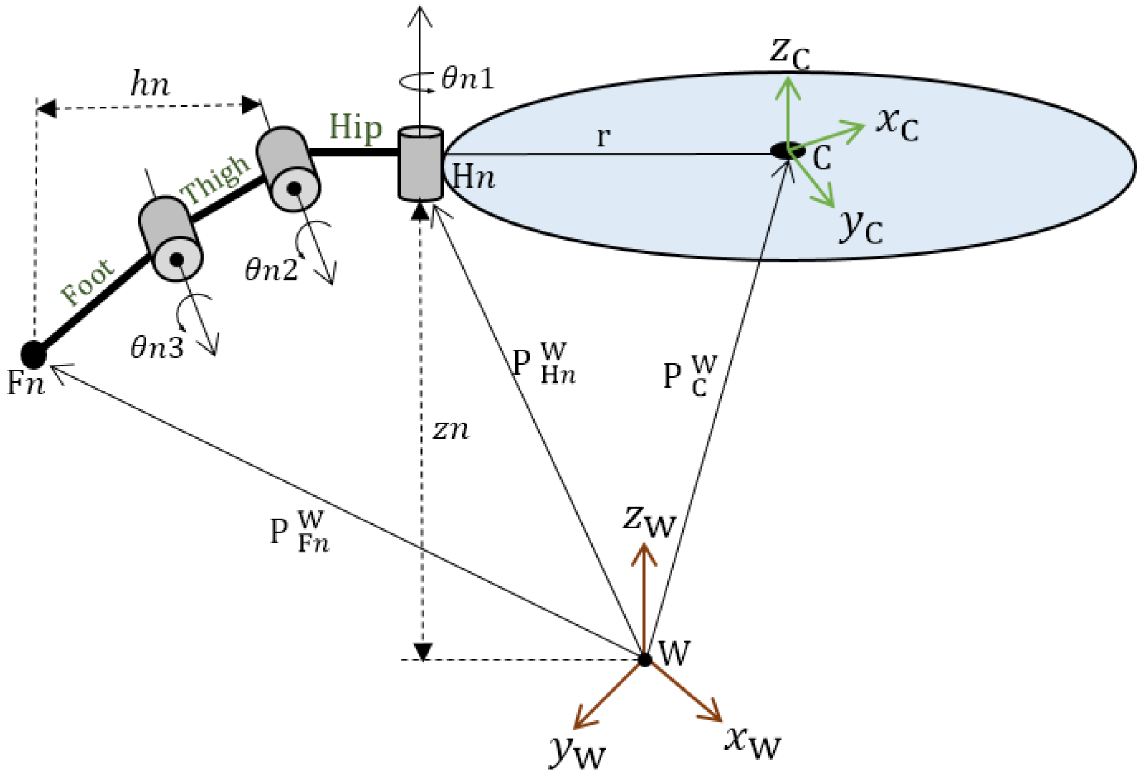

Figure 3.10: Mechanics Scheme Shows the Texture of the Leg n in 3D Space along with Hexapod's Body

As mentioned in the discussion above, and shown in the Figure 3.10 the position of the center of Hexapod's body P^{W}_{C} with respect to the world frame is given. Besides, the locations of the Leg's terminals P^{W}_{Fn} are also present. As seen previously in the subsection that discusses about the inverse kinematics of the Hexapod's leg via the geometry, it is possible to define the parameters of the Leg's joints depending on knowing the position of the Leg's terminal that taken with respect to the Head coordinate frame. Subsequently, finding the point Fn in the parameters of the frame Hn is the top priority.

$$P^{W}_{Fn} = P^{W}_{Hn} + P_{W}{}^{Hn}_{Fn} \tag{3.39}$$

Equation (3.39) defines a vectorial equation taken due to the Figure 3.10. The vector $\mathrm{P}_w{}_{Fn}^{Hn}$ explains the relationship between the frames Fn and Hn in world coordinate frame. In order to isolate the vector P_{Fn}^{Hn} from $\mathrm{P}_w{}_{Fn}^{Hn}$ the following equation have to be accepted.

$$\mathrm{P}_w{}_{Fn}^{Hn} = \mathrm{R}_{Hn}^{W} . \mathrm{P}_{Fn}^{Hn} \tag{3.40}$$

In equation (3.40) the rotation transformation matrix R_{Hn}^{W} that gives the frame Hn with respect to the fixed coordinate W can be found in the following equation.

$$\mathrm{R}_{Hn}^{W} = \mathrm{R}_{C}^{W} . \mathrm{Rot}\,(\mathrm{z}\,, (n-1).\frac{pi}{3}). \tag{3.41}$$

Also the vector P_{Hn}^{W} can be obtained as follow

$$\mathrm{P}_{Hn}^{W} = \mathrm{P}_{C}^{W} . \begin{bmatrix} \mathrm{r}.\sin((n-1).pi/3) \\ \mathrm{r}.\cos((n-1).pi/3) \\ 0 \end{bmatrix} \tag{3.42}$$

Using the equations (3.40), (3.41) and (3.42) the equation (3.39) may be reconstructed as in following equation aiming to find the vector P_{Fn}^{Hn}

$$\mathrm{P}_{Fn}^{Hn} = (\mathrm{P}_{Fn}^{W} - \mathrm{P}_{Hn}^{W}).(\mathrm{R}_{Hn}^{W})^{-1} \tag{3.43}$$

Once the position P_{Fn}^{Hn} is found, identifying the Joint's parameters that associated with the Hexapod's leg n can be defined using the technique mentioned previously through the equations (3.1) up to (3.7).

3.4.4 Direct Kinematics Study for the NOROS

For any parallel robot, direct kinematics survey aims to define the coordinate frame that associated with the center of gravity with regard to the global reference frame. Although the hexapod robot regarded as a semi-parallel manipulator the same trace have to behold [47]. In this survey, several substantive hypotheses will be accepted allow to perform the direct problem with ease and simplicity. The first assumption states that the Hexapod follows a stable tripod locomotion, that means during the robot locomotion there are 3 legs distributed by symmetry support the Hexapod's body continuously. These three legs in addition to the Hexapod's platform which has a hemisphere shape and the terrain will form a three degree of freedom parallel manipulator. Through this parallel manipulator, defining the position and orientation of the center of mass frame is a quite possible. It is also conceivable to state that any extra supporting leg will be thought as a redundant leg. The second hypothesis will be based on the first assumption and complement it. It declares that during the displacement of the Hexapod, the platform should be move on parallel to the ground. The question here is what the reason behind such an assumption? The answer will be the first assumption. According to the mentioned parallel manipulator of three degree of freedom that consists of three legs each of them has 3 joints connected with a servo motors and a passive joint represent the point contact between the leg and the ground, this passive joint should be kinematically modelled as 2 degree of freedom instead of 3 degree of freedom in order to maintain the symmetric state for the robot due to Grubler-Kutzbach criterion. This change in modeling the passive joint will require assuming that the robot is moving parallel to the ground. After finding the coordinate associated with the center of mass of the Hexapod, the second stage of direct kinematics study of the Hexapod takes a place. The purpose of this phase is to recognize the coordinate systems associated with each swinging Leg's terminal with regard to the world coordinate system in a serial manner starting from the center of the mass coordinate system.

To facilitate the study, this survey will be separated into several steps so that each phase will be explained separately. Firstly, depending on the presupposition, the three terminal points that represent the connections between the legs and the ground are known, subsequently the positions that define the locations of the head joints can be independently found. This technique will be reviewed through the following figure and equations

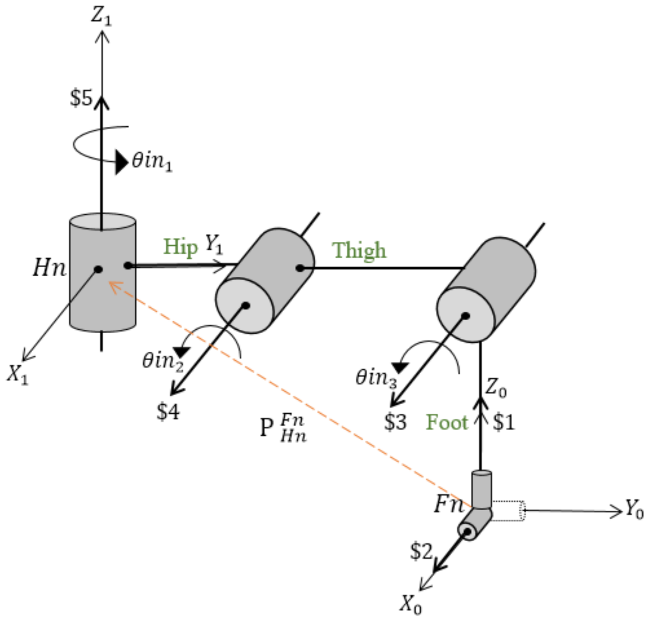

Figure 3.11: The Mechanism of the Hexapod's Leg that Support the Body and Serve to Displace the Robot in 3-DOF

The technique that mentioned above aims to find the position of the coordinate associated with the Head joints of supporting legs wrt the global reference frame [50-51]. The following equations can find the position Hn with respect to the reference frame W written due to the parameters of product of exponential assortment.

$$\mathrm{P}_{Hn}^{\mathrm{W}} = \mathrm{P}_{Fn}^{\mathrm{W}} . \mathrm{P}_{Hn}^{Fn}(\theta) \tag{3.44}$$

$$\mathrm{P}_{Hn}^{Fn}(\theta) = e^{\theta 1.[\hat{\$}_1]} . e^{\theta 2.[\hat{\$}_2]} . e^{\theta 3.[\hat{\$}_3]} . e^{\theta 4.[\hat{\$}_4]} . e^{\theta 5.[\hat{\$}_5]} . \mathrm{P}_{Hn}^{Fn}(0) \tag{3.45}$$

The parameters of the equation (3.45) are explained through the next table. The initial position of the point Hn in the parameter of the coordinate Fn is given as follow

$$\mathrm{P}_{Hn}^{Fn}(0) = [0 \quad -(t1+t2) \quad t3]^T \tag{3.46}$$

The parameter n in previous equations indicates to the series numbers of the Hexapod's legs as 1, 3, 5 or 2, 4, 6.

Table 3.5: The Parameters of the Hexapod's Leg that Support the Body and Serve to Displace the Robot in 3-DOF

Joints	Screws direction	Point located on the screws	Angles
terminal	$[0 \quad 0 \quad 1]^T$	$[0 \quad 0 \quad 0]^T$	θin_1
terminal	$[1 \quad 0 \quad 0]^T$	$[0 \quad 0 \quad 0]^T$	$\theta in_2 + \theta in_3$
Lap	$[1 \quad 0 \quad 0]^T$	$[0 \quad 0 \quad t3]^T$	$-\theta in_3,$
Trochanter	$[1 \quad 0 \quad 0]^T$	$[0 \quad -t2 \quad t3]^T$	$-\theta in_2$
Head	$[0 \quad 0 \quad 1]^T$	$[0 \quad -(t2+t1) \quad t3]^T$	$-\theta in_1$

The second step of the direct analysis come after finding the positions of the Head joints that associated with the supporting legs. Assuming that the position vectors of the points H1, H2 and H3 are located in the parameter of the world coordinate, now the objective is to find the position and the orientation of the center of the mass coordinate frame.

In order to find the position of the mass center, the following procedure has to be performed. Firstly, as long as the center of gravity lying in the center of the Hexapod's circular platform, it is also existing in the center of the triangle formed by the points H1, H2 and H3 or H2, H4 and H6. Subsequently, The position of the centroid given easily by the following vectorial equation

$$\mathrm{P}_{C}^{\mathrm{W}} = {}^{1}\!/_{3} \cdot \left(\mathrm{P}_{H1}^{\mathrm{W}} + \mathrm{P}_{H3}^{\mathrm{W}} + \mathrm{P}_{H5}^{\mathrm{W}}\right) \tag{3.47}$$

Secondly, there is a need to confirm the result that appeared in the previous equation due to the fact that states the center of the triangle ΔH1H3H5 does not necessarily have to be the center of the Hexapod's platform. The centroid of the mentioned triangle and the centroid of the moving platform are identical if the following vectorial equations are realized.

$$\sqrt{3}.\mathrm{r} = \sqrt{\left(\mathrm{P}_{H1_x}^{\mathrm{W}} - \mathrm{P}_{H3_x}^{\mathrm{W}}\right)^2 + \left(\mathrm{P}_{H1_y}^{\mathrm{W}} - \mathrm{P}_{H3_y}^{\mathrm{W}}\right)^2 + \left(\mathrm{P}_{H1_z}^{\mathrm{W}} - \mathrm{P}_{H3_z}^{\mathrm{W}}\right)^2} \tag{3.48}$$

$$\sqrt{3}.\mathrm{r} = \sqrt{\left(\mathrm{P}_{H1_x}^{\mathrm{W}} - \mathrm{P}_{H5_x}^{\mathrm{W}}\right)^2 + \left(\mathrm{P}_{H1_y}^{\mathrm{W}} - \mathrm{P}_{H5_y}^{\mathrm{W}}\right)^2 + \left(\mathrm{P}_{H1_z}^{\mathrm{W}} - \mathrm{P}_{H5_z}^{\mathrm{W}}\right)^2} \tag{3.49}$$

$$\sqrt{3}.\mathrm{r} = \sqrt{\left(\mathrm{P}_{H3_x}^{\mathrm{W}} - \mathrm{P}_{H5_x}^{\mathrm{W}}\right)^2 + \left(\mathrm{P}_{H3_y}^{\mathrm{W}} - \mathrm{P}_{H5_y}^{\mathrm{W}}\right)^2 + \left(\mathrm{P}_{H3_z}^{\mathrm{W}} - \mathrm{P}_{H5_z}^{\mathrm{W}}\right)^2} \tag{3.50}$$

After finding the position of the center of mass, it is possible to define the orientation of the coordinate associated WRT world coordinate frame using the next equations due to the notation is given in the following figure

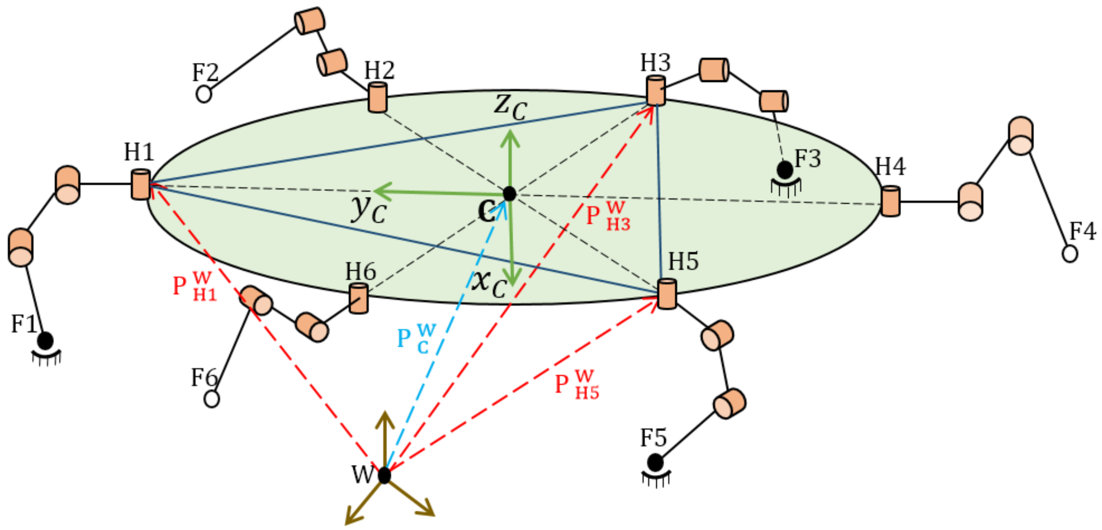

Figure 3.12: Kinematics Scheme of the Hexapod Illustrating the Configuration which Forms the Basis for the Direct Kinematics.

$$\widehat{x_C} = \frac{\left(\mathrm{P}_{H5}^{\mathrm{W}} - \mathrm{P}_{H3}^{\mathrm{W}}\right)}{\sqrt{\left(\mathrm{P}_{H5_x}^{\mathrm{W}} - \mathrm{P}_{H3_x}^{\mathrm{W}}\right)^2 + \left(\mathrm{P}_{H5_y}^{\mathrm{W}} - \mathrm{P}_{H3_y}^{\mathrm{W}}\right)^2 + \left(\mathrm{P}_{H5_z}^{\mathrm{W}} - \mathrm{P}_{H3_z}^{\mathrm{W}}\right)^2}} \tag{3.51}$$

$$\widehat{y_C} = \frac{\left(\mathrm{P}\,^{\mathrm{W}}_{H1} - \mathrm{P}\,^{\mathrm{W}}_{C}\right)}{\sqrt{\left(\mathrm{P}\,^{\mathrm{W}}_{H1_x} - \mathrm{P}\,^{\mathrm{W}}_{C\ x}\right)^2 + \left(\mathrm{P}\,^{\mathrm{W}}_{H1_y} - \mathrm{P}\,^{\mathrm{W}}_{C\ y}\right)^2 + \left(\mathrm{P}\,^{\mathrm{W}}_{H5_z} - \mathrm{P}\,^{\mathrm{W}}_{C\ z}\right)^2}} \tag{3.52}$$

$$\widehat{z_C} = \widehat{x_C} \times \widehat{y_C} \tag{3.53}$$

Eventually, according to the coordinate frame that associated with the center of mass of the Hexapod that found in the previous direct kinematics analysis, the coordinate that attached to the swinging Leg's terminals can be identified using direct kinematics approach from the C coordinate system to the Fn coordinate frames. Here, the variable n define the number of the swinging leg. This step explained through the subsequent equation.

$$\mathrm{T}\,^{W}_{Fn}(\theta) = \mathrm{T}\,^{W}_{C} . \mathrm{T}\,^{C}_{Hn}\,\mathrm{T}\,^{Hn}_{Fn}(\theta) \tag{3.54}$$

In equation (3.54), the transformation matrix $\mathrm{T}\,^{C}_{Hn}$ given in equation (3.38) and the coordinate frame Fn WRT the frame Hn will be found serially similar to the technique explained through the equation (3.32). It should be noted that each redundant supporting leg will be handled as swinging leg through the equation (3.54). Sometimes the Hexapod robots mentioned as a semi-parallel manipulator or serial-parallel robot, the reason behind this is cleared in this analysis, while the moving body of the hexapod along with the ground and supporting legs considered as a parallel manipulator where the coordinate frame that attached with the centroid is found on this basis. In contrast, the coordinates that associated with the Leg's terminal are located based on serial approach.

3.5 Mobility Analysis for the Hexapod

Kinematically, understanding the behavior of the robot displacement in space considered a very significant factor to give an authentic analysis. Studying the mobility aims to identify how many variables can be adequate to give the position of the studied body WRT fixed coordinate system [45]. The maximum number of variables that are in need to recognize any body displacing in 3-D space is six, three of them to define the position where the other to define the orientation. When the kinematic chain connected in serial manner, the determination of DOF is straightforward. In this condition, the number of active joints specify the mobility such that the total number of the joints and the DOF of the manipulator are balanced. In contrast, the situation becomes more difficult when considering the closed chains. Several theories were found for this purpose but perhaps the most famous *Grubler-Kutzbach* standard and the reciprocity-based technique which mentioned in the second chapter. Both methods will be discussed in the next subsections in order to handle the mobility of the Hexapod.

3.5.1 The Mobility Discussion for the Hexapod Using the Conventional Method

The conventional or C-G-K standard considered as one of the oldest and most famous technique to define the mobility of the kinematic manipulator whether it is an open or closed chain. This method depends on knowing the number and the style of the connections besides to the number of the linkage that forms the structural of the robot. Due to this criterion, the numbers of DOF can be recognized by the next equation.

$$\mathrm{M} = \partial(e - v - 1) + \sum_{j=1}^{v} m_j \tag{3.55}$$

The parameters of the equation (3.55) described as follow: M represents the overall DOF that associated with the robot, the parameter ∂ defined as the DOF related with the workspace. In the case that the moving body takes planer motion, ∂ will defined as 3. However, for spatial movement ∂ substituted by 6. The variables v and e realized respectively as the number of the joints and the links that form the robot mechanism. Lastly, the parameter m_j expressed as the number of DOF that formative by the joint j.

Three main specifications should be achieved by the closed chains robot in order to be described as symmetric manipulator. The first condition, the mobility of the robot and the Leg's number should be the same. The second, the structures of the Robot's legs are conformable. Eventually, Robot's legs have an identical number of effective joints. If any of the mentioned above conditions are breached, the manipulator will be classified as an asymmetric robot.

In any symmetric parallel robot, following properties are realized. The mobility value and the number of the robot's legs are identical to the number of circuits in which each circuit consists of two neighboring legs connected with the ground and the platform.

$$\mathrm{M} = t = l + 1 \tag{3.56}$$

In equation (3.56), the parameter t indicates to the number of the Robot's leg while, l recognized as the number of independent circuit. Moreover, the *Euler* neutralization is given in the posterior equation

$$l = v + 1 - e \tag{3.57}$$

The Leg's connectivity Ci is defined as the number of DOF of all the joints that combines the leg, the overall connectivity is given as follow

$$\sum_{i=1}^{t} Ci = \sum_{j=1}^{v} m_j \tag{3.58}$$

By substituting the equation (3.57) into the equation (3.55)

$$\sum_{j=1}^{v} m_j = \mathrm{M} + \partial . l \tag{3.59}$$

The number of independent circuit l may be excluded in equation (3.59) if the equation (3.56) used for this purpose

$$\sum_{j=1}^{v} m_j = \sum_{i=1}^{t} Ci = (\partial + 1). \mathrm{M} - \partial \tag{3.60}$$

Moreover, the Leg's connectivity realized through the following equation

$$\mathrm{M} \leq Ci \leq \partial \tag{3.61}$$

With regard to the Hexapod, there are two cases define the mobility analysis of the Hexapod robot. The first case, when all the Robot's leg are contacting the terrain and supporting the body structure. With this consideration, the NOROS will emulate a symmetric general parallel manipulator with six limbs and six DOF so that three parameters is used to define the center of gravity of the robot while the other determine the orientation of the coordinate system that associated with the center. It is preferable to make sure of this expectation through the previous equations. If the equation (3.55) applied so that the number of the Hexapod's links included the body and the ground is $e = 20$, the number of the joints associated with the robot $v = 24$, $\partial = 6$ and $\sum m_j$ =36. Then $\mathrm{M} = 6$ DOF. Here, the joints that model the relation between the Leg's terminal and the territory are taken without limitations, that's mean spherical joints are chosen for this purpose. The number of connectivities in each leg Ci is equal to six. The second case, when the Hexapod parallel manipulator loses Leg or more in order to locomotion. During the previous mobility analysis, the Hexapod robot handled as a comprehensive parallel manipulator but this thesis aims to study the Hexapod mobile robot. Supposing that the Hexapod robot follows a stable tripod locomotion, three legs are chosen symmetrically to displacing to the new positions while the other three legs assist the body and serve to push the robot. In order to handle the Hexapod based on the symmetric situation, the number of legs that support the body must be equal to the number of DOF of the centroid. However, depending on the stability analysis of the Hexapod, at least three legs differentiated in a symmetric manner must take the supporting role, in this case, the number of DOF should equal three. As mentioned previously, any additional leg support the body will be handled as a redundant leg. Moreover, through the equations (3.60) and (3.61), it is possible to identify the allowed number of connectivities in each leg in which the Hexapod robot maintains the symmetric condition. Due to the equation (3.61), the connectivity in each leg should be between three and six, and the equation (3.60) defines the overall number of connectivities in the Hexapod robot by 15 connectivities. Subsequently, five connectivities take a place in each leg. Knowing that 3 revolute joints related with servo motors, so that the passive joint that formed instead of the point of contact between the Leg’s terminal and the ground modeled as universal joint with two DOF in order to realize the Hexapod as a symmetric robot.

3.5.2 Mobility Analysis for the Hexapod Using Reciprocal Based Technique

Recalling the subsection 2.6.2 that discussed the definition of the mobility using the theory of reciprocal screws. This technique uses 4 essential phase to identify the number of the DOF and the type of motion performed by the robot. For the purpose of conducting this survey for the Hexapod, assuming that the robot performs a stable 3+3 locomotion. Hence, the configuration of the Hexapod's leg that fit with this assumption illustrated in the figure 3.11. We can notice that the contact point of the Leg's terminal on the terrain may be considered as a spherical joint with three degree of passive joint. However we can use universal joint instead of spherical joint in order to maintain the state of symmetric condition. In this case, the body of the Hexapod will process in parallel to the supporting plane formed by supporting feet. The first step to define the mobility analysis through this technique will be finding the basis for the displacement system formed by the screws associated with the Leg's joints of the hexapod robot. It is observable that the system of motion consists of 5 linearly independent screw lines since it belongs to different planes. Basis for such a system can be given in the subsequent equation.

$$\begin{cases} \$1_{\mathrm{B}} = [1 \quad 0 \quad 0 \quad 0 \quad 0 \quad 0]^{\mathrm{T}} \\ \$2_{\mathrm{B}} = [0 \quad 0 \quad 1 \quad 0 \quad 0 \quad 0]^{\mathrm{T}} \\ \$3_{\mathrm{B}} = [0 \quad 0 \quad 0 \quad 1 \quad 0 \quad 0]^{\mathrm{T}} \\ \$4_{\mathrm{B}} = [0 \quad 0 \quad 0 \quad 0 \quad 1 \quad 0]^{\mathrm{T}} \\ \$5_{\mathrm{B}} = [0 \quad 0 \quad 0 \quad 0 \quad 0 \quad 1]^{\mathrm{T}} \end{cases} \tag{3.62}$$

The second step aims to define a reciprocity system associated with each leg independently relying on the theory of reciprocal screws. There is a 1 reciprocal system according to 5 screw systems. By using the observation rules that derived from the theory of reciprocity, it is easy to find the basis of 1 reciprocal system

$$\$1_{\mathrm{r}} = [0 \quad 0 \quad 0 \quad 0 \quad 1 \quad 0]^{\mathrm{T}} \tag{3.63}$$

By following the same approach, we can find the reciprocal system that related with the other two Hexapod's legs. Also, these reciprocal systems are a moment vectors with the direction of Y-axis. These three reciprocal systems are not identical since Y-

axes will be distinct. Hence, the system that made up of the three reciprocal systems, each associated with one Hexapod's leg, composes the restraint system of the moving body. The following steps summarized in finding the restraint system of moving body in the parameters of the world frame. Because of the restraint system component of moment vectors, it is possible to define this system as following

$$\begin{cases} \mathrm{L1} = [0 \quad 0 \quad 0 \quad x1 \quad y1 \quad z1]^{\mathrm{T}} \\ \mathrm{L2} = [0 \quad 0 \quad 0 \quad x2 \quad y2 \quad z2]^{\mathrm{T}} \\ \mathrm{L3} = [0 \quad 0 \quad 0 \quad x3 \quad y3 \quad z3]^{\mathrm{T}} \end{cases} \tag{3.64}$$

Finally, the system of displacement of the mobile body can be found by using the theory of reciprocal screws of the system represented in the equation (3.64). The basis of the reciprocal system that represents the motion type of the robot and can be given in the subsequent equation

$$\begin{cases} \mathrm{L1}_r = [0 \quad 0 \quad 0 \quad 1 \quad 0 \quad 0]^{\mathrm{T}} \\ \mathrm{L2}_r = [0 \quad 0 \quad 0 \quad 0 \quad 1 \quad 0]^{\mathrm{T}} \\ \mathrm{L3}_r = [0 \quad 0 \quad 0 \quad 0 \quad 0 \quad 1]^{\mathrm{T}} \end{cases} \tag{3.65}$$

It is clear that, the centroid of the Hexapod robot possesses three DOF so that the movement has a translation type.

3.6 Jacobian Survey of the Hexapod Robot

The analysis of this section will be According to the explanation in the subsection 2.5.2.2 that mentioned in the second chapter which discusses the derivation of the Jacobian matrix and finding the velocity based on the theory of screws. Also, the technique referred in the passage 2.6.3 can leads to facilitate the survey pretty much by using the theory of reciprocal screws. Moreover, this study will be mainly based on the assumption that the Hexapod robot displaces due to the stable 3+3 locomotion mentioned earlier. The figure 3.13 explains the architecture of the Robot's leg in which the velocities of the joints are shown. The direct velocity of the center of gravity of the *NOROS* due to the equation (2.47) will be stated as follow

$$\$_c = [\hat{\$}_{(1,j)} \quad \cdots \quad \hat{\$}_{(5,j)}].[c_{(1,j)} \quad \cdots \quad c_{(5,j)}]^T, j = 1,2,3 \qquad (3.66)$$

In equation (3.66), $\$_c$ represents the twist that associated with the centroid of the mobile platform which is considered as the combination of the angular and linear velocity of that center. Also, $\hat{\$}_{(i,j)}$ defined as the screw vector that associated with the joint i and located in the Hexapod's leg j. The intensity $c_{(i,j)}$ considered as the velocity or the joint rate related to the joint i.

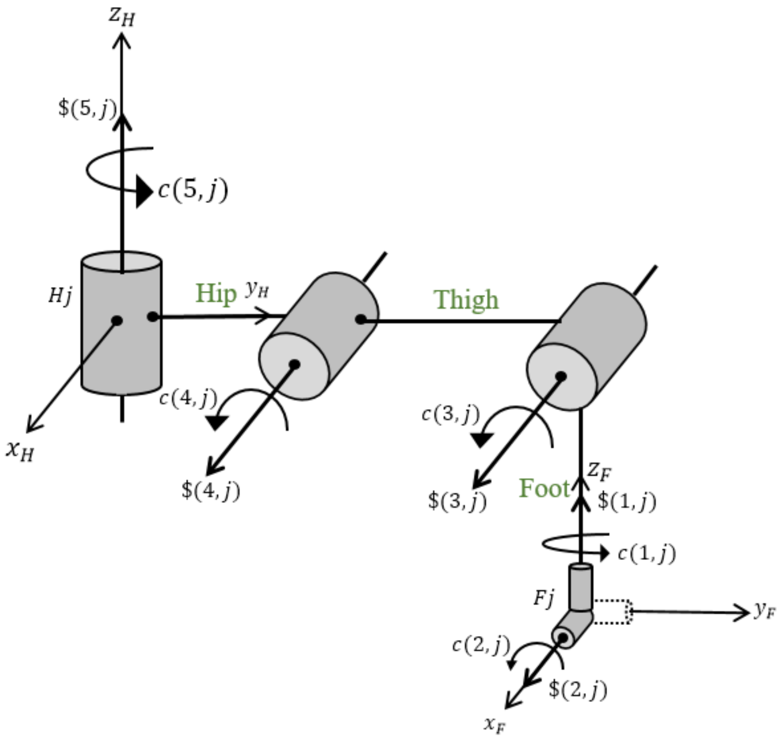

Figure 3.13: The Mechanism of a Hexapod Leg defines the Screws and the Rates that Associated with its Joints.

Equation (3.66) could be spread to form the equation that hold the number (3.67)

$$\begin{bmatrix} W \\ v \end{bmatrix} = \hat{\$}_{(1,j)}.c_{(1,j)} + \hat{\$}_{(2,j)}.c_{(2,j)} + \hat{\$}_{(3,j)}.c_{(3,j)} + \hat{\$}_{(4,j)}.c_{(4,j)} + \hat{\$}_{(5,j)}.c_{(5,j)} \qquad (3.67)$$

The system of screws that shown in the figure 3.13 has a basis given through the equation (3.62) and reciprocal system specified in the equation (3.63). Thereafter, the reciprocal screw may be applied on the equation (3.67) due to Klein formularization.

$$\left\{\$1_{\mathrm{r}}\ ;\ \begin{bmatrix} w \\ v \end{bmatrix}\right\} = [0 \quad 0 \quad 0 \quad 0 \quad 0 \quad 0]^{\mathrm{T}} \tag{3.68}$$

Now, to solve the problem of existence two passive joints, we are in need to find a screw that is reciprocal only to the screws that are associated with the passive joint. It is observable that the screw given in the next equation satisfies the cancellation property.

$$\$2_{\mathrm{r}} = [0 \quad 1 \quad 0 \quad 0 \quad 0 \quad 0]^{\mathrm{T}} \tag{3.69}$$

Subsequently, using the same product technique that used in equation (3.68), but instead of using the screw $\$1_{\mathrm{r}}$, the screw $\$2_{\mathrm{r}}$ is used to achieve the cancellation target.

$$\left\{\$2_{\mathrm{r}}\ ;\ \begin{bmatrix} w \\ v \end{bmatrix}\right\} = \left\{\$2_{\mathrm{r}}\ ;\ \hat{\$}_{(1,j)}\right\}.c_{(1,j)} + \left\{\$2_{\mathrm{r}}\ ;\ \hat{\$}_{(2,j)}\right\}.c_{(2,j)} + \left\{\$2_{\mathrm{r}}\ ;\ \hat{\$}_{(3,j)}\right\}.c_{(3,j)} \tag{3.70}$$

The first part of the equations (3.68) and (3.70) could be written in the matrix form as follow

$$\left\{\$1_{\mathrm{r}}\ ;\ \begin{bmatrix} w \\ v \end{bmatrix}\right\} = [\$1_{\mathrm{r}}]^{\mathrm{T}}.\begin{bmatrix} 0_{3\times3} & 1_{3\times3} \\ 1_{3\times3} & 0_{3\times3} \end{bmatrix}.\begin{bmatrix} w \\ v \end{bmatrix} \tag{3.71}$$

$$\left\{\$2_{\mathrm{r}}\ ;\ \begin{bmatrix} w \\ v \end{bmatrix}\right\} = [\$2_{\mathrm{r}}]^{\mathrm{T}}.\begin{bmatrix} 0_{3\times3} & 1_{3\times3} \\ 1_{3\times3} & 0_{3\times3} \end{bmatrix}.\begin{bmatrix} w \\ v \end{bmatrix} \tag{3.72}$$

Depending on the analysis discussed above, system can be derived from the previous equations in order to find the direct velocity of the center of gravity of the *NOROS* robot. This system is formed in the equation (3.73)

$$\begin{bmatrix} [\$1_{\mathrm{r}}]^{\mathrm{T}} \\ [\$2_{\mathrm{r}}]^{\mathrm{T}} \end{bmatrix} \cdot \begin{bmatrix} 0_{3\times3} & 1_{3\times3} \\ 1_{3\times3} & 0_{3\times3} \end{bmatrix} \cdot \begin{bmatrix} w \\ v \end{bmatrix}$$
$$= \begin{bmatrix} 0 \\ \{\$2_{\mathrm{r}}\ ;\ \hat{\$}_{(1,j)}\}.\, c_{(1,j)} + \{\$2_{\mathrm{r}}\ ;\ \hat{\$}_{(2,j)}\}.\, c_{(2,j)} + \{\$2_{\mathrm{r}}\ ;\ \hat{\$}_{(3,j)}\}.\, c_{(3,j)} \end{bmatrix} \tag{3.73}$$

Chapter 4

LOCOMOTION ANALYSIS

4.1 Introduction

The study of locomotion thought as the main factor of the robots that able to navigate in the surroundings. The survey of locomotion is interested in finding the most optimum sequential series of steps for moving in forward or backward direction, rotating around some axis, changing the direction of moving, overcoming the pitfalls that are in the way and in some cases resistance to stumbling when a fault occurs or loss of some leg. The majority of the gait discussion established on the theory of metamorphic [52] which is involved in handling the structure of the machinery that modifies the formation of the mechanism structure, the mobility and the functionality of its chains to adjust the various assignments. All the criteria of the metamorphism theory apply fully to the Hexapod robot [47]. Hexapod robot possesses numerous style of balanced locomotion including uniform and unorganized gait. Usually, the balanced uniform locomotion grouped depends on how many legs assist the Robot's body through the locomotion period. According to this standard, three essential locomotion manner are found which are tripod, quadruped and 5-legged locomotion style [49]. It is noticeable that, there are no less than 3 assistant legs according to the Hexapod stability conditions [53]. In contrast, sometimes when the Hexapod performs special tasks such as bypassing obstacles, it follows an unorganized movement. This movement is named as free locomotion [54]. In this study, the attention will be directed only towards the balanced tripod locomotion.

4.2 The Stability Modes for the Hexapod Robot

Although when the three legs of the hexapod robot contacting the ground can achieve the compulsory condition of the stable state as explained before, there are other factors to ensure the balance during Robot movement. The stability edge defined as the state that ensures the center of the gravity of the Hexapod robot located inside the shape that specified by the supporting Leg's contact points constantly during the locomotion [52-53]. According to the definition of the stability edge, three cases can be derived which are the stable, critical, and unsteady state. The previously mentioned cases explained in the following figure.

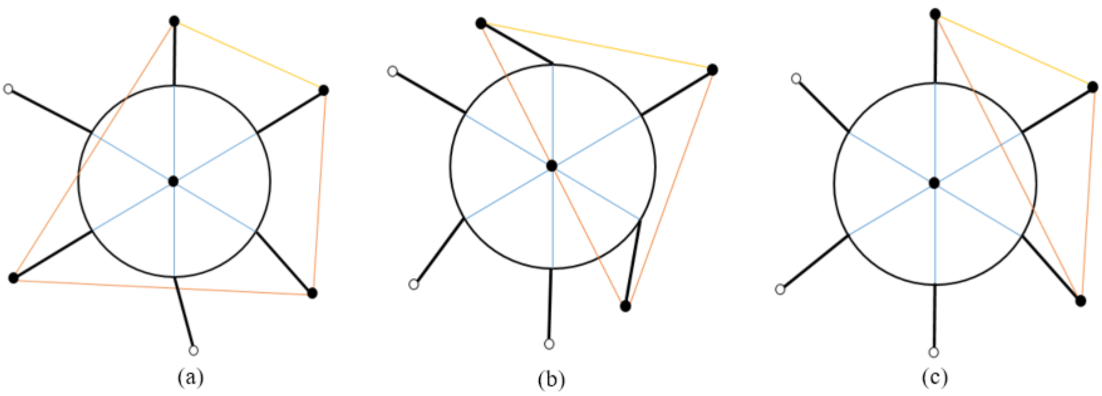

Figure 4.1: The three Supposed Cases that Illustrate the Stability of the Hexapod Robot (a) Stable State (b) Critical State (c) Unsteady State

In the figure 4.1 the bold points that define the polygon refer to the point contact between the supporting leg and the terrain, while the empty points indicate the swinging Leg's terminal.

4.3 Stable Tripod Locomotion Analysis for the Hexapod Robot

The uniform tripod hexapod locomotion defined by possessing 3 limbs assisting the Hexapod's platform and serve to move the robot forward, while the other legs fluctuate in order to displace the Leg's terminals to the another position [53]. As mentioned in the previous sections, the combination of these two motions makes the robot classified as a hybrid robot in which the three assistant limbs in addition to the terrain and body modeled as an equivalent manipulator, while the swinging leg studied serially. Throughout the elementary and substituting stages, all the legs will be contacting the ground. In this case, the Hexapod handled as a parallel manipulator with the center of mass possesses 6 DOFs. The robot researcher Wang et al introduces 3 styles of stable 3+3 locomotion [49], which are a mammal, insect, and hybrid insect-mammal gait. Through this survey, two of the previously mentioned styles which are the mammal and insect locomotion will be studied in details in the next subsections.

4.3.1 The Definition of the Stable 3+3 Mammal Locomotion

During this locomotion, the Hexapod's leg displaced in a columnar pattern similar to the mammalians in which the paths will be forward the limbs and have a line form. Moreover, the Head joint of the Robot's leg is inoperative through the motion. The forward locomotion according to the mammal gait can be summarized as follow, the anterior assistant limbs fall back while the posterior limbs stand out. In contrast, the frontal reeling legs emerge and the rearward legs retreat. During the elementary period of the 3+3 mammal locomotion, the limbs are disseminated equivalently around the Hexapod's body so that the motion of the hexapod according to this gait possesses only two trends. A completed round of the stable tripod locomotion may be separated into certain periods. The subsequent figure explains in detail a full cycle of the Hexapod's locomotion depending on the tripod mammal gait

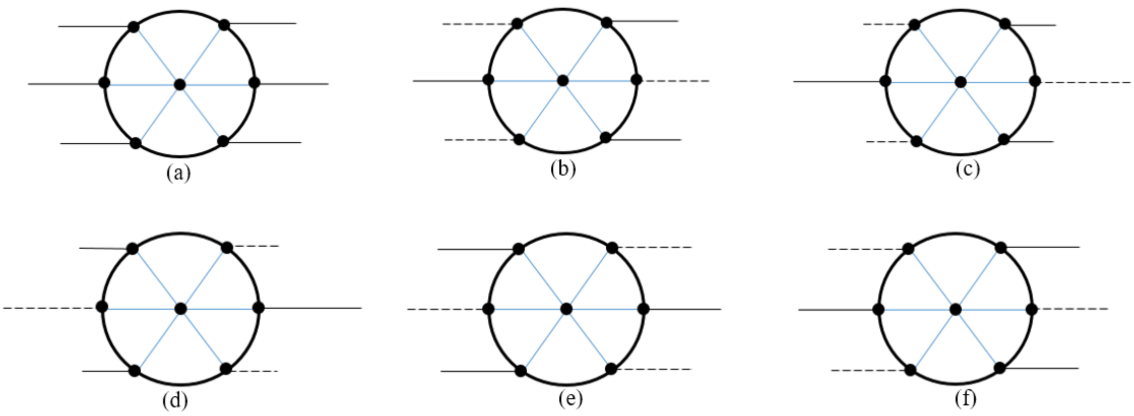

Figure 4.2: A Hexapod's Locomotion Cycle According to the Tripod Mammal Gait (a) Initial State (b) The First Switching Phase (c) The First Moving Phase (d) The Second Switching Period (e) The Second Moving Period (f) Final Switching Period

4.3.2 Kinematic Modeling of the Duty Cycle of the Mammal Kick of Gait

This survey aims to simulate a duty cycle steps according to the mammal locomotion regarding the structure of the *NOROS* hexapod. Before embarking on this analysis, the assumptions written in the subsection 3.4.1 should be accepted. Also, the definition of the coordinates that received in 3.4.2 will be considered in this study. The relations between the Hexapod coordinate systems during the initial condition will be as follow; y-axis of the center of the mass coordinate will be along the Hip link of the first leg when the Head joint has zero angle, z_C will be columnar to the plane that shaped by the footholds of the Hexapod legs and x_C defined by the cross product formula. The axes of the world coordinate frame during initial condition x_W, y_W and z_W have the same directions of the center of the mass coordinate axes, but the origin will be on the ground and along the z_C. Also, the axes of the Head and Foot coordinate frames have the same initial configuration of the center of the mass coordinate system. Six stages could be modeled to represent the duty cycle displacement of the hexapod when following the mammal gait. These stages are initial phase, first switching period, first moving phase, second switching period, second moving phase and third switching phase. Each of them will be discussed separately.

4.3.2.1 Initial Phase of the Mammal Locomotion

The duty cycle of the mammal kick of gait starts when all the six legs of the hexapod touching the ground, supporting the body and positioned towards the moving direction. In this case, we can consider the set of six legs, ground and moving platform as a parallel manipulator with 6 degrees of freedom. Commonly, spherical joints take a place instead of the ends of legs that touching the ground. The following figure illustrates the structure of the Hexapod robot during the initial phase.

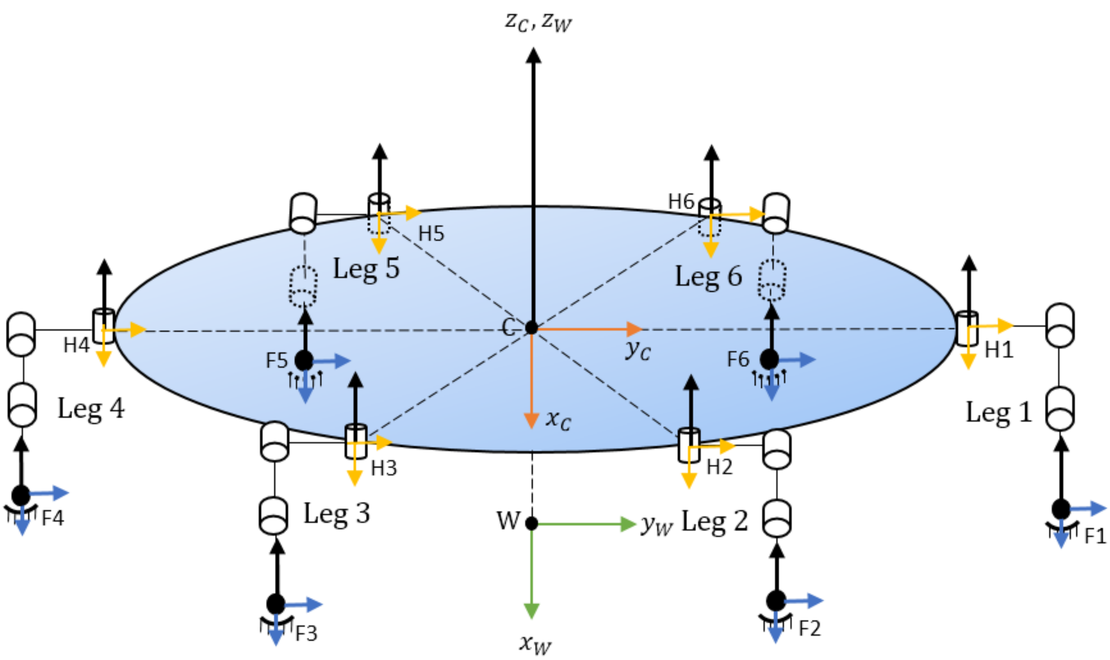

Figure 4.3: The initial Configuration of the Hexapod According to the Mammal Locomotion

4.3.2.2 The First Switching Period of the Mammal Locomotion

In this stage, three legs are chosen symmetrically, such as the legs 2, 4, 6 that changes their situations from assistant phase to swinging phase, while the other legs still supporting the body of the hexapod. Figure 4.4 shows the variation that occurs during the first switching period.

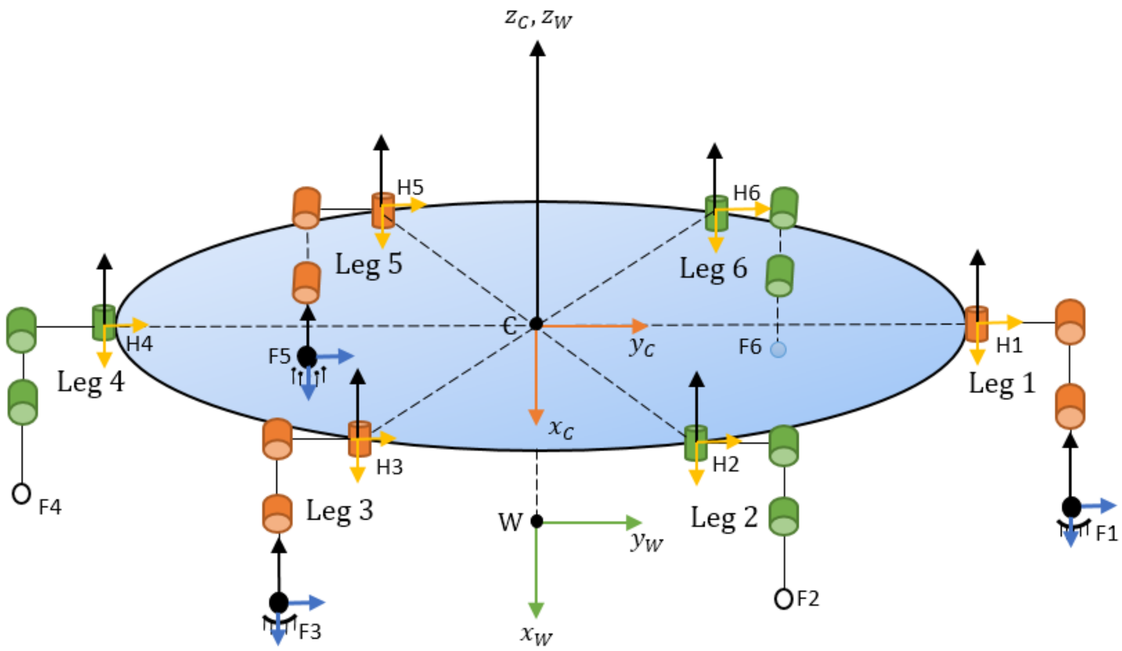

Figure 4.4: The First Switching Phase Configuration of the Hexapod According to the Mammal Locomotion

In figure 4.4, the Hexapod's leg that its joints colored in red refers to the assistant case, while the green defines the swinging leg. This color rule will be followed in the subsequent figures. It is noticeable notice that during the first switching period all the joints still in the initial conditions and all the legs are on the ground. This step aims to prepare the first set of the legs to support the platform and pushing the robot forward, while the other set of legs prepared to fluctuate. The following figure shows a view from the top clarifies the hexapod during this stage in which it defines the assistant shape that formed by the confluence points between the Leg's terminals and the ground. The mentioned shape is an equilateral triangle.

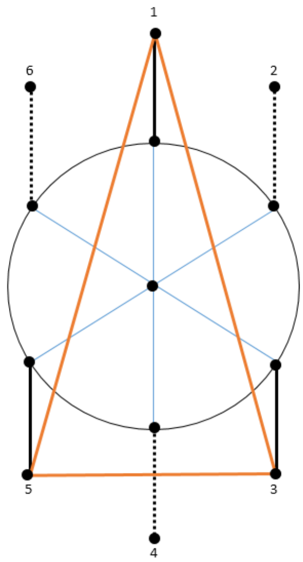

Figure 4.5: A View from the Top Explains the Hexapod Stability Case during the First Switch Period of the Mammal Locomotion

4.3.2.3 The First Moving Phase of the Mammal Locomotion

During this phase the first supporting legs set changed their configuration symmetrically, pushing the body of the hexapod forward, at the same time other set of legs swinging forward. Ending this step ensures that all the legs are on the ground. The following figure illustrates the variations during the first moving phase.

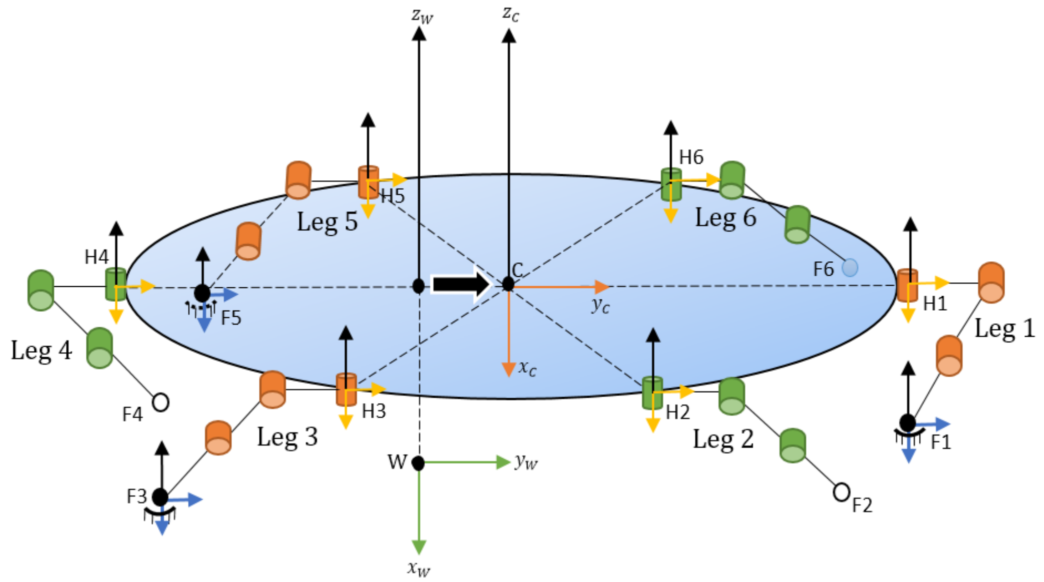

Figure 4.6: The First Moving Phase Configuration of the Hexapod According to the Mammal Locomotion

4.3.2.4 The Second Switching Phase of the Mammal Locomotion

During this phase, switching between the sets of the supporting legs and swinging legs happen. This step aims to prepare the set of the legs that are supporting the body in the previous phase to swinging and prepare the other legs that are responsible to swing in the previous phase to support the body polygon of the hexapod and pushing the body forward. We can notice that during this preparation, all the limbs are on the ground.

4.3.2.5 The Second Moving Phase of the Mammal Locomotion

During this phase the supporting legs set changed their configuration symmetrically, pushing the body of the hexapod forward, at the same time another set of legs swinging forward. Ending this step ensures that all the legs are on the ground. The Figure 4.6 illustrates the variations during the second moving phase

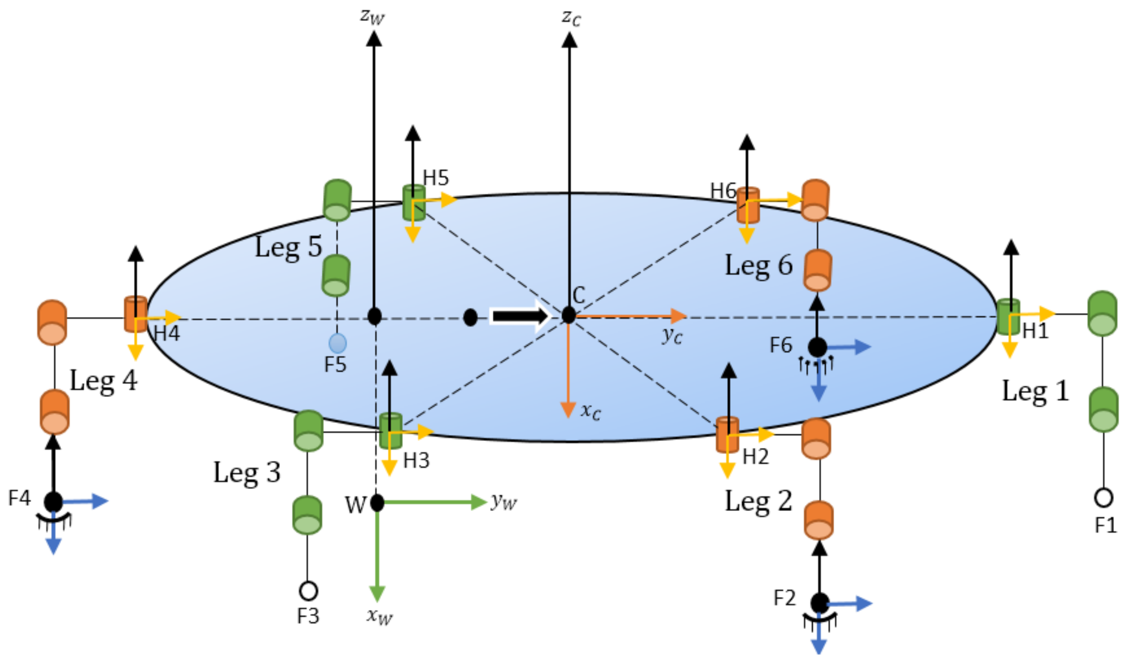

Figure 4.7: The second moving phase configuration of the Hexapod according to the mammal locomotion

4.3.2.6 The Third Switching Phase of the Mammal Locomotion

During this phase, switching between the sets of the supporting legs and swinging legs happen. This step aims to prepare the set of the legs that are supporting the body in the previous phase to swinging and prepare the other legs that are responsible for swinging in the previous phase to support the body polygon of the hexapod and pushing the body forward. We can notice that during this preparation, all the limbs are on the ground. Once this period is done, the full cycle of mammal kick of gait has been modeled.

Appendix A includes a program written in Matlab environment explains in details a Hexapod Locomotion's full duty cycle according to the mammal gait and the parameters that explained in the section 4.3.2.

4.3.3 The Definition of the Stable 3+3 Insect Locomotion

Hexapod's Insect locomotion also considered as one of the maximum essential method used to transport the Hexapod robot from one place to another. This process based on replication of the biological walking manner of the insects and reptiles. Kinetically, tripod insect locomotion defined as a sequence of motion occurs on both side of the Hexapod's moving platform so that the interior and posterior leg belonging to the same tip are working in harmony and the internal leg works in a reverse manner [55]. Tripod insect locomotion and mammal locomotion are compatible in initial conditions. However, they have an incompatible mobile tendency. A scheme of the hexapod robot that illustrates the initial configuration of the hexapod in case of the insect wave locomotion is sketched in Figure 4.8

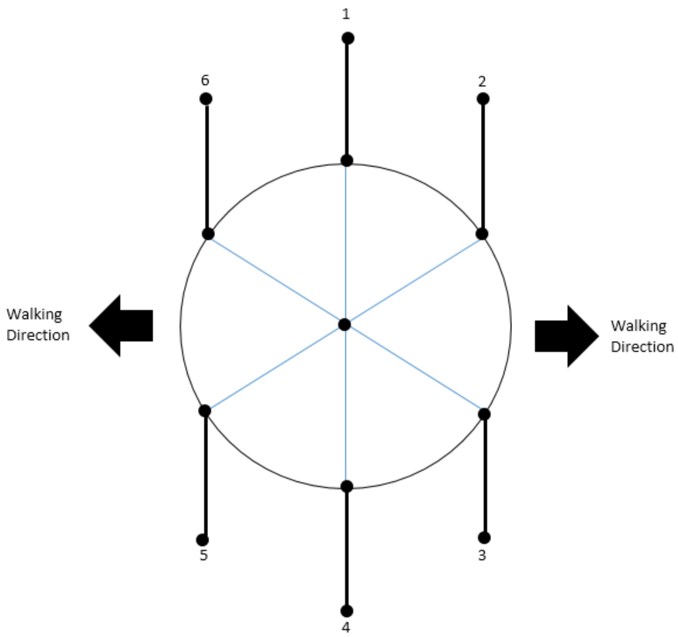

Figure 4.8: Illustration of the Hexapod's Primary Configuration According to the 3+3 Insect Gait

4.3.4 Kinematic Modeling of the Duty Cycle of the Insect Gait

This study targets to mimic a duty cycle phases of the insect locomotion due to the structure of the Hexapod robot. Before the establishment of this analysis, the presumption mentioned in the subsection 3.4.1 should be acknowledged. Moreover, the description of the coordinates that established in 3.4.2 will be considered in this section. Also, as stated above, the insect and mammal locomotion participated in the same primary state that shown in figure 4.3, for this reason, the relations between the coordinate system that cited in the section 4.3.2 during this phase are recognized. Lastly, the two mentioned locomotion has the same duty cycle Steps separation.

Throughout the first moving stage according to the insect wave gait, the first set of supporting legs modify their alignment evenly, shove the Hexapod's body forward, in parallel, the other set of legs swinging to transport the Leg's terminal to another place. Figure 4.9 illustrates the variations during the first moving phase.

During the second converting phase, switching between the sets of the supporting legs and swinging legs happen. This step aims to prepare the set of the legs that are supporting the body in the previous phase to swinging and prepare the other legs that are responsible for swinging in the previous phase to support the body polygon of the hexapod and pushing the body forward. We can notice that during this preparation, all the limbs are on the ground. Figure 4.10 clarifies the variation during this period. In figure 4.10 the dense line refers to the assistant leg, while the dotted line mentions the swinging leg.

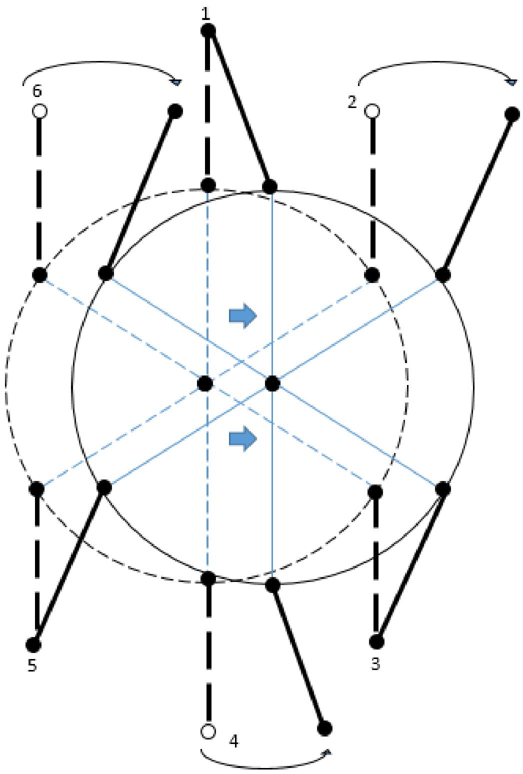

Figure 4.9: Illustration the First Moving Phase Configuration of the Hexapod According to the Insect Locomotion

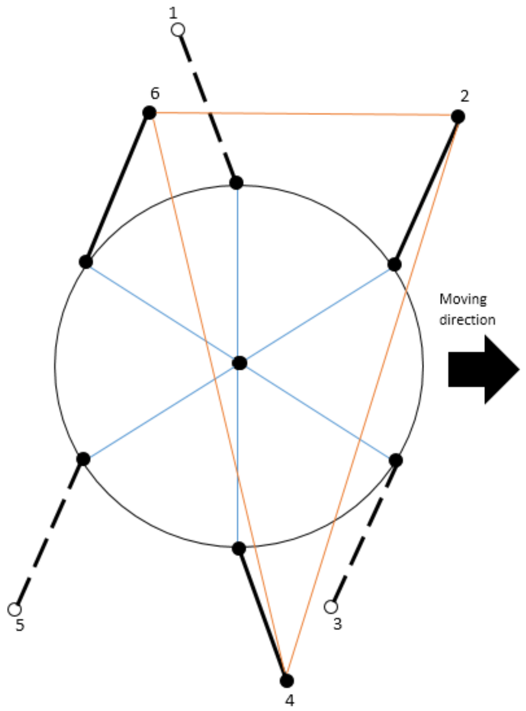

Figure 4.10: Illustration the Hexapod Structure and Supporting Polygon during the Second Phase According to the Insect Locomotion

Through this phase, the first supporting legs set adjusting their configuration symmetrically in order to push the body of the robot ahead, while the another set of legs swinging forward. Completing this step ensures that all the legs are on the ground.

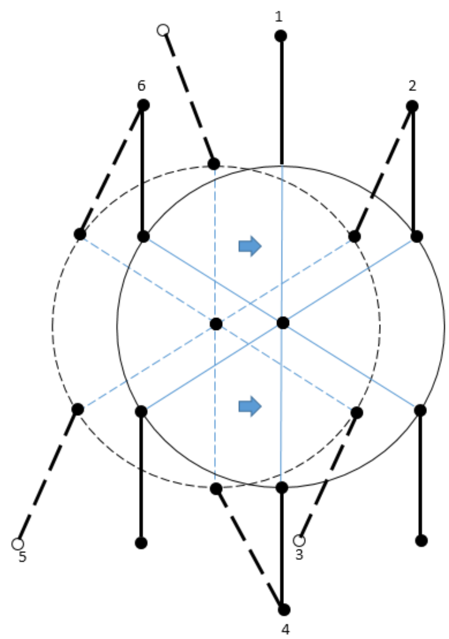

Figure 4.11: Illustration the Second Moving Phase Configuration of the Hexapod According to the Insect Locomotion

In figure 4.9 and figure 4.11 the dotted lines refer to the Hexapod configuration before the second moving phase starting, and the solid lines indicate to the Hexapod's structure after the end of this stage.

Chapter 5

KINEMATIC REPRESENTATION

5.1 Introduction

The kinematic survey of any mechanical structure or robotic texture demands a methodical technique can represent the framework of that construction. In this meaning, the topological representation of the kinematic structure places the Robot parts in a certain order by two main elements, the vertex, and the edge. Basically, this representation scheme aims to form a matrix structure gives advanced prospects of the controlling equalizations. To this end, assorted species have been suggested to build a kinematic graphs models. *Wittenburg* [56] was one of the first in this field, he proposed a methodical representation relevant to modeling a linkage of solid bodies through the graph. In [57] the mathematician Arczewski grants additions related to defining some special mechanical equipment as the springs and dampers. *Jain* was able to build on the graph representation to derive dynamic motion equations [58]. Networking technique representation [59] has been enormous investigated kinematically and dynamically by *Uyguroğlu M.K.* This survey included some 3-D mechanical system such as grinders and gears. Moreover, *Demirel H* and *Uyguroğlu M.K* introduced a new methodology [60] based on the direct and indirect graph in order to avoid the obstacles of both, this method named T-T graph. These research [61-64] were dedicated to analyze the velocity equations and define the mobility in the closed chains manipulator by using some techniques related to the theory of graph representation. In this chapter, the configurations and functionality of Hexapod robot will be studied in details kinematically through the theory of the graph representation.

5.2 Fundamental Concepts of Graph Theory

Mathematically, graphs are textures established by assembling two mathematical creatures called nodes and lines, in like manner, Graph theory is the area of knowledge that handles with the relevance among these two objects. The mentality of the physicists and logician *Leonhard Euler* must be mentioned when talking about the theory of graphs. He was the first recognized scientist publishes about one of the extremely difficult and confusing topology problems at that time famed as the bridges of *königsberg* [65]. Afterward, the mathematicians *Louis Cauchy Jean* and *Simon L'Huilier* were able to develop the Euler's formulas forming the basis of what is called today topological graph theory [66]. For the time being, graph representation theory becomes participatory in many engineering and medical science implementations. Moreover, evolving a new topological method, especially in the start of this century, had a considerable effectiveness on different sides of our modern science [67].

5.2.1 Fundamental Terminologies

Ordinarily, any graph representation specified using two collections of elements. The first set referred as vertices or nodes group so that it could be represented as $N = \{n_1, n_2, \dots\ n_i\}$. The second indicated as edges or lines set, it can be symbolized as $L = \{l_1, l_2, \dots\ l_i\}$. The previous two sets determine the graph representation as $G = \{N, L\}$. The subsequent terms are verified in the theory of graph representation [68].

- If the two vertices n_1 and n_2 that form the two ends of the line l are coincident with each other, then the line l forms a circuit or loop.
- The two lines l_1 and l_2 recognized as a parallel lines if they possess conformable two ending points.

- The term Null graph represents any graph that has no nodes in its structure.
- The term insignificant defines any graphs that has only one nodes in his structure.
- Any graph become empty if it doesn't have any line.
- The lines l_1 and l_2 are contiguous if exists a node connects between them
- Two nodes defined as adjacent if exists a line connects these two nodes.
- The number of lines that connects with a node n defined as the degree of n and indicated by $deg\ (n)$.
- Droopy node n is a node that has $deg\ (n)\ = 1$, by the same token, any line connects with a droopy node considered as droopy line.
- A node n that has zero degree defined as separate node.
- A set of lines C is considered as a subgraph of X if $C\ \in\ X$.
- Considering a graph X and two subgraphs of X, $C1$ and $C2$, If $X = C1\ \cup\ C2$ and $C1\ \cap\ C2 = 0$, then $C1$ and $C2$ are defined as consummated subgraphs.
- Any edge sequence could be considered as an edge train, if all edges in the sequence show for only once.
- If the two ends of the edge train are different, then the edge train called open edge train.
- The term path refers to the open edge train that internal nodes have degree equal to two.
- Connected graph refers to the graph that has a path passes through each two nodes.
- Any series of lines T belongs to the connected graph $X\ (N, L)$ that fulfill some requirements considered as a tree. These requirements include the following: the elements of T is connected, all the nodes in the graph are included in the T, there is no loop included in T and T has precisely $n - 1$ lines, where n refers to the

number of combined nodes. The remaining lines of X that are not in T form a set called co-tree.

- The term cut node refers to the set of lines $n \in X$ that satisfy the property: if l eliminated from the graph X, the resulting graph has combinations more than in the graph X.
- The graph X could be separated into two or more portions depending on the selected cut set.
- Consider the graph $X = (N, L)$ and the sequence of lines l belonging to the graph X. Then, l considered as a cut set if the resulting of $X - l$ gives precisely two detached parts.
- If the graph X consists of several parts, assuming that these parts are connected, consequently one tree is defined for each parts. The combination of all these trees forms the forest. The set of lines that are not belonging to the forest forms co-forest.
- Branches and chords refer to the lines that form the tree (forest) and co-tree (co-forest) respectively.
- The rank and the nullity are defined as the number of lines that shape the tree (forest) and co-tree (co-forest) respectively.
- In the domain of graph theory, the term spanning tree refers to the tree that has the least number of lines connected its nodes. Predominantly, diverse spanning trees exist in the connected graph. In case of the graph is disconnect, the term spanning forest uses instead of spanning tree.
- The definition of the spanning tree leads to the two essential terminologies, fundamental loop and fundamental cut-set. Considering a connected graph X and the spanning tree T belonging to X, depending on the chosen spanning tree T, each

line in the graph X that isn't member in the spanning tree T forms a circuit together with the path consists of a unique subset of lines belonging to the spanning tree T. This circuit or loop called fundamental loop. The definition of the fundamental loop clarify that the number of the fundamental loops are identical to the number of the nullity of the graph X. The fundamental cut-set refers to the special subset of the graph X that has only line belongs to the spanning tree T, in which if this subset is removed from the graph, the graph will divided into exactly two sections.

- In the domain of graph theory, the idiom directed graph indicates to the graph that possesses a directed lines. Each directed line specify the transmission between its two terminal nodes.
- Considering a directed graph $X = (N, L)$ has n nodes and l lines. In this case, the incident array R is defined as a matrix has $(n \times l)$ elements. The element $R_{x,y}$ equal to 1 or -1 if the directed line y coincident with the terminal x.
- In the directed graph, the definition circuit matrix refers to the matrix that relate between the edges of the graph and oriented circuits belonging to the graph. Considering the circuit matrix $C = [c_{(x,y)}]$, the element of C takes 1 if the edge y belonging to the circuit x and both have the same orientation, if they have opposite direction, $c_{(x,y)}$ takes -1. In the case the edge y doesn't belong to the circuit x, $c_{(x,y)}$ will takes 0.
- The word walk in the theory of graph indicates to the sequence of lines in which a sequence of nodes form a connections between these lines. The walk becomes a trail if all the lines duplicate at most for once. A walk turns out to be a path when the lines and nodes that form the walk visited once except the first and the last nodes. If the walk is close sequence, in this case the path is called circuit.

5.3 Functional Representation of the Hexapod Robot

The functional representation of the mechanism chain recognized as the schematic drawing of the mechanism in which all the elements of the robot drawing similar to their construction. Hence, only functional elements essential to the structure are shown. The following figure illustrates the functionality representation of the Hexapod robot.

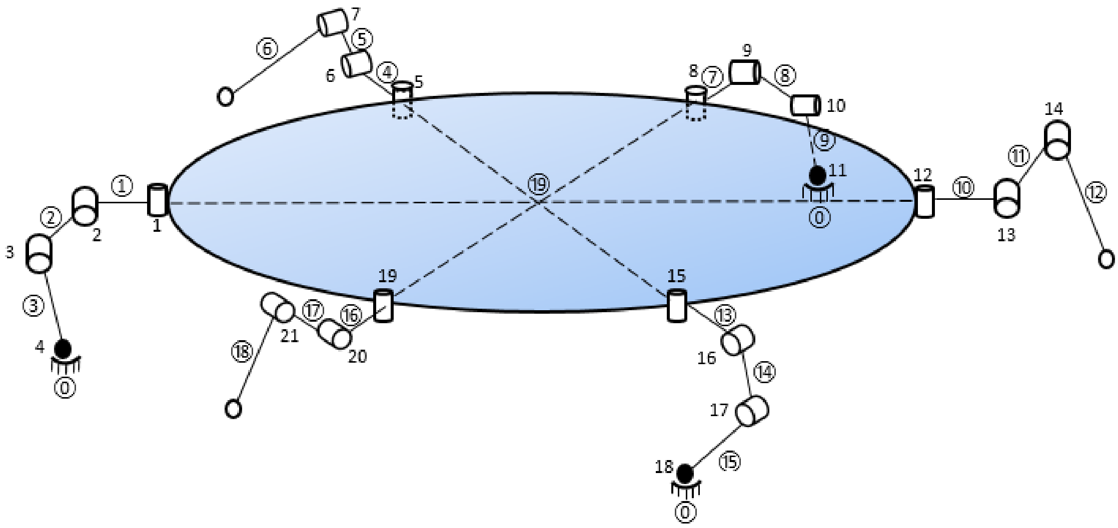

Figure 5.1: The Functionality of the Hexapod According to the Stable Tripod State

Figure 5.1 explains the functionality of the robot during some moving phase according to the stable 3+3 locomotion. In this case, the robot hexapod has 20 moving body and 21 joints. Here, the points of the legs that are touching the ground are considered as the universal joints due to the mobility analysis in the third chapter.

5.4 Graph Representation of the Hexapod Texture

The representation of any robot structure using the theory of graph aims to define the Robot's parts joints and links as elements belonging to the environment of the graph theory i.e. joints and links replaced by edges and vertices respectively. Generally, this graph named as the topological graph, and characterized by it possesses no directions in its structure. Sometimes, the topological graph referred as $\mathrm{T} = (V, E)$, so that V defines the group of all the vertices in the graph and E recognized as the group that includes all the edges. Moreover, this graph representation regarded as a simple because of there is only one edge pass throw any two vertices. In this notation, the variables n and m identified as the number of the joints and links respectively in which the joints will be listed as $i = 1 \ldots n$ while the links indicated as $j = 0 \ldots m - 1$. Subsequently, an arbitrary edge located in the topological graph will be defined as $e_i = (v_\alpha, v_\beta)$. The topological graphs have studied widely in [69]. Figure 5.2 describes the graph representation of the closed chains that formed by the Hexapod's leg that in contact with the terrain, the ground and the Hexapod's body.

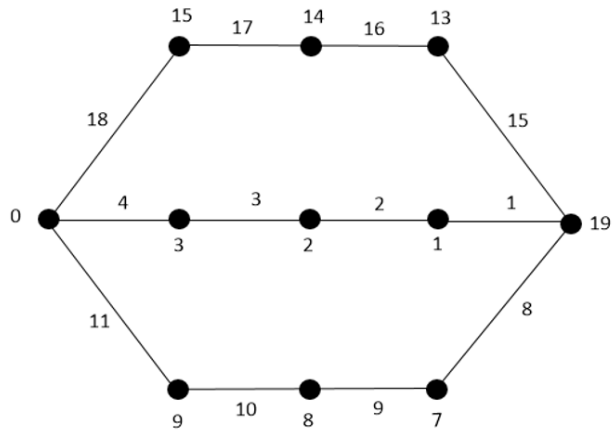

Figure 5.2: Topological Graph Representation of the Portion of the Hexapod Robot that Forms a Closed Chains Manipulator

It is noticeable that, since all the edged paths originating from the ground link have distinct edge labels, therefore the graph shown in figure 5.2 is regarded as a canonical graph.

5.5 Oriented Graph Representation of the Hexapod

In the theory of graph, the oriented topological graph recognized as the scheme that its edges specified by arrows in the sake of determining the steering motion through the kinematic joints that form the robot movement. Subsequently, if the edge $e_i = (v_\alpha, v_\beta)$ exists in the oriented graph that leads to the edge (v_β, v_α) is not resident in that graph. Moreover, consider the edge e_i that reside in the graph $\overrightarrow{T}$, in this case the link α known as the source and the link β defined as the head. The following figure illustrates the movement directions of the joints that exist in the figure 5.2

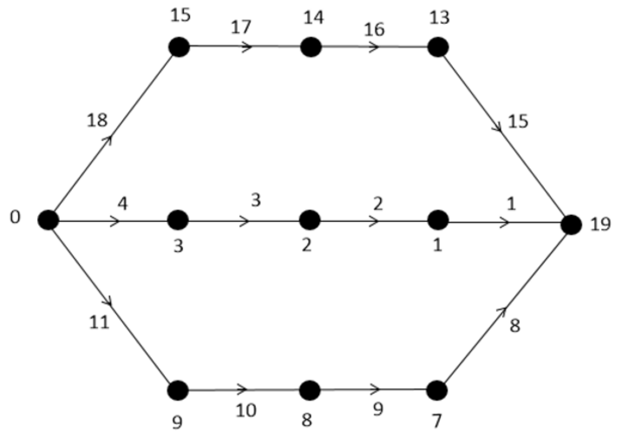

Figure 5.3: Oriented Topological Graph Representation of the Portion of the Hexapod Robot that Forms a Closed Chains Manipulator

5.6 The Predecessor Relevance of the Spanning Tree

Consider the definition of the spanning tree of the topological graph introduced in the second chapter. The configuration of this graph characterized as any two vertices possess only one trace passing each other. The spanning tree can be helpful in order to re-analysis the structure of the closed chains that formed by the three legs of the Hexapod. The spanning tree can be characterized as $ƌ = (V, E^{ƌ})$. The following figure clarifies a spanning tree related to the topology configuration of the closed chains that have been built by the structure of the three leg of the Hexapod that has a contact with the ground.

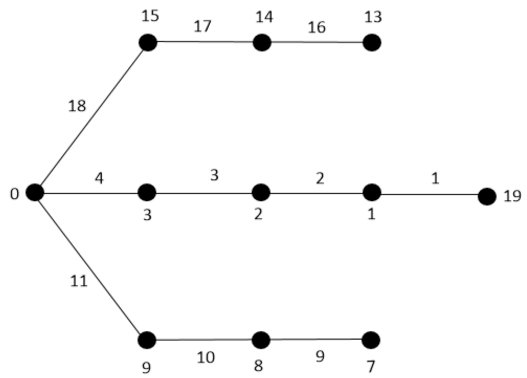

Figure 5.4: A Spanning Tree of the Portion of the Hexapod Robot that Forms a Closed Chains Manipulator

Kinematically, the ordering relevance between the components of the kinematic chains is extremely important in order to allocate the motion orientation. Hence, the importance of steering the edges of the spanning tree take place. Moreover, the direct root topological graph recognized as the topology that characterized by existing oriented trace came out from the fixed platform directed to all the vertices allocated in the graph. The subsequent graph shows the root-directed tree according to the spanning tree that explained in the figure 5.4. The term predecessor defined as the ordering relevance between two vertices belonging to the root-directed tree so that there is an oriented line passing through both of them.

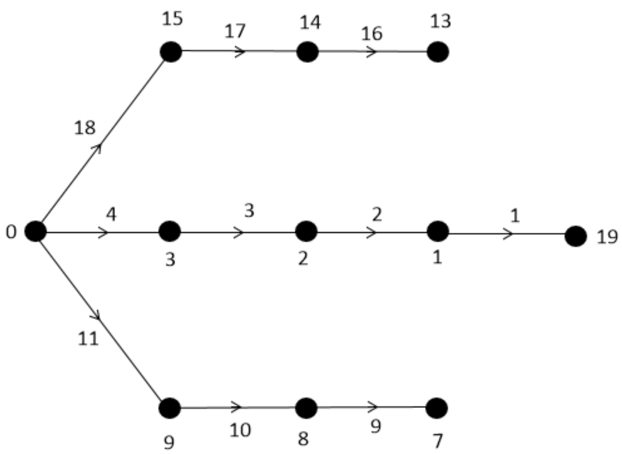

Figure 5.5: The Root-Directed Tree According to the Closed Chains Formed by the three Assistant Leg of the Hexapod

Consider the guided edges $\overrightarrow{e_{\imath 1}} = (v_\alpha, v_\beta)$ and $\overrightarrow{e_{\imath 2}} = (v_\beta, v_\gamma)$ are belonging to the root-directed tree. Then, the following properties are satisfied; it is possible to identify the edges as $v_\alpha = v_\beta - 1$ and $v_\beta = v_\gamma - 1$ according to the $\overrightarrow{e_{\imath 1}}$ and $\overrightarrow{e_{\imath 2}}$ respectively. Also, the predecessor relevance of the two mentioned edges as follows $e_{i1} = e_{i2} - 1$.

5.7 The Fundamental Cycle

According to the determination of the Fundamental loops that introduced in the second chapter, the root-directed tree that provided in the figure 5.5 possesses two co-tree edges so that each of them identify an essential loop. Through the following figure, the fundamental circuits $A8$ and $A15$ will be shown.

5.8 The Relationship between the Kinematics and the Graph Theory

As referenced in the kinematic section, any solid body can be symbolized using a uniform matrix. Basically, this matrix demonstrates the linkage between a system of coordinate installed on the body and the external reference system. Consequently, the relation among the body v_α and the reference system will be denoted as $T(v_\alpha)$. Moreover, take into the consideration a joint Ji relates two bodies v_α, v_β w ith each other. Also, suppose that the transmission direction of the joint Ji will be from the body v_β to v_α. Consequently, the relation between the bodies symbolized as $\overrightarrow{Ji}$ = (v_β, v_α). Hence, the joint $\overrightarrow{Ji}$ could be expressed as the following equation

$$D(Ji) = \left(T(v_\beta)\right)^{-1}.T(v_\alpha) \tag{5.1}$$

In equation (5.1), $D(Ji)$ represents the uniform transformation of the coordinate system that located at the body v_α with respect to the coordinate that existing on the body v_β.

The plurality of kinematic techniques handle the joints as a set of a 1-DOF revolute or translation joint in order to simplify the analysis. However, the screw vector can model these type of joints easily. Then, the joint configuration $D(Ji)$ can be given as

$$D(Ji) = \exp([\$], \theta i) \tag{5.2}$$

5.8.1 The Configurations of the Kinematic Structure

As discussed earlier, the determination of the consecutive relation of the motion directions through the joints is a critical objective to find out the configuration of a body belongs to that mechanism. However, through the theory of graph, it is possible to identify any Link's configuration by observing the differences between the oriented topological graph and the root-directed tree. Let the variable $\varrho(i)$ indicates to the configuration of the joint i. Consequently, there are three distinct cases for an arbitrary joint (v_β, v_α) that belongs to the oriented topological graph. The first state occurs when the joint (v_β, v_α) belongs to all of the directed topological graph and the root-directed tree. In this case, the variable $\varrho((v_\beta, v_\alpha))$ substituted by 1. The second situation arises when the joint (v_β, v_α) belongs to directed topological graph and (v_α, v_β) belongs to the root-directed graph. Then, the variable $\varrho((v_\beta, v_\alpha))$ replaced by -1. Lastly, when the joint (v_β, v_α) existing only in the directed topology graph. Hence, $\varrho((v_\beta, v_\alpha))$ will be zero.

According to the discussion above, the equation (5.2) can turn into a more formal form depending on the variable $\varrho(i)$.

$$D(Ji) = \exp(\varrho(Ji).([\$], \theta i)) \tag{5.3}$$

Moreover, we can derive any Body's configuration $T(v_\alpha)$ according to the equation (5.3) as follow

$$T(v_\alpha) = D(Jr). \dots\ D(Ji-1). D(Ji) \quad (5.4)$$

As an example with regards to the structure of the Hexapod robot. It is possible to define the configuration of the moving platform body 19 due to the root directed tree and the oriented topological graph that was shown in figures 5.3 and 5.5

$$T(19) = D(4). D(3). D(2). D(1) \quad (5.5)$$

Supposing that the joint that characterizes the point contact of the Hexapod's leg with the ground modeled as a 1-dof joint. Then, the equation 5.5 could be expanded as follow.

$$T(19) = \exp([\$4], \theta 4)). \exp([\$3], \theta 3)). \exp([\$2], \theta 2)). \exp([\$1], \theta 1)) \quad (5.6)$$

5.9 Kinematic Restraints

In kinematics, the analyzing of the closed loops manipulators considered as one of the enormously problematic issues due to the dependencies between the loops and because of existence high ordered passive joints. However, the theory of graph involves several techniques can be helpful to solve these complications. The cut body and cut joints methods can make a difference in the way of handling the parallel manipulator.

5.9.1 The Cut Joint Methodology

Supposing that the fundamental circuit $A15$ that was shown in Figure 5.6. This circuit consists of two open kinematic chains in addition to the co-tree joint $J(13,19)$. Hence, the joint $J15$ is handled as an eliminated joint and discarded from the fundamental circuit $A15$. Subsequently, a system of restraint is shaped due to the eliminated joint $J15$ as following

$$u15(13,19) = 0 \quad (5.7)$$

In this case, it is possible to define the links 13 and 19 by applying the equation (5.4) provided that all the joint that award the configuration of the links are composed of low kinematic pairs.

$$T(13) = D(18).D(17).D(16)$$
$$T(19) = D(4).D(3).D(2).D(1) \quad (5.8)$$

Thereafter, the equations (5.7) and (5.8) will define the kinematic constraints of the fundamental circuit $A15$ [42]. This methodology can be extremely valuable in the case of existing only one high ordered joint in each closed kinematic loop.

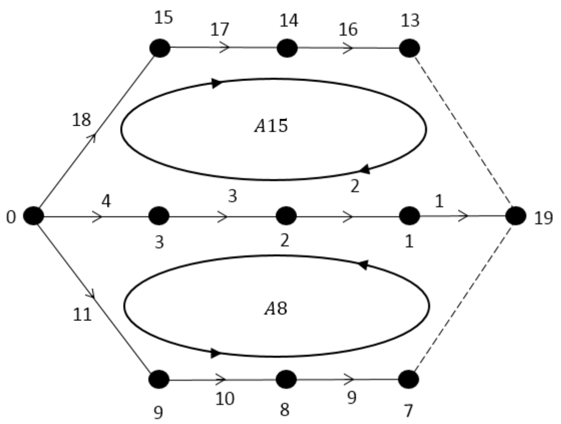

Figure 5.6: Fundamental Circuits Corresponding to the Root Directed Tree

5.9.2 The Cut Body Method

As a replacement of rejecting the Fundamental Loop’s chord, this tactic handles with the whole loop including the cut joint as a locked kinematic series. In this methodology, identifying a uniformity function to label the joints are needed in order to form the restricted system for each closed loop. Hence, the mentioned function will be defined due to the alignment of the Joint’s direction in the directed root spanning tree and the Fundamental circuit. Subsequently, if the mentioned directions are identical the alignment function $6(Ji)$ of the joint i has a value equal to one. In contrast, if the directions are opposed. Then, the function $6(Ji)$ has -1 value.

According to the structure of the Hexapod that represents three legs touching the ground, the Figure 5.6 exemplifies the Fundamental circuits $A15$ and $A8$ corresponding to the root directed tree. Subsequently, the assembling in A_{15}, for example, is as follows $1 <_{15} 2 <_{15} 3 <_{15} 4 <_{15} 18 <_{15} 17 <_{15} 16 <_{15} 15$. Then, the Sequential arrangement of the relation of all the joints in the fundamental cycle leads to the closing state for A_i.

$$F_i = \begin{bmatrix} 1 & 0 & 0 & 0 \\ 0 & 1 & 0 & 0 \\ 0 & 0 & 1 & 0 \\ 0 & 0 & 0 & 1 \end{bmatrix} \tag{5.9}$$

Where F_i in the equation (5.9) for the sequence of joints $m <_i \ldots <_i i$ is given as follows

$$F_i = exp(\varrho(m).([\$m], \theta m). \ldots . exp(\varrho(i).([\$i], \theta i) \tag{5.10}$$

According to the Figure 5.6 the system of loop restrictions for the fundamental cycles $A15$ and $A8$ is given due to the equation (5.9) and (5.10) as following

$$F_{15} = I_{4\times4} , F_8 = I_{4\times4} \tag{5.11}$$

Where

$$\begin{gathered} F_{15} = \mathrm{D}(1)^{-1}.\mathrm{D}(2)^{-1}.\mathrm{D}(3)^{-1}.\mathrm{D}(4)^{-1}.\mathrm{D}(18).\mathrm{D}(17).\mathrm{D}(16).\mathrm{D}(15) \\ F_8 = \mathrm{D}(1)^{-1}.\mathrm{D}(2)^{-1}.\mathrm{D}(3)^{-1}.\mathrm{D}(4)^{-1}.\mathrm{D}(11).\mathrm{D}(10).\mathrm{D}(9).\mathrm{D}(8) \end{gathered} \tag{5.12}$$

In equation (5.12) $\mathrm{D}(i)$ represents the configuration of the joint i that should be possess only 1 degree of freedom.

Chapter 6

CONCLUSION AND FUTURE WORK

6.1 Conclusion

The integration process between the Kinematics and Locomotion analysis is an indispensable element when investigating the Legged Robots so that giving accurate sequences of joint's movements that capable of accomplishing the Robot's tasks may be done correctly only by knowing the kinetic structure and conducting the appropriate kinematic analysis. In this Thesis, an overall kinematic analysis includes dealing with the problem of the hexapod’s single leg via geometric approach, (D-H) convention and the theory of screws. It is noticeable that, despite the importance of the (D-H) convention, the screw theory demonstrates ease in application, implementation and extraction of results. Moreover, the geometric approach cannot be dispensed with because of its importance in achieving the Hexapod’s inverse kinematics. This dissertation also demonstrates a new vectorial technique to hold the direct kinematics using the product of exponential method and some techniques related to the parallel manipulator analysis. Besides, the process of finding the inverse kinematics is implemented using the geometry-based approach. Furthermore, a comparison process to find the mobility of the Hexapod between the conventional method and the reciprocity-based method shows the superiority of the second one in terms of their ability to predict the way of movement. Also, the screw theory utilizes in this thesis in order to perform the velocity analysis of the hexagonal Hexapod structure with the full assistance of the reciprocal theory.

The Hexapod's locomotion analysis and the stabilization edge discussed and implemented during a full working cycle regarding two essential Mobile Robot's gait which are the insect and the mammal locomotion. Furthermore, the relationship between the Hexapod architecture and the graph theory illustrated using some issues related to the network model approach aiming to build a kinetic representation of the Hexapod's construction.

6.2 Future Work

In this thesis, several hypotheses imposed aiming to carry out the kinematic survey of the Hexapod on the basis that it is a symmetric manipulator in term of kinetics, but the truth is slightly different. When the Hexapod starts moving, the Robot's body must lose three degrees of freedom in order keep the robot in kinetic symmetry. This means that the robot must walk parallel to the ground. However, in order to perform certain tasks, such as crossing obstacles and walking on the slopes, we must handle the Hexapod as an asymmetrical robot. Subsequently, the kinematic modeling of the Hexapod without limitations will be the focus of future work.

REFERENCES

[1] Arena, P., Fortuna, L., Frasca, M., Patané, L., & Pavone, M. (2005, May). Climbing obstacles via bio-inspired CNN-CPG and adaptive attitude control. In *Circuits and Systems, 2005. ISCAS 2005. IEEE International Symposium on* (pp. 5214-5217). IEEE.

[2] Cho, J., Park, S., & Kim, K. (2014). Design of mechanical stiffness switch for hydraulic quadruped robot legs inspired by equine distal forelimb. *Electronics Letters, 51*(1), 33-35.

[3] Morgansen, K. A., Triplett, B. I., & Klein, D. J. (2007). Geometric methods for modeling and control of free-swimming fin-actuated underwater vehicles. *IEEE Transactions on Robotics*, *23*(6), 1184-1199.

[4] Celaya, E., & Porta, J. M. (1998). A control structure for the locomotion of a legged robot on difficult terrain. *IEEE Robotics & Automation Magazine*, *5*(2), 43-51.

[5] Clemente, D. C. (2011). *Gait Optimization for Multi-legged Walking Robots, with Application to a Lunar Hexapod*. Stanford University.

[6] Yi, S. J., McGill, S. G., Zhang, B. T., Hong, D., & Lee, D. D. (2012, November). Active stabilization of a humanoid robot for real-time imitation of a human operator. In *Humanoid Robots (Humanoids), 2012 12th IEEE-RAS International Conference on* (pp. 761-766). IEEE.

[7] Grimaldi, D. A. (2010). 400 million years on six legs: on the origin and early evolution of Hexapoda. *Arthropod structure & development*, *39*(2), 191-203.

[8] Nonami, K., Barai, R. K., Irawan, A., & Daud, M. R. (2014). *Hydraulically actuated hexapod robots* (pp. 78-104). Springer: London, UK.

[9] Tedeschi, F., & Carbone, G. (2014). Design issues for hexapod walking robots. *Robotics*, *3*(2), 181-206.

[10] Yang, J. M., & Kim, J. H. (1999). Optimal fault tolerant gait sequence of the hexapod robot with overlapping reachable areas and crab walking. *IEEE Transactions on Systems, Man, and Cybernetics-Part A: Systems and Humans*, *29*(2), 224-235.

[11] Raibert, M. H. (1986). *Legged robots that balance*. MIT press.

[12] Petternella, M., & Salinari, S. (1973). Simulation by digital computer of walking machine control system. In *IFAC, IIC, and ANIPLA, Symposium on Automatic Control in Space, 5 Th, Genoa, Italy*.

[13] Okhotsimski, D. E., & Platonov, A. K. (1973, August). Control algorithm of the walker climbing over obstacles. In *Proceedings of the 3rd international joint conference on Artificial intelligence* (pp. 317-323). Morgan Kaufmann Publishers Inc.

[14] Devjanin, E. A., Gurfinkel, V. S., Gurfinkel, E. V., Kartashev, V. A., Lensky, A. V., Shneider, A. Y., & Shtilman, L. G. (1983). The six-legged walking robot capable of terrain adaptation. *Mechanism and Machine Theory*, *18*(4), 257-260.

[15] McGhee, R. B. (1977, December). Control of legged locomotion systems. In *Proceedings of the 18th Automatic Control Conference, San Francisco, CA, USA* (Vol. 38, p. 205215).

[16] Byrd, J. S., & DeVries, K. R. (1990). A six-legged telerobot for nuclear applications development. *The International Journal of Robotics Research*, *9*(2), 43-52.

[17] Nelson, G. M., Quinn, R. D., Bachmann, R. J., Flannigan, W. C., Ritzmann, R. E., & Watson, J. T. (1997, April). Design and simulation of a cockroach-like hexapod robot. In *Robotics and Automation, 1997. Proceedings. 1997 IEEE International Conference on* (Vol. 2, pp. 1106-1111). IEEE.

[18] Roennau, A., Heppner, G., Pfotzer, L., & Dillmann, R. (2013, July). Lauron V: Optimized leg configuration for the design of a bio-inspired walking robot. In *Proc. Conference on Climbing and Walking Robots (CLAWAR)*.

[19] Lewinger, W. A., Branicky, M. S., & Quinn, R. D. (2006). Insect-inspired, actively compliant hexapod capable of object manipulation. *Climbing and Walking Robots*, 65-72.

[20] Saunders, A., Goldman, D. I., Full, R. J., & Buehler, M. (2006, May). The rise climbing robot: body and leg design. In *Defense and Security Symposium* (pp. 623017-623017). International Society for Optics and Photonics.

[21] Hauser, K., Bretl, T., Latombe, J. C., Harada, K., & Wilcox, B. (2008). Motion planning for legged robots on varied terrain. *The International Journal of Robotics Research*, *27*(11-12), 1325-1349.

[22] Kang, H., Shim, H., Jun, B. H., & Lee, P. M. (2011). Design of Underwater Link and Joint for the Development of Multi-Legged Underwater Robot CR200. *Proc. of MTS/IEEE Oceans*.

[23] Roy, S. S., Singh, A. K., & Pratihar, D. K. (2009). Analysis of six-legged walking robots. In *Proceedings of the forteenth national conference on machine and mechanisms (NaCoMM-2009), Durgapur, India* (pp. 259-65).

[24] Chu, S. K., & Pang, G. H. (2002). Comparison between different models of hexapod robot in fault-tolerant gait. *IEEE Transactions on Systems, Man, and Cybernetics-Part A: Systems and Humans*, *32*(6), 752-756.

[25] Preumont, A., Alexandre, P., & Ghuys, D. (1991, June). Gait analysis and implementation of a six leg walking machine. In *Advanced Robotics, 1991.'Robots in Unstructured Environments', 91 ICAR. Fifth International Conference on* (pp. 941-945). IEEE.

[26] Takahashi, Y., Arai, T., Mae, Y., Inoue, K., & Koyachi, N. (2000). Development of multi-limb robot with omnidirectional manipulability and mobility. In *Intelligent Robots and Systems, 2000. (IROS 2000). Proceedings. 2000 IEEE/RSJ International Conference on* (Vol. 3, pp. 2012-2017). IEEE.

[27] Tsai, L. W. (1999). *Robot analysis: the mechanics of serial and parallel manipulators*. John Wiley & Sons.

[28] Murray, R. M., Li, Z., Sastry, S. S., & Sastry, S. S. (1994). *A mathematical introduction to robotic manipulation*. CRC press.

[29] Rocha, C. R., Tonetto, C. P., & Dias, A. (2011). A comparison between the Denavit–Hartenberg and the screw-based methods used in kinematic modeling of robot manipulators. *Robotics and Computer-Integrated Manufacturing*, *27*(4), 723-728.

[30] Hartenberg, R. S., & Denavit, J. (1955). A kinematic notation for lower pair mechanisms based on matrices. *Journal of applied mechanics*, *77*(2), 215-221.

[31] Ohwovoriole, M. S., & Roth, B. (1981). An extension of screw theory. *ASME J. Mech. Des*, *103*(4), 725-735.

[32] Davidson, J. K., & Hunt, K. H. (2004). *Robots and screw theory: applications of kinematics and statics to robotics*. Oxford University Press on Demand.

[33] Dimentberg, F. M. E. (1968). *The screw calculus and its applications in mechanics* (No. FTD-HT-23-1632-67). FOREIGN TECHNOLOGY DIV WRIGHT-PATTERSONAFB OH.

[34] Rodrigues' rotation formula (2017). In *Wikipedia*. Retrieved from https://en.wikipedia.org/wiki/Rodrigues%27_rotation_formula

[35] Tsai, L. W., & Roth, B. (1972). Design of dyads with helical, cylindrical, spherical, revolute and prismatic joints. *Mechanism and Machine Theory*, *7*(1), 85-102.

[36] Plücker coordinates (2017). In *Wikipedia*. Retrieved from https://en.wikipedia.org/wiki/Pl%C3%BCcker_coordinates

[37] Ball, R. S. (1998). *A Treatise on the Theory of Screws*. Cambridge university press.

[38] Screw theory (2016). In *Wikipedia*. Retrieved from https://en.wikipedia.org/wiki/Screw_theory

[39] Park, F. C., & Lynch, K. (2012). Introduction to Robotics: Mechanics, Planning, and Control.

[40] Jacobian matrix and determinant (2017). In *Wikipedia*. Retrieved from https://en.wikipedia.org/wiki/Jacobian_matrix_and_determinant#Jacobian_matrix

[41] Mohamed, M. G., & Duffy, J. (1985). A direct determination of the instantaneous kinematics of fully parallel robot manipulators. *Journal of mechanisms, transmissions, and automation in design*, *107*(2), 226-229.

[42] Arabyan, A., & Wu, F. (1998). An improved formulation for constrained mechanical systems. *Multibody System Dynamics*, *2*(1), 49-69.

[43] Tsai, L. W. (1998). The Jacobian analysis of a parallel manipulator using reciprocal screws. In *Advances in Robot Kinematics: Analysis and Control* (pp. 327-336). Springer Netherlands.

[44] Zhao, J., Li, B., Yang, X., & Yu, H. (2009). Geometrical method to determine the reciprocal screws and applications to parallel manipulators. *Robotica*, *27*(06), 929-940.

[45] Chebychev–Grübler–Kutzbach criterion (2016). In *Wikipedia*. Retrieved from https://en.wikipedia.org/wiki/Chebychev%E2%80%93Gr%C3%BCbler%E2%80%93Kutzbach_criterion

[46] Rovetta, A., & Paul, E. C. (2004). New robot concept for Mars soil exploration: Mechanics and functionality. *ASTRA*, 2-4.

[47] Xilun, X. K. D. (2013). Typical gait analysis of a six-legged robot in the context of metamorphic mechanism theory. *Chinese Journal of Mechanical Engineering*, *26*(4), 1.

[48] Ding, X., & Yang, F. (2016). Study on hexapod robot manipulation using legs. *Robotica*, *34*(02), 468-481.

[49] Wang, Z. Y., Ding, X. L., & Rovetta, A. (2010). Analysis of typical locomotion of a symmetric hexapod robot. *Robotica*, *28*(06), 893-907.

[50] Sandoval-Castro, X. Y., Garcia-Murillo, M., Perez-Resendiz, L. A., & Castillo-Castañeda, E. (2013). Kinematics of hex-piderix-a six-legged robot-using screw theory. *International Journal of Advanced Robotic Systems*, *10*(1), 19.

[51] Dai, J. S., Zoppi, M., & Kong, X. (2012). *Advances in reconfigurable mechanisms and Robots I*. Springer.

[52] Ding, X. L., & XU, K. (2009). Design and analysis of a novel metamorphic wheel-legged rover mechanism [J]. *Journal of Central South University (Science and Technology)*, *40*(1), 91-101.

[53] Lee, T. T., Liao, C. M., & Chen, T. K. (1988). On the stability properties of hexapod tripod gait. *IEEE Journal on Robotics and Automation*, *4*(4), 427-434.

[54] Kwak, S. H. (1986). *A computer simulation study of a free gait motion coordination algorithm for rough-terrain locomotion by a hexapod walking machine* (Doctoral dissertation, The Ohio State University).

[55] Eslami, S. M. (2009). Evolving Robust Control Strategies for Simulated Animats.

[56] Wittenburg, J. Dynamics of Systems of Rigid Bodies. 1977, BG Teubner.

[57] Arczewski, K. (1992). Graph theoretical approach—II. Determination of generalized forces fora class of systems consisting of particles and springs. *Journal of the Franklin Institute*, *329*(3), 483-491.

[58] Jain, A. (2011). Graph theoretic foundations of multibody dynamics. *Multibody system dynamics*, *26*(3), 307-333.

[59] Uyguroğlu, M. K. (1998). *The Network Model Approach to the Kinematic and Dynamic Analysis of the Three Dimensional Mechanical Systems*. Eastern Mediterranean University.

[60] Uyguroğlu, M., & Demirel, H. (2005). TSAI–TOKAD (T–T) graph: the combination of non-oriented and oriented graphs for the kinematics of articulated gear mechanisms. *Meccanica*, *40*(3), 223-232.

[61] Simoni, R., Doria, C. M., & Martins, D. (2013). Symmetry and invariants of kinematic chains and parallel manipulators. *Robotica*, *31*(01), 61-70.

[62] Wohlhart, K. (2004). Screw spaces and connectivities in multiloop linkages. In *On Advances in Robot Kinematics* (pp. 97-104). Springer Netherlands.

[63] Davies, T. H. (2015). A network approach to mechanisms and machines: Some lessons learned. *Mechanism and Machine Theory*, *89*, 14-27

[64] Kim, H. S., & Tsai, L. W. (2002). Evaluation of a Cartesian parallel manipulator. In *Advances in robot kinematics* (pp. 21-28). Springer Netherlands.

[65] Gribkovskaia, I., Halskau, Ø., & Laporte, G. (2007). The bridges of Königsberg—a historical perspective. *Networks*, *49*(3), 199-203.

[66] Biggs, N., Lloyd, E. K., & Wilson, R. J. (1976). *Graph Theory, 1736-1936*. Oxford University Press.

[67] Biggs, N., Biggs, N. L., Biggs, N. L., & Biggs, N. L. (1974). *Algebraic graph theory* (Vol. 2). Cambridge: Cambridge university press.

[68] Uyguroğlu, M.K., EE 529-Circuits and Systems: Graduate course in Electrical Engineering, EMU University, Department of Electrical and Electronic Engineering, TRNC-Turkey: 3 Credit Hours.

[69] Carricato, M., & Parenti-Castelli, V. (2002). Singularity-free fully-isotropic translational parallel mechanisms. *The International Journal of Robotics Research*, *21*(2), 161-174.

APPENDICES

Appendix A: Position Analysis of a Duty Cycle According to the Mammal Locomotion for the Hexapod Robot (Matlab)

```
function mammallocomotion
% the lengths of the Leg's links and the Radios
l1=1; l2=1; l3=1; r=1;
% supporting legs analysis
% the first supporting leg, leg 1
% the Joint's variables, during this phase, all are zero
t1=0; t2=0; t3=0;
% the intial configuration of the first leg H1 WRT F1
gf1h10=[1 0 0 0;0 1 0 -l1;0 0 1 l2+l3;0 0 0 1];
% the configuration of the screw axes
w1=[1 0 0]; w2=[1 0 0]; w3=[1 0 0];
q1=[0 0 0]; q2=[0 0 l3]; q3=[0 0 l3+l2];
% the matrices that expresses the screws of the first leg
s1=poe(w1,q1);s2=poe(w2,q2);s3=poe(w3,q3);
% applying the product of exponential to obtain H1 WRT F1
gf1h1=expm(s1*t3)*expm(s2*t2)*expm(s3*t1)*gf1h10
% getting the frame F1 WRT global frame
T0f1=[1 0 0 0;0 1 0 r+l1;0 0 1 0;0 0 0 1];
% getting the frame H1 WRT global frame
g0h1=T0f1*gf1h1;
% getting the position of H1 and F1 WRT global frame
pof1=T0f1(1:3,4);  poh1=g0h1(1:3,4);
% second supporting leg 'leg3' %%%
% the intial configuration of the second supporting leg
H3 WRT F3
gf3h30=[1 0 0 0;0 1 0 l1;0 0 1 l2+l3;0 0 0 1];
% the configuration of the screw axes
w1=[1 0 0]; w2=[1 0 0]; w3=[1 0 0];
q1=[0 0 0]; q2=[0 0 l3]; q3=[0 0 l3+l2];
% the matrices that expresses the screws of the first leg
s1=poe(w1,q1);s2=poe(w2,q2);s3=poe(w3,q3);
% applying the product of exponential to obtain H3 WRT F3
gf3h3=expm(s1*t3)*expm(s2*t2)*expm(s3*t1)*gf3h30
% getting the frame F3 WRT global frame
T0f3=[1 0 0 r*cos(pi/6);0 1 0 (-r*sin(pi/6))-l1;0 0 1 0;0
0 0 1];
% getting the frame H3 WRT global frame
g0h3=T0f3*gf3h3;
% getting the position of H3 and F3 WRT global frame
pof3=T0f3(1:3,4); poh3=g0h3(1:3,4);
% the third supporting leg, leg 5
% the intial configuration of the third supporting leg H5
WRT F5
gf5h50=[1 0 0 0;0 1 0 l1;0 0 1 l2+l3;0 0 0 1];
% the configuration of the screw axes
```

```
w1=[1 0 0]; w2=[1 0 0];w3=[1 0 0];
q1=[0 0 0]; q2=[0 0 l3]; q3=[0 0 l3+l2];
% the matrices that expresses the screws of the first leg
s1=poe(w1,q1);s2=poe(w2,q2);s3=poe(w3,q3);
% applying the product of exponential to obtain H5 WRT F5
gf5h5=expm(s1*t3)*expm(s2*t2)*expm(s3*t1)*gf5h50
% getting the frame F5 WRT global frame
T0f5=[1 0 0 r*cos(5*pi/6);0 1 0 (-r*sin(5*pi/6))-l1;0 0 1
0;0 0 0 1];
% getting the frame H5 WRT global frame
g0h5=T0f5*gf5h5;
% getting the position of H3 and F3 WRT global frame
pof5=T0f5(1:3,4); poh5=g0h5(1:3,4);
% finding the configuration of mass center WRT global
frame
% verifying technique
n1=(poh1(1,1)-poh3(1,1)).^2;  n2=(poh1(2,1)-
poh3(2,1)).^2;
n3=(poh1(3,1)-poh3(3,1)).^2;  k1=sqrt(n1+n2+n3)
n4=(poh1(1,1)-poh5(1,1)).^2;  n5=(poh1(2,1)-
poh5(2,1)).^2;
n6=(poh1(3,1)-poh5(3,1)).^2;  k2=sqrt(n4+n5+n6)
n7=(poh1(1,1)-poh5(1,1)).^2;  n8=(poh1(2,1)-
poh5(2,1)).^2;
n9=(poh1(3,1)-poh5(3,1)).^2;  k3=sqrt(n7+n8+n9);
k=sqrt(3)*r;
if k1==k2 && k2==k3  disp('the centroid is found')
% finding the position of the centroid
cx=(poh1(1,1)+poh3(1,1)+poh5(1,1))/3;
cy=(poh1(2,1)+poh3(2,1)+poh5(2,1))/3;
cz=(poh1(3,1)+poh3(3,1)+poh5(3,1))/3;
poc=[cx;cy;cz];
% finding the orientation of the centroid WRT global
frame
vy=(poh1(1:3,1)-poc(1:3,1));
vy=vy(1:3,1)/sqrt(vy(1,1)^2+vy(2,1)^2+vy(3,1)^2);
vx=(poh3(1:3,1)-poh5(1:3,1));
vx=vx/sqrt(vx(1,1)^2+vx(2,1)^2+vx(3,1)^2);
vz=cross(vx,vy);
% drawing the position of H1,H3,H5 WRT global frame
drawpos(poh1,poh3,poh5,4)
% drawing the position of F1,F3,F5 WRT global frame
drawpos(pof1,pof3,pof5,3)
% drawing the position CENTER OF MASS WRT global frame
poc=[cx cy cz];
starts = zeros(3,3);ends = [poc; 0 0 0; 0 0 0];
quiver3(starts(:,1), starts(:,1), starts(:,1), ends(:,1),
ends(:,2), ends(:,3), 'black')
else disp('something went wrong')
end
% the first swingin leg, leg'2'
```

```
% the intial configuration of the first leg H2 WRT F2
gh2f20=[1 0 0 0;0 1 0 l1;0 0 1 -(l2+l3);0 0 0 1];
% the configuration of the screw axes
w1=[1 0 0]; w2=[1 0 0];
q1=[0 l1 0]; q2=[0 l1 -l2];
% the matrices that expresses the screws of the leg 2
s1=poe(w1,q1);s2=poe(w2,q2);
% applying the product of exponential to obtain F2 WRT H2
gh2f2=expm(t1*s1)*expm(t2*s2)*gh2f20;
% the relation between the centroid frame and H2 frame
gch2=[1 0 0 r*cos(pi/6);0 1 0 r*sin(pi/6);0 0 1 0;0 0 0
1];
% the relation between the centroid frame and the global
frame
g0c= [1 0 0 0;0 1 0 0;0 0 1 2;0 0 0 1];
% getting the frame F2 wrt global reference frame.
g0f2= g0c*gch2*gh2f2;pof2=g0f2(1:3,4);
% getting the position of H2 wrt global reference frame.
g0h2=g0c*gch2; p0h2=g0h2(1:3,4);
% the second swingin leg, leg'4'
% the intial configuration of the first leg H4 WRT F4
gh4f40=[1 0 0 0;0 1 0 -l1;0 0 1 -l2-l3;0 0 0 1];
% the configuration of the screw axes
w1=[1 0 0]; w2=[1 0 0];
q1=[0 -l1 0];q2=[0 -l1 -l2];
% the matrices that expresses the screws of the leg 4
s1=poe(w1,q1);s2=poe(w2,q2);
% applying the product of exponential to obtain F4 WRT H4
gh4f4=expm(t1*s1)*expm(t2*s2)*gh4f40;
% the relation between the centroid frame and H4 frame
gch4=[1 0 0 0;0 1 0 -r;0 0 1 0;0 0 0 1];
% getting the frame F4 wrt global reference frame.
g0f4=g0c*gch4*gh4f4;pof4=g0f4(1:3,4);
% getting the position of H4 wrt global reference frame.
g0h4=g0c*gch4; p0h4=g0h4(1:3,4);
% the third swingin leg, leg'6'
% the intial configuration of the first leg H6 WRT F6
gh6f60=[1 0 0 0;0 1 0 l1;0 0 1 -l2-l3;0 0 0 1];
% the configuration of the screw axes
w1=[1 0 0];w2=[1 0 0];q1=[0 l1 0];q2=[0 l1 -l2];
% the matrices that expresses the screws of the leg 6
s1=poe(w1,q1);s2=poe(w2,q2);
% applying the product of exponential to obtain F6 WRT H6
gh6f6=expm(t1*s1)*expm(t2*s2)*gh6f60
% the relation between the centroid frame and H6 frame
gch6=[1 0 0 -r*cos(pi/6);0 1 0 r*sin(pi/6); 0 0 1 0;0 0 0
1];
% getting the frame F6 wrt global reference frame.
g0f6=g0c*gch6*gh6f6;pof6=g0f6(1:3,4);
% getting the position of H6 wrt global reference frame.
g0h6=g0c*gch6;p0h6=g0h6(1:3,4);
```

```
% drawing the position of F2,F4,F6 WRT global frame
drawpos(pof2,pof4,pof6,2);
% drawing the position of H2,H4,H6 WRT global frame
drawpos(p0h2,p0h4,p0h6,1);

%%%%%% first moving stage
clear all;
figure;
% the lengths of the Leg's links and the Radios
l1=1; l2=1; l3=1; r=1;
% supporting legs analysis
% the first supporting leg, leg 1
% the Joint's variables, during this phase
t1in=-pi/6; t2in=0;
t1=-t1in;t2=-t2in;t3=t1in+t2in;
% the intial configuration of the first leg H1 WRT F1
gf1h10=[1 0 0 0;0 1 0 -l1;0 0 1 l2+l3;0 0 0 1];
% the configuration of the screw axes
w1=[1 0 0];w2=[1 0 0];w3=[1 0 0];
q1=[0 0 0];q2=[0 0 l3];q3=[0 0 l3+l2];
% the matrices that expresses the screws of the first leg
s1=poe(w1,q1);s2=poe(w2,q2);s3=poe(w3,q3);
% applying the product of exponential to obtain H1 WRT F1
gf1h1=expm(s1*t3)*expm(s2*t2)*expm(s3*t1)*gf1h10
% getting the frame F1 WRT global frame
T0f1=[1 0 0 0;0 1 0 r+l1;0 0 1 0;0 0 0 1];
% getting the frame H1 WRT global frame
g0h1=T0f1*gf1h1
% getting the position of H1 and F1 WRT global frame
pof1=T0f1(1:3,4);  poh1=g0h1(1:3,4);
% second supporting leg 'leg3' %%%
% the intial configuration of the second supporting leg
H3 WRT F3
gf3h30=[1 0 0 0;0 1 0 l1;0 0 1 l2+l3;0 0 0 1];
% the configuration of the screw axes
w1=[1 0 0];w2=[1 0 0];w3=[1 0 0];
q1=[0 0 0];q2=[0 0 l3];q3=[0 0 l3+l2];
% the matrices that expresses the screws of the first leg
s1=poe(w1,q1);s2=poe(w2,q2);s3=poe(w3,q3);
% applying the product of exponential to obtain H3 WRT F3
gf3h3=expm(s1*t3)*expm(s2*t2)*expm(s3*t1)*gf3h30;
% getting the frame F3 WRT global frame
T0f3=[1 0 0  r*cos(pi/6);0 1 0 (-r*sin(pi/6))-l1; 0 0 1
0;0 0 0 1];
% getting the frame H3 WRT global frame
g0h3=T0f3*gf3h3;
% getting the position of H3 and F3 WRT global frame
pof3=T0f3(1:3,4); poh3=g0h3(1:3,4);
% the third supporting leg, leg 5
% the intial configuration of the third supporting leg H5
WRT F5
```

```
gf5h50=[1 0 0 0;0 1 0 l1;0 0 1 l2+l3;0 0 0 1];
% the configuration of the screw axes
w1=[1 0 0];w2=[1 0 0];w3=[1 0 0];
q1=[0 0 0];q2=[0 0 l3];q3=[0 0 l3+l2];
% the matrices that expresses the screws of the first leg
s1=poe(w1,q1);s2=poe(w2,q2);s3=poe(w3,q3);
% applying the product of exponential to obtain H5 WRT F5
gf5h5=expm(s1*t3)*expm(s2*t2)*expm(s3*t1)*gf5h50;
% getting the frame F5 WRT global frame
T0f5=[1 0 0 r*cos(5*pi/6);0 1 0 (-r*sin(5*pi/6))-l1;0 0 1
0;0 0 0 1];
% getting the frame H5 WRT global frame
g0h5=T0f5*gf5h5;
% getting the position of H3 and F3 WRT global frame
pof5=T0f5(1:3,4); poh5=g0h5(1:3,4);
% finding the configuration of mass center WRT global
frame
% verifying technique
n1=(poh1(1,1)-poh3(1,1)).^2;  n2=(poh1(2,1)-
poh3(2,1)).^2;
n3=(poh1(3,1)-poh3(3,1)).^2;  k1=sqrt(n1+n2+n3)
n4=(poh1(1,1)-poh5(1,1)).^2;  n5=(poh1(2,1)-
poh5(2,1)).^2;
n6=(poh1(3,1)-poh5(3,1)).^2;  k2=sqrt(n4+n5+n6)
n7=(poh1(1,1)-poh5(1,1)).^2;  n8=(poh1(2,1)-
poh5(2,1)).^2;
n9=(poh1(3,1)-poh5(3,1)).^2;  k3=sqrt(n7+n8+n9);
k=sqrt(3)*r;
if k1==k2 && k2==k3  disp('the centroid is found')
% finding the position of the centroid
cx=(poh1(1,1)+poh3(1,1)+poh5(1,1))/3;
cy=(poh1(2,1)+poh3(2,1)+poh5(2,1))/3;
cz=(poh1(3,1)+poh3(3,1)+poh5(3,1))/3;
poc=[cx;cy;cz];
% finding the orientation of the centroid WRT global
frame
vy=(poh1(1:3,1)-poc(1:3,1));
vy=vy(1:3,1)/sqrt(vy(1,1)^2+vy(2,1)^2+vy(3,1)^2)
vx=(poh3(1:3,1)-poh5(1:3,1));
vx=vx/sqrt(vx(1,1)^2+vx(2,1)^2+vx(3,1)^2)
vz=cross(vx,vy);
% drawing the position of H1,H3,H5 WRT global frame
drawpos(poh1,poh3,poh5,4);
% drawing the position of F1,F3,F5 WRT global frame
drawpos(pof1,pof3,pof5,3);
% drawing the position CENTER OF MASS WRT global frame
poc=[cx cy cz];
starts = zeros(3,3);ends = [poc; 0 0 0; 0 0 0];
quiver3(starts(:,1), starts(:,1), starts(:,1), ends(:,1),
ends(:,2), ends(:,3), 'black')
else disp('something went wrong')
```

```
end
% the first swingin leg, leg'2'
t1=pi/6; t2=0;
% the intial configuration of the first leg H2 WRT F2
gh2f20=[1 0 0 0;0 1 0 l1;0 0 1 -(l2+l3);0 0 0 1];
% the configuration of the screw axes
w1=[1 0 0];w2=[1 0 0];q1=[0 l1 0];q2=[0 l1 -l2];
% the matrices that expresses the screws of the leg 2
s1=poe(w1,q1);s2=poe(w2,q2);
% applying the product of exponential to obtain F2 WRT H2
gh2f2=expm(t1*s1)*expm(t2*s2)*gh2f20;
% the relation between the new centroid frame and H2
frame
gcnewh2=[1 0 0 r*cos(pi/6);0 1 0 r*sin(pi/6);0 0 1 0;0 0
0 1];
% the relation between the new centroid frame and the
global frame
g0cnew= [1 0 0 cx;0 1 0 cy;0 0 1 cz;0 0 0 1];
% getting the frame F2 wrt global reference frame.
g0f2=g0cnew*gcnewh2*gh2f2;pof2=g0f2(1:3,4)
% getting the position of H2 wrt global reference frame.
g0h2=g0cnew*gcnewh2; p0h2=g0h2(1:3,4);
% the second swingin leg, leg'4'
t1=pi/6;t2=0;
% the intial configuration of the first leg H4 WRT F4
gh4f40=[1 0 0 0;0 1 0 -l1;0 0 1 -l2-l3;0 0 0 1];
% the configuration of the screw axes
w1=[1 0 0];w2=[1 0 0];q1=[0 -l1 0];q2=[0 -l1 -l2];
% the matrices that expresses the screws of the leg 4
s1=poe(w1,q1);s2=poe(w2,q2);
% applying the product of exponential to obtain F4 WRT H4
gh4f4=expm(t1*s1)*expm(t2*s2)*gh4f40
% the relation between the new centroid frame and H4
frame
gcnewh4=[1 0 0 0;0 1 0 -r;0 0 1 0;0 0 0 1];
% the relation between the new centroid frame and global
frame
g0cnew=[1 0 0 cx;0 1 0 cy;0 0 1 cz;0 0 0 1];
% getting the frame F4 wrt global reference frame.
g0f4=g0cnew*gcnewh4*gh4f4; pof4=g0f4(1:3,4)
% getting the position of H4 wrt global reference frame.
g0h4=g0cnew*gcnewh4;  p0h4=g0h4(1:3,4);
% the third swingin leg, leg'6'
% the intial configuration of the first leg H6 WRT F6
gh6f60=[1 0 0 0;0 1 0 l1;0 0 1 -l2-l3;0 0 0 1];
% the configuration of the screw axes
w1=[1 0 0];w2=[1 0 0];q1=[0 l1 0];q2=[0 l1 -l2];
% the matrices that expresses the screws of the leg 6
s1=poe(w1,q1);s2=poe(w2,q2);
% applying the product of exponential to obtain F6 WRT H6
gh6f6=expm(t1*s1)*expm(t2*s2)*gh6f60;
```

```
% the relation between the centroid frame and H6 frame
gcnewh6=[1 0 0 -r*cos(pi/6);0 1 0 r*sin(pi/6);0 0 1 0 ;0
0 0 1];
% getting the frame F6 wrt global reference frame.
g0f6=g0cnew*gcnewh6*gh6f6; pof6=g0f6(1:3,4);
% getting the position of H6 wrt global reference frame.
g0h6=g0cnew*gcnewh6;p0h6=g0h6(1:3,4);
% drawing the position of F2,F4,F6 WRT global frame
drawpos(pof2,pof4,pof6,2)
% drawing the position of H2,H4,H6 WRT global frame
drawpos(p0h2,p0h4,p0h6,1)

% the second moving phase
clear all;
figure;
% the lengths of the Leg's links and the Radios
l1=1; l2=1; l3=1; r=1;
% supporting legs analysis
% the first supporting leg, leg 2
% the Joint's variables, during this phase
t1in=-pi/6;t2in=0;
t1=-t1in;t2=-t2in;t3=t1in+t2in;
% the intial configuration of the first supporting leg H2
WRT F2
gf2h20=[1 0 0 0; 0 1 0 -l1-(l2+l3)*sin(pi/6)
        0 0 1 (l1+l2)*cos(pi/6);0 0 0 1];
% the configuration of the screw axes
w1=[1 0 0];w2=[1 0 0];w3=[1 0 0];
q1=[0 0 0];q2=[0 -l3*sin(pi/6) l3*cos(pi/6)];
q3=[0 -(l3+l2)*sin(pi/6) (l3+l2)*cos(pi/6)];
% the matrices that expresses the screws of the first leg
s1=poe(w1,q1);s2=poe(w2,q2);s3=poe(w3,q3);
% applying the product of exponential to obtain H2 WRT F2
gf2h2=expm(s1*t3)*expm(s2*t2)*expm(s3*t1)*gf2h20;
% getting the frame F2 WRT global frame
T0f2=[1 0 0 0.8661;0 1 0 3.5000;0 0 1 0.0000;0 0 0 1];
% getting the frame H2 WRT global frame
g0h2=T0f2*gf2h2;
% getting the position of H2 and F2 WRT global frame
pof2=T0f2(1:3,4);
poh2=g0h2(1:3,4);
% second supporting leg 'leg4' %%%
% the intial configuration of the second supporting leg
H4 WRT F4
gf4h40=[1 0 0 0
         0 1 0 -l1+(l2+l3)*sin(pi/6)
         0 0 1 (l2+l3)*cos(pi/6)
         0 0 0 1];
% the configuration of the screw axes
w1=[1 0 0]; w2=[1 0 0];w3=[1 0 0];
q1=[0 0 0];q2=[0 -l3*sin(pi/6) l3*cos(pi/6)];
```

```
q3=[0 -(l3+l2)*sin(pi/6) (l3+l2)*cos(pi/6)];
% the matrices that expresses the screws of the first leg
s1=poe(w1,q1);s2=poe(w2,q2);s3=poe(w3,q3);
% applying the product of exponential to obtain H4 WRT F4
gf4h4=expm(s1*t3)*expm(s2*t2)*expm(s3*t1)*gf4h40
% getting the frame F4 WRT global frame
T0f4=[1 0 0 0;0 1 0 0;0 0 1 0;0 0 0 1];
% getting the frame H4 WRT global frame
g0h4=T0f4*gf4h4
% getting the position of H4 and F4 WRT global frame
pof4=T0f4(1:3,4);
poh4=g0h4(1:3,4);
% the third supporting leg, leg 6
% the intial configuration of the third supporting leg H6
WRT F6
gf6h60=[1 0 0 0
        0 1 0 -l1-(l2+l3)*sin(pi/6)
        0 0 1 (l1+l2)*cos(pi/6)
        0 0 0 1];
% the configuration of the screw axes
w1=[1 0 0];w2=[1 0 0];w3=[1 0 0];
q1=[0 0 0];q2=[0 -l3*sin(pi/6) l3*cos(pi/6)];
q3=[0 -(l3+l2)*sin(pi/6) (l3+l2)*cos(pi/6)];
% the matrices that expresses the screws of the
supporting leg 6
s1=poe(w1,q1);s2=poe(w2,q2);s3=poe(w3,q3);
% applying the product of exponential to obtain H6 WRT F6
gf6h6=expm(s1*t3)*expm(s2*t2)*expm(s3*t1)*gf6h60
% getting the frame F6 WRT global frame
T0f6=[1 0 0 -0.8661;0 1 0 3.5000;0 0 1 0;0 0 0 1];
% getting the frame H6 WRT global frame
g0h6=T0f6*gf6h6;
% getting the position of H6 and F6 WRT global frame
pof6=T0f6(1:3,4);
poh6=g0h6(1:3,4);
% finding the configuration of mass center WRT global
frame
% verifying technique
n1=(poh4(1,1)-poh2(1,1)).^2; n2=(poh4(2,1)-poh2(2,1)).^2;
n3=(poh4(3,1)-poh2(3,1)).^2; k1=sqrt(n1+n2+n3)
n4=(poh4(1,1)-poh6(1,1)).^2; n5=(poh4(2,1)-poh6(2,1)).^2;
n6=(poh4(3,1)-poh6(3,1)).^2; k2=sqrt(n4+n5+n6)
n7=(poh2(1,1)-poh6(1,1)).^2; n8=(poh2(2,1)-poh6(2,1)).^2;
n9=(poh2(3,1)-poh6(3,1)).^2; k3=sqrt(n7+n8+n9);
k=sqrt(3)*r
if k1==k2 && k2==k3  disp('the centroid is found')
% finding the position of the centroid
cx=(poh2(1,1)+poh4(1,1)+poh6(1,1))/3
cy=(poh2(2,1)+poh4(2,1)+poh6(2,1))/3
cz=(poh2(3,1)+poh4(3,1)+poh6(3,1))/3
poc=[cx; cy ;cz];
```

```
% finding the orientation of the centroid WRT global
frame
vy=(poc(1:3,1)-poh4(1:3,1));
vy=vy(1:3,1)/sqrt(vy(1,1)^2+vy(2,1)^2+vy(3,1)^2)
vx=(poh2(1:3,1)-poh6(1:3,1));
vx=vx/sqrt(vx(1,1)^2+vx(2,1)^2+vx(3,1)^2)
vz=cross(vx,vy)
else disp('something went wrong')
end
% the first swingin leg, leg'1'
t1=pi/6; t2=0;
% the intial configuration of the first leg H1 WRT F1
gh1f10=[1 0 0 0;0 1 0 0;0 0 1 -1.7321;0 0 0 1];
% the configuration of the screw axes
w1=[1 0 0];w2=[1 0 0];
q1=[0 l1 0];q2=[0 l1-l2*sin(pi/6) -l2*cos(pi/6)];
% the matrices that expresses the screws of the leg 1
s1=poe(w1,q1);s2=poe(w2,q2);
% applying the product of exponential to obtain F1 WRT H1
gh1f1=expm(t1*s1)*expm(t2*s2)*gh1f10
% the relation between the new centroid frame and H1
frame
gcnewh1=[1 0 0 0;0 1 0 r;0 0 1 0;0 0 0 1];
% the relation between the new centroid frame and the
global frame
g0cnew= [1 0 0 cx;0 1 0 cy;0 0 1 cz;0 0 0 1];
% getting the frame F1 wrt global reference frame.
g0f1=g0cnew*gcnewh1*gh1f1;pof1=g0f1(1:3,4)
% getting the position of H1 wrt global reference frame.
g0h1=g0cnew*gcnewh1;p0h1=g0h1(1:3,4);
% the second swingin leg, leg'3'
t1=pi/6;t2=0 ;
% the intial configuration of the first leg H3 WRT F3
gh3f30=[1 0 0 0;0 1 0 -2;0 0 1 -1.7321;0 0 0 1];
% the configuration of the screw axes
w1=[1 0 0];w2=[1 0 0];
q1=[0 -l1 0];q2=[0 -l1+(l2*sin(pi/6)) -l2*cos(pi/6)];
% the matrices that expresses the screws of the leg 3
s1=poe(w1,q1);s2=poe(w2,q2);
% applying the product of exponential to obtain F3 WRT H3
gh3f3=expm(t1*s1)*expm(t2*s2)*gh3f30
% the relation between the new centroid frame and H3
frame
gcnewh3=[1 0 0 r*cos(pi/6);0 1 0 -r*sin(pi/6);0 0 1 0;0 0
0 1];
% the relation between the new centroid frame and global
frame
g0cnew=[1 0 0 cx;0 1 0 cy;0 0 1 cz;0 0 0 1];
% getting the frame F3 wrt global reference frame.
g0f3=g0cnew*gcnewh3*gh3f3; pof3=g0f3(1:3,4);
% getting the position of H3 wrt global reference frame.
```

```
g0h3=g0cnew*gcnewh3;  p0h3=g0h3(1:3,4);
% the third swingin leg, leg'5'
% the intial configuration of the first leg H5 WRT F5
gh5f50=[1 0 0 0;0 1 0 -2;0 0 1 -1.7321;0 0 0 1];
% the configuration of the screw axes
w1=[1 0 0];w2=[1 0 0];
q1=[0 -l1 0];q2=[0 -l1+(l2*sin(pi/6)) -l2*cos(pi/6)];
% the matrices that expresses the screws of the leg 5
s1=poe(w1,q1);s2=poe(w2,q2);
% applying the product of exponential to obtain F5 WRT H5
gh5f5=expm(t1*s1)*expm(t2*s2)*gh5f50;
% the relation between the centroid frame and H5 frame
gcnewh5=[1 0 0 -r*cos(pi/6);0 1 0 -r*sin(pi/6);0 0 1 0;0
0 0 1];
% getting the frame F5 wrt global reference frame.
g0f5=g0cnew*gcnewh5*gh5f5; pof5=g0f5(1:3,4);
% getting the position of H5 wrt global reference frame.
g0h5=g0cnew*gcnewh5;p0h5=g0h5(1:3,4);
% drawing the position of H1,H3,H5 WRT global frame
drawpos(p0h1,p0h3,p0h5,4)
% drawing the position of F1,F3,F5 WRT global frame
drawpos(pof1,pof3,pof5,3)
% drawing the position of F2,F4,F6 WRT global frame
drawpos(pof2,pof4,pof6,2)
% drawing the position of H2,H4,H6 WRT global frame
drawpos(poh2,poh4,poh6,1)
% drawing the position CENTER OF MASS WRT global frame
starts=zeros(3,3); ends = [[cx cy cz]; 0 0 0; 0 0 0];
quiver3(starts(:,1), starts(:,1), starts(:,1), ends(:,1),
ends(:,2), ends(:,3), 'black')
end
function pof=poe(w1,q1)
ww1=[0     -w1(3)   w1(2);...
w1(3)   0     -w1(1);...
-w1(2)   w1(1)    0  ];
v1=transp(cross(q1,w1));
pof=[ww1(1:3,1:3) v1(1:3,1);0 0 0 0];
end
function drawpos(p1,p2,p3,color)
pb1 = [p1(1,1) p1(2,1)  p1(3,1)];
pb2 = [p2(1,1) p2(2,1)  p2(3,1)];
pb3 = [p3(1,1) p3(2,1)  p3(3,1)];
starts = zeros(3,3); ends = [pb1; pb2; pb3];
if color==1
quiver3(starts(:,1),starts(:,1),starts(:,1),ends(:,1),end
s(:,2),ends(:,3),'yellow')
else if color==2
quiver3(starts(:,1),starts(:,1),starts(:,1),ends(:,1),end
s(:,2),ends(:,3),'red')
else if color==3
```

```
quiver3(starts(:,1),starts(:,1),starts(:,1),ends(:,1),end
s(:,2),ends(:,3),'blue')
else if color==4
quiver3(starts(:,1),starts(:,1),
starts(:,1),ends(:,1),ends(:,2),ends(:,3),'green')
hold on;axis equal

    end
    end
    end
end
end
```

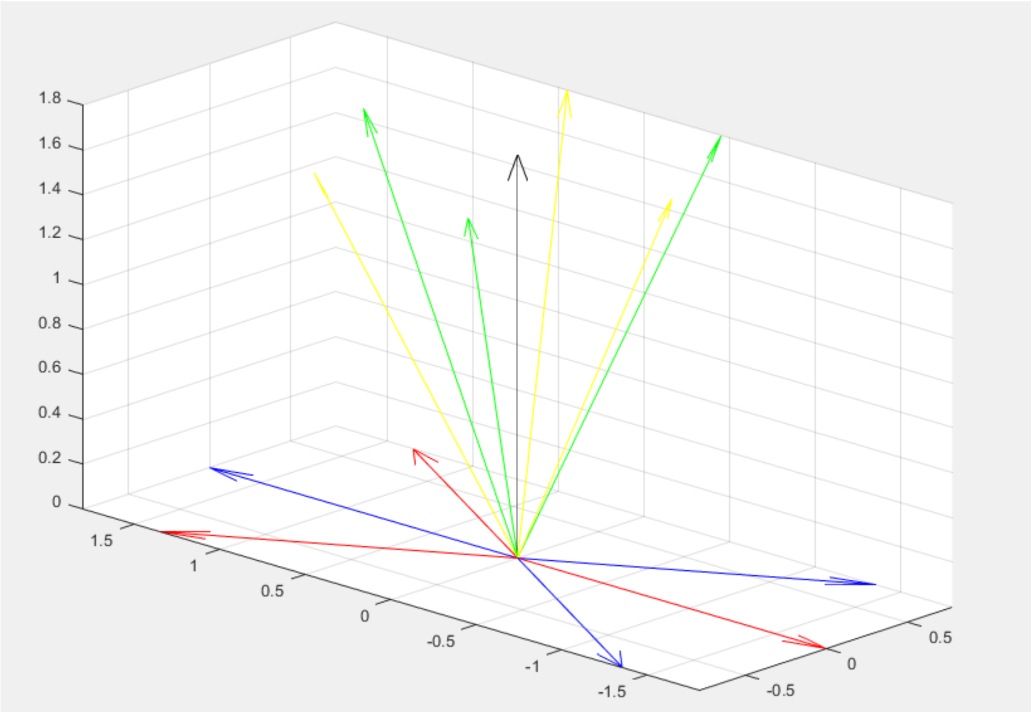

Figure A.1: Position kinematic analysis of the Hexapod robot according to the first switching period of the mammal Locomotion

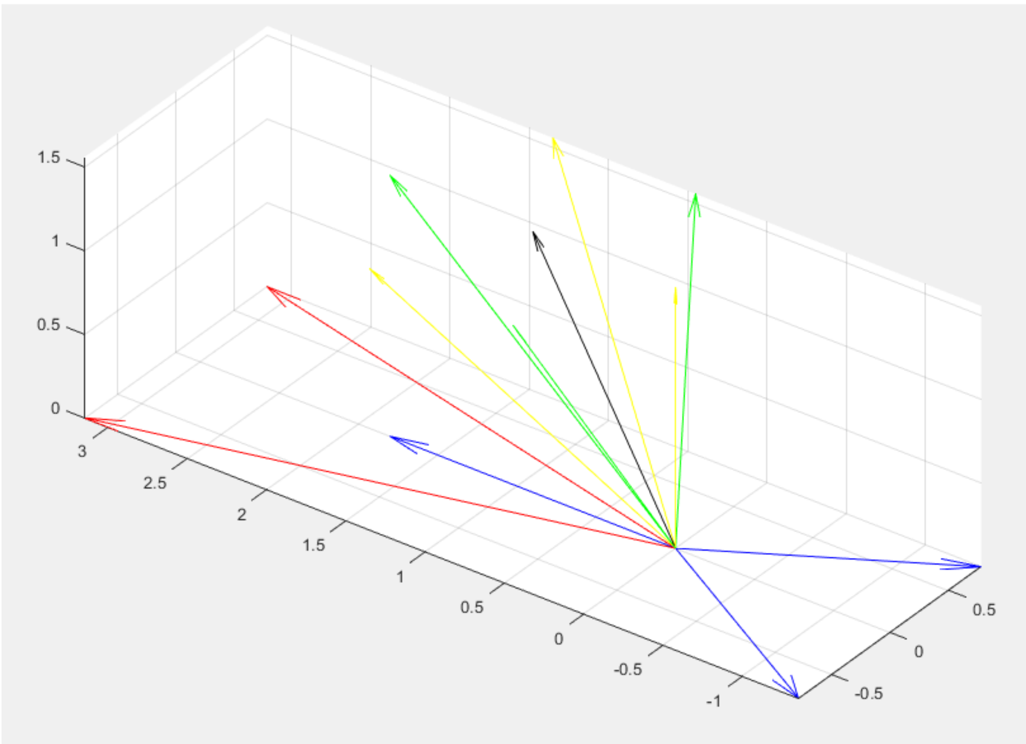

Figure A.2: Position kinematic analysis of the Hexapod robot according to the first moving period of the mammal Locomotion

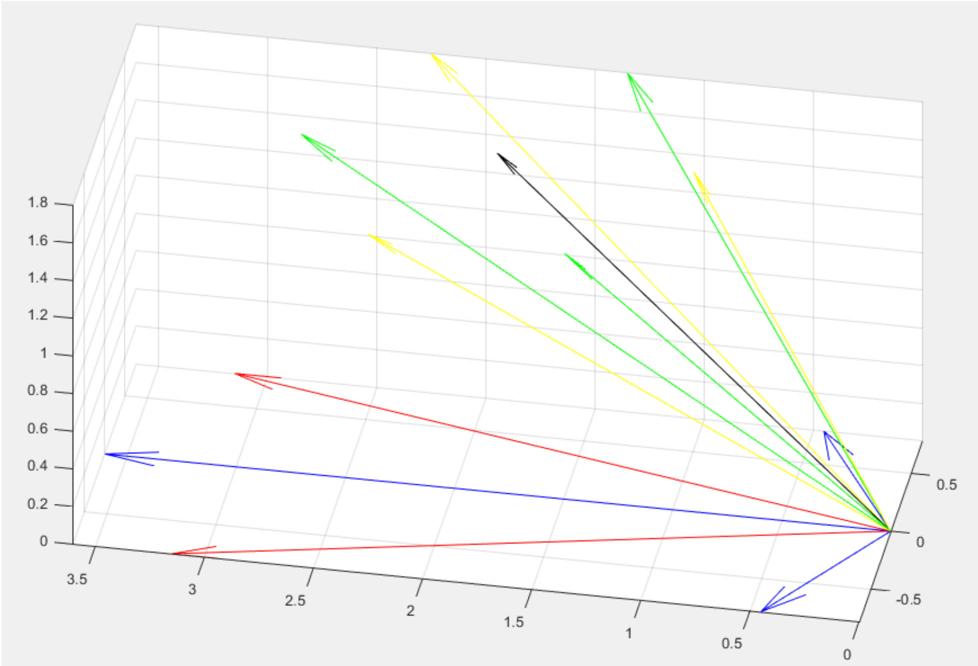

Figure A.3: Position kinematic analysis of the Hexapod robot according to the second moving period of the mammal Locomotion

Appendix B: Kinematic Analysis of a Duty Cycle According to the Insect Locomotion for the Hexapod Robot (Matlab)

```
function insectlocomotion
% the lengths of the Leg's links and the Radios
l1=1; l2=1; l3=1; r=1;
% supporting legs analysis
% the first supporting leg, leg 1
% the Joint's variables, during this phase, all are zero
t1=0; t2=0; t3=0;
% the intial configuration of the first leg H1 WRT F1
gf1h10= [1 0 0 0;0 1 0 -l1;0 0 1 l2+l3;0 0 0 1];
% the configuration of the screw axes
w1= [1 0 0]; w2= [1 0 0]; w3= [1 0 0];
q1= [0 0 0]; q2= [0 0 l3]; q3= [0 0 l3+l2];
% the matrices that expresses the screws of the first leg
s1=poe(w1,q1);s2=poe(w2,q2);s3=poe(w3,q3);
% applying the product of exponential to obtain H1 WRT F1
gf1h1=expm(s1*t3)*expm(s2*t2)*expm(s3*t1)*gf1h10
% getting the frame F1 WRT global frame
T0f1= [1 0 0 0;0 1 0 r+l1;0 0 1 0;0 0 0 1];
% getting the frame H1 WRT global frame
g0h1=T0f1*gf1h1;
% getting the position of H1 and F1 WRT global frame
pof1= T0f1(1:3,4);  poh1=g0h1(1:3,4);
% second supporting leg 'leg3' %%%
% the intial configuration of the second supporting leg
H3 WRT F3
gf3h30= [1 0 0 0;0 1 0 l1;0 0 1 l2+l3;0 0 0 1];
% the configuration of the screw axes
w1= [1 0 0]; w2= [1 0 0]; w3= [1 0 0];
q1= [0 0 0]; q2= [0 0 l3]; q3= [0 0 l3+l2];
% the matrices that expresses the screws of the first leg
s1=poe(w1,q1);s2=poe(w2,q2);s3=poe(w3,q3);
% applying the product of exponential to obtain H3 WRT F3
gf3h3=expm(s1*t3)*expm(s2*t2)*expm(s3*t1)*gf3h30
% getting the frame F3 WRT global frame
T0f3=[1 0 0 r*cos(pi/6);0 1 0 (-r*sin(pi/6))-l1;0 0 1 0;0
0 0 1];
% getting the frame H3 WRT global frame
g0h3=T0f3*gf3h3;
% getting the position of H3 and F3 WRT global frame
pof3=T0f3(1:3,4); poh3=g0h3(1:3,4);
% the third supporting leg, leg 5
% the intial configuration of the third supporting leg H5
WRT F5
gf5h50=[1 0 0 0;0 1 0 l1;0 0 1 l2+l3;0 0 0 1];
% the configuration of the screw axes
```

```
w1=[1 0 0]; w2=[1 0 0];w3=[1 0 0];
q1=[0 0 0]; q2=[0 0 l3]; q3=[0 0 l3+l2];
% the matrices that expresses the screws of the first leg
s1=poe(w1,q1);s2=poe(w2,q2);s3=poe(w3,q3);
% applying the product of exponential to obtain H5 WRT F5
gf5h5=expm(s1*t3)*expm(s2*t2)*expm(s3*t1)*gf5h50
% getting the frame F5 WRT global frame
T0f5=[1 0 0 r*cos(5*pi/6);0 1 0 (-r*sin(5*pi/6))-l1;0 0 1
0;0 0 0 1];
% getting the frame H5 WRT global frame
g0h5=T0f5*gf5h5;
% getting the position of H3 and F3 WRT global frame
pof5=T0f5(1:3,4); poh5=g0h5(1:3,4);
% finding the configuration of mass center WRT global
frame
% verifying technique
n1=(poh1(1,1)-poh3(1,1)).^2;  n2=(poh1(2,1)-
poh3(2,1)).^2;
n3=(poh1(3,1)-poh3(3,1)).^2;  k1=sqrt(n1+n2+n3)
n4=(poh1(1,1)-poh5(1,1)).^2;  n5=(poh1(2,1)-
poh5(2,1)).^2;
n6=(poh1(3,1)-poh5(3,1)).^2;  k2=sqrt(n4+n5+n6)
n7=(poh1(1,1)-poh5(1,1)).^2;  n8=(poh1(2,1)-
poh5(2,1)).^2;
n9=(poh1(3,1)-poh5(3,1)).^2;  k3=sqrt(n7+n8+n9);
k=sqrt(3)*r;
if k1==k2 && k2==k3  disp('the centroid is found')
% finding the position of the centroid
cx=(poh1(1,1)+poh3(1,1)+poh5(1,1))/3;
cy=(poh1(2,1)+poh3(2,1)+poh5(2,1))/3;
cz=(poh1(3,1)+poh3(3,1)+poh5(3,1))/3;
poc=[cx;cy;cz];
% finding the orientation of the centroid WRT global
frame
vy=(poh1(1:3,1)-poc(1:3,1));
vy=vy(1:3,1)/sqrt(vy(1,1)^2+vy(2,1)^2+vy(3,1)^2);
vx=(poh3(1:3,1)-poh5(1:3,1));
vx=vx/sqrt(vx(1,1)^2+vx(2,1)^2+vx(3,1)^2);
vz=cross(vx,vy);
% drawing the position of H1,H3,H5 WRT global frame
drawpos(poh1,poh3,poh5,4)
% drawing the position of F1,F3,F5 WRT global frame
drawpos(pof1,pof3,pof5,3)
% drawing the position CENTER OF MASS WRT global frame
poc=[cx cy cz];
starts = zeros(3,3);ends = [poc; 0 0 0; 0 0 0];
quiver3(starts(:,1), starts(:,1), starts(:,1), ends(:,1),
ends(:,2), ends(:,3), 'black')
else disp('something went wrong')
end
% the first swingin leg, leg'2'
```

```
% the intial configuration of the first leg H2 WRT F2
gh2f20=[1 0 0 0;0 1 0 l1;0 0 1 -(l2+l3);0 0 0 1];
% the configuration of the screw axes
w1=[1 0 0]; w2=[1 0 0];
q1=[0 l1 0]; q2=[0 l1 -l2];
% the matrices that expresses the screws of the leg 2
s1=poe(w1,q1);s2=poe(w2,q2);
% applying the product of exponential to obtain F2 WRT H2
gh2f2=expm(t1*s1)*expm(t2*s2)*gh2f20;
% the relation between the centroid frame and H2 frame
gch2=[1 0 0 r*cos(pi/6);0 1 0 r*sin(pi/6);0 0 1 0;0 0 0
1];
% the relation between the centroid frame and the global
frame
g0c= [1 0 0 0;0 1 0 0;0 0 1 2;0 0 0 1];
% getting the frame F2 wrt global reference frame.
g0f2= g0c*gch2*gh2f2;pof2=g0f2(1:3,4);
% getting the position of H2 wrt global reference frame.
g0h2=g0c*gch2; p0h2=g0h2(1:3,4);
% the second swingin leg, leg'4'
% the intial configuration of the first leg H4 WRT F4
gh4f40=[1 0 0 0;0 1 0 -l1;0 0 1 -l2-l3;0 0 0 1];
% the configuration of the screw axes
w1=[1 0 0]; w2=[1 0 0];
q1=[0 -l1 0];q2=[0 -l1 -l2];
% the matrices that expresses the screws of the leg 4
s1=poe(w1,q1);s2=poe(w2,q2);
% applying the product of exponential to obtain F4 WRT H4
gh4f4=expm(t1*s1)*expm(t2*s2)*gh4f40;
% the relation between the centroid frame and H4 frame
gch4=[1 0 0 0;0 1 0 -r;0 0 1 0;0 0 0 1];
% getting the frame F4 wrt global reference frame.
g0f4=g0c*gch4*gh4f4;pof4=g0f4(1:3,4);
% getting the position of H4 wrt global reference frame.
g0h4=g0c*gch4; p0h4=g0h4(1:3,4);
% the third swingin leg, leg'6'
% the intial configuration of the first leg H6 WRT F6
gh6f60=[1 0 0 0;0 1 0 l1;0 0 1 -l2-l3;0 0 0 1];
% the configuration of the screw axes
w1=[1 0 0];w2=[1 0 0];q1=[0 l1 0];q2=[0 l1 -l2];
% the matrices that expresses the screws of the leg 6
s1=poe(w1,q1);s2=poe(w2,q2);
% applying the product of exponential to obtain F6 WRT H6
gh6f6=expm(t1*s1)*expm(t2*s2)*gh6f60
% the relation between the centroid frame and H6 frame
gch6=[1 0 0 -r*cos(pi/6);0 1 0 r*sin(pi/6); 0 0 1 0;0 0 0
1];
% getting the frame F6 wrt global reference frame.
g0f6=g0c*gch6*gh6f6;pof6=g0f6(1:3,4);
% getting the position of H6 wrt global reference frame.
g0h6=g0c*gch6;p0h6=g0h6(1:3,4);
```

```
% drawing the position of F2,F4,F6 WRT global frame
drawpos(pof2,pof4,pof6,2);
% drawing the position of H2,H4,H6 WRT global frame
drawpos(p0h2,p0h4,p0h6,1);
%%%%%% first moving stage
clear all;
figure;
% the lengths of the Leg's links and the Radios
l1=1; l2=1; l3=1; r=1;
% supporting legs analysis
% the first supporting leg, leg 1
% the Joint's variables, during this phase
t1in=pi/6; t2in=pi/40.56; t3in=0;
t1=-t1in;t2=-t2in;t3=-t3in;t4=t2in+t3in;t5=t1in;
% the intial configuration of the first leg H1 WRT F1
gf1h10=[1 0 0 0;0 1 0 -l1;0 0 1 l2+l3;0 0 0 1];
% the configuration of the screw axes
w0=[0 0 1];w1=[1 0 0];w2=[1 0 0];w3=[1 0 0];w4=[0 0 1];
q0=[0 0 0];q1=[0 0 0];q2=[0 0 l3];q3=[0 0 l3+l2];q4=[0 -
l1 0];
% the matrices that expresses the screws of the first leg
s0=poe(w0,q0);s1=poe(w1,q1);s2=poe(w2,q2);s3=poe(w3,q3);s
4=poe(w4,q4);
% applying the product of exponential to obtain H1 WRT F1
gf1h1=expm(s0*t5)*expm(s1*t4)*expm(s2*t3)*expm(s3*t2)*exp
m(s4*t1)*gf1h10;
% getting the frame F1 WRT global frame
T0f1=[1 0 0 0;0 1 0 r+l1;0 0 1 0;0 0 0 1];
% getting the frame H1 WRT global frame
g0h1=T0f1*gf1h1
% getting the position of H1 and F1 WRT global frame
pof1=T0f1(1:3,4);  poh1=g0h1(1:3,4);
% second supporting leg 'leg3' %%%
% the Joint's variables, during this phase
t1in=-pi/6; t2in=-pi/40.56; t3in=0;
t1=-t1in;t2=-t2in;t3=-t3in;t4=t2in+t3in;t5=t1in;
% the intial configuration of the second supporting leg
H3 WRT F3
gf3h30=[1 0 0 0;0 1 0 l1;0 0 1 l2+l3;0 0 0 1];
% the configuration of the screw axes
w0=[0 0 1];w1=[1 0 0];w2=[1 0 0];w3=[1 0 0];w4=[0 0 1];
q0=[0 0 0];q1=[0 0 0];q2=[0 0 l3];q3=[0 0 l3+l2];q4=[0 l1
0];
% the matrices that expresses the screws of the first leg
s0=poe(w0,q0);s1=poe(w1,q1);s2=poe(w2,q2);s3=poe(w3,q3);s
4=poe(w4,q4);
% applying the product of exponential to obtain H3 WRT F3
gf3h3=expm(s0*t5)*expm(s1*t4)*expm(s2*t3)*expm(s3*t2)*exp
m(s4*t1)*gf3h30;
% getting the frame F3 WRT global frame
```

```
T0f3=[1 0 0  r*cos(pi/6);0 1 0 (-r*sin(pi/6))-l1; 0 0 1
0;0 0 0 1];
% getting the frame H3 WRT global frame
g0h3=T0f3*gf3h3;
% getting the position of H3 and F3 WRT global frame
pof3=T0f3(1:3,4); poh3=g0h3(1:3,4);
% the third supporting leg, leg 5
% the Joint's variables, during this phase
t1in=-pi/6; t2in=-pi/40.56; t3in=0;
t1=-t1in;t2=-t2in;t3=-t3in;t4=t2in+t3in;t5=t1in;
% the intial configuration of the third supporting leg H5
WRT F5
gf5h50=[1 0 0 0;0 1 0 l1;0 0 1 l2+l3;0 0 0 1];
% the configuration of the screw axes
w0=[0 0 1];w1=[1 0 0];w2=[1 0 0];w3=[1 0 0];w4=[0 0 1];
q0=[0 0 0];q1=[0 0 0];q2=[0 0 l3];q3=[0 0 l3+l2];q4=[0 l1
0];
% the matrices that expresses the screws of the first leg
s0=poe(w0,q0);s1=poe(w1,q1);s2=poe(w2,q2);s3=poe(w3,q3);s
4=poe(w4,q4);
% applying the product of exponential to obtain H5 WRT F5
gf5h5=expm(s0*t5)*expm(s1*t4)*expm(s2*t3)*expm(s3*t2)*exp
m(s4*t1)*gf5h50;
% getting the frame F5 WRT global frame
T0f5=[1 0 0 -r*cos(pi/6);0 1 0 (-r*sin(pi/6))-l1;0 0 1
0;0 0 0 1];
% getting the frame H5 WRT global frame
g0h5=T0f5*gf5h5;
% getting the position of H3 and F3 WRT global frame
pof5=T0f5(1:3,4); poh5=g0h5(1:3,4);
% finding the configuration of mass center WRT global
frame
% verifying technique
n1=(poh1(1,1)-poh3(1,1)).^2;  n2=(poh1(2,1)-
poh3(2,1)).^2;
n3=(poh1(3,1)-poh3(3,1)).^2;  k1=sqrt(n1+n2+n3)
n4=(poh1(1,1)-poh5(1,1)).^2;  n5=(poh1(2,1)-
poh5(2,1)).^2;
n6=(poh1(3,1)-poh5(3,1)).^2;  k2=sqrt(n4+n5+n6)
n7=(poh1(1,1)-poh5(1,1)).^2;  n8=(poh1(2,1)-
poh5(2,1)).^2;
n9=(poh1(3,1)-poh5(3,1)).^2;  k3=sqrt(n7+n8+n9);
k=sqrt(3)*r;
if k==k && k==k  disp('the centroid is found')
% finding the position of the centroid
cx=(poh1(1,1)+poh3(1,1)+poh5(1,1))/3;
cy=(poh1(2,1)+poh3(2,1)+poh5(2,1))/3;
cz=(poh1(3,1)+poh3(3,1)+poh5(3,1))/3;
poc=[cx;cy;cz];
% finding the orientation of the centroid WRT global
frame
```

```
vy=(poh1(1:3,1)-poc(1:3,1));
vy=vy(1:3,1)/sqrt(vy(1,1)^2+vy(2,1)^2+vy(3,1)^2)
vx=(poh3(1:3,1)-poh5(1:3,1));
vx=vx/sqrt(vx(1,1)^2+vx(2,1)^2+vx(3,1)^2)
vz=cross(vx,vy);
% drawing the position of H1,H3,H5 WRT global frame
drawpos(poh1,poh3,poh5,4);
% drawing the position of F1,F3,F5 WRT global frame
drawpos(pof1,pof3,pof5,3);
% drawing the position CENTER OF MASS WRT global frame
poc=[cx cy cz];
starts = zeros(3,3);ends = [poc; 0 0 0; 0 0 0];
quiver3(starts(:,1), starts(:,1), starts(:,1), ends(:,1),
ends(:,2), ends(:,3), 'black')
else disp('something went wrong')
end
% the first swingin leg, leg'2'
% the Joint's variables, during this phase
t1=-pi/6; t2=-pi/40.56; t3=0;
% the intial configuration of the first leg H2 WRT F2
gh2f20=[1 0 0 0;0 1 0 l1;0 0 1 -(l2+l3);0 0 0 1];
% the configuration of the screw axes
w1=[0 0 1];w2=[1 0 0];w3=[1 0 0];q1=[0 0 0]; q2=[0 l1
0];q3=[0 l1 -l2];
% the matrices that expresses the screws of the leg 2
s1=poe(w1,q1);s2=poe(w2,q2);s3=poe(w3,q3);
% applying the product of exponential to obtain F2 WRT H2
gh2f2=expm(t1*s1)*expm(t2*s2)*expm(t3*s3)*gh2f20;
% the relation between the new centroid frame and H2
frame
gcnewh2=[1 0 0 r*cos(pi/6);0 1 0 r*sin(pi/6);0 0 1 0;0 0
0 1];
% the relation between the new centroid frame and the
global frame
g0cnew= [1 0 0 cx;0 1 0 cy;0 0 1 cz;0 0 0 1];
% getting the frame F2 wrt global reference frame.
g0f2=g0cnew*gcnewh2*gh2f2;pof2=g0f2(1:3,4)
% getting the position of H2 wrt global reference frame.
g0h2=g0cnew*gcnewh2; p0h2=g0h2(1:3,4);
% the second swingin leg, leg'4'
% the Joint's variables, during this phase
t1=pi/6; t2=pi/40.56; t3=0;
% the intial configuration of the first leg H4 WRT F4
gh4f40=[1 0 0 0;0 1 0 -l1;0 0 1 -l2-l3;0 0 0 1];
% the configuration of the screw axes
w1=[0 0 1];w2=[1 0 0];w3=[1 0 0];q1=[0 0 0]; q2=[0 -l1
0];q3=[0 -l1 -l2];
% the matrices that expresses the screws of the leg 4
s1=poe(w1,q1);s2=poe(w2,q2);s3=poe(w3,q3);
% applying the product of exponential to obtain F4 WRT H4
gh4f4=expm(t1*s1)*expm(t2*s2)*expm(t3*s3)*gh4f40
```

```
% the relation between the new centroid frame and H4
frame
gcnewh4=[1 0 0 0;0 1 0 -r;0 0 1 0;0 0 0 1];
% the relation between the new centroid frame and global
frame
g0cnew=[1 0 0 cx;0 1 0 cy;0 0 1 cz;0 0 0 1];
% getting the frame F4 wrt global reference frame.
g0f4=g0cnew*gcnewh4*gh4f4; pof4=g0f4(1:3,4)
% getting the position of H4 wrt global reference frame.
g0h4=g0cnew*gcnewh4;  p0h4=g0h4(1:3,4);
% the third swingin leg, leg'6'
% the Joint's variables, during this phase
t1=-pi/6; t2=-pi/40.56; t3=0;
% the intial configuration of the first leg H6 WRT F6
gh6f60=[1 0 0 0;0 1 0 l1;0 0 1 -l2-l3;0 0 0 1];
% the configuration of the screw axes
w1=[0 0 1];w2=[1 0 0];w3=[1 0 0];q1=[0 0 0]; q2=[0 l1
0];q3=[0 l1 -l2];
% the matrices that expresses the screws of the leg 6
s1=poe(w1,q1);s2=poe(w2,q2);s3=poe(w3,q3);
% applying the product of exponential to obtain F6 WRT H6
gh6f6=expm(t1*s1)*expm(t2*s2)*expm(t3*s3)*gh6f60;
% the relation between the centroid frame and H6 frame
gcnewh6=[1 0 0 -r*cos(pi/6);0 1 0 r*sin(pi/6);0 0 1 0 ;0
0 0 1];
% getting the frame F6 wrt global reference frame.
g0f6=g0cnew*gcnewh6*gh6f6; pof6=g0f6(1:3,4);
% getting the position of H6 wrt global reference frame.
g0h6=g0cnew*gcnewh6;p0h6=g0h6(1:3,4);
% drawing the position of F2,F4,F6 WRT global frame
drawpos(pof2,pof4,pof6,2)
% drawing the position of H2,H4,H6 WRT global frame
drawpos(p0h2,p0h4,p0h6,1)
% the second moving phase
clear all;
figure;
% the lengths of the Leg's links and the Radios
l1=1; l2=1; l3=1; r=1;
% supporting legs analysis
% the first supporting leg, leg 2
% the Joint's variables, during this phase
t1in=pi/6;t2in=pi/40.56;t3in=0;
t1=-t1in;t2=-t2in;t3=-t3in;t4=t2in+t3in;t5=t1in;
% the intial configuration of the first supporting leg H2
WRT F2
gf2h20=[1 0 0 -0.5000; 0 1 0 -0.8660
        0 0 1 2.0000;0 0 0 1];
% the configuration of the screw axes
w0=[0 0 1];w1=[1 0 0];w2=[1 0 0];w3=[1 0 0];w4=[0 0 1];
q0=[0 0 0];q1=[0 0 0];q2=[0 0 l3];q3=[0  0 (l3+l2)];q4=[0
-l1 0 ]
```

```
% the matrices that expresses the screws of the first leg
s0=poe(w0,q0);s1=poe(w1,q1);s2=poe(w2,q2);s3=poe(w3,q3);s
4=poe(w4,q4);
% applying the product of exponential to obtain H2 WRT F2
gf2h2=expm(s0*t5)*expm(s1*t4)*expm(s2*t3)*expm(s3*t2)*exp
m(s4*t1)*gf2h20;
% getting the frame F2 WRT global frame
T0f2=[1 0 0 1.9434;0 1 0 1.3660;0 0 1 0.0000;0 0 0 1];
% getting the frame H2 WRT global frame
g0h2=T0f2*gf2h2;
% getting the position of H2 and F2 WRT global frame
pof2=T0f2(1:3,4);
poh2=g0h2(1:3,4);
% second supporting leg 'leg4' %%%
% the Joint's variables, during this phase
t1in=-pi/6;t2in=-pi/40.56;t3in=0;
t1=-t1in;t2=-t2in;t3=-t3in;t4=t2in+t3in;t5=t1in;
% the intial configuration of the second supporting leg
H4 WRT F4
gf4h40=[1 0 0 -0.500
        0 1 0  0.8660
        0 0 1  2.000
        0 0 0  1];
% the configuration of the screw axes
w0=[0 0 1];w1=[1 0 0];w2=[1 0 0];w3=[1 0 0];w4=[0 0 1];
q0=[0 0 0];q1=[0 0 0];q2=[0 0 l3];q3=[0  0 (l3+l2)];q4=[0
l1 0 ]
% the matrices that expresses the screws of the first leg
s0=poe(w0,q0);s1=poe(w1,q1);s2=poe(w2,q2);s3=poe(w3,q3);s
4=poe(w4,q4);
% applying the product of exponential to obtain H4 WRT F4
gf4h4=expm(s0*t5)*expm(s1*t4)*expm(s2*t3)*expm(s3*t2)*exp
m(s4*t1)*gf4h40
% getting the frame F4 WRT global frame
T0f4=[1 0 0 1.0774;0 1 0 -1.8660;0 0 1 0;0 0 0 1];
% getting the frame H4 WRT global frame
g0h4=T0f4*gf4h4
% getting the position of H4 and F4 WRT global frame
pof4=T0f4(1:3,4);
poh4=g0h4(1:3,4);
% the third supporting leg, leg 6
% the Joint's variables, during this phase
t1in=pi/6;t2in=pi/40.56;t3in=0;
t1=-t1in;t2=-t2in;t3=-t3in;t4=t2in+t3in;t5=t1in;
% the intial configuration of the third supporting leg H6
WRT F6
gf6h60=[1 0 0 -0.5000
        0 1 0 -0.8660
        0 0 1 2.0000
        0 0 0 1];
% the configuration of the screw axes
```

```
w0=[0 0 1];w1=[1 0 0];w2=[1 0 0];w3=[1 0 0];w4=[0 0 1];
q0=[0 0 0];q1=[0 0 0];q2=[0 0 l3];q3=[0  0 (l3+l2)];q4=[0
-l1 0 ]
% the matrices that expresses the screws of the
supporting leg 6
s0=poe(w0,q0);s1=poe(w1,q1);s2=poe(w2,q2);s3=poe(w3,q3);s
4=poe(w4,q4);
% applying the product of exponential to obtain H6 WRT F6
gf6h6=expm(s0*t5)*expm(s1*t4)*expm(s2*t3)*expm(s3*t2)*exp
m(s4*t1)*gf6h60
% getting the frame F6 WRT global frame
T0f6=[1 0 0 0.2114;0 1 0 1.3660;0 0 1 0;0 0 0 1];
% getting the frame H6 WRT global frame
g0h6=T0f6*gf6h6;
% getting the position of H6 and F6 WRT global frame
pof6=T0f6(1:3,4);
poh6=g0h6(1:3,4);
% finding the configuration of mass center WRT global
frame
% verifying technique
n1=(poh4(1,1)-poh2(1,1)).^2; n2=(poh4(2,1)-poh2(2,1)).^2;
n3=(poh4(3,1)-poh2(3,1)).^2; k1=sqrt(n1+n2+n3)
n4=(poh4(1,1)-poh6(1,1)).^2; n5=(poh4(2,1)-poh6(2,1)).^2;
n6=(poh4(3,1)-poh6(3,1)).^2; k2=sqrt(n4+n5+n6)
n7=(poh2(1,1)-poh6(1,1)).^2; n8=(poh2(2,1)-poh6(2,1)).^2;
n9=(poh2(3,1)-poh6(3,1)).^2; k3=sqrt(n7+n8+n9);
k=sqrt(3)*r
if k1==k2 && k2==k3  disp('the centroid is found')
% finding the position of the centroid
cx=(poh2(1,1)+poh4(1,1)+poh6(1,1))/3
cy=(poh2(2,1)+poh4(2,1)+poh6(2,1))/3
cz=(poh2(3,1)+poh4(3,1)+poh6(3,1))/3
poc=[cx; cy ;cz];
% finding the orientation of the centroid WRT global
frame
vy=(poc(1:3,1)-poh4(1:3,1));
vy=vy(1:3,1)/sqrt(vy(1,1)^2+vy(2,1)^2+vy(3,1)^2)
vx=(poh2(1:3,1)-poh6(1:3,1));
vx=vx/sqrt(vx(1,1)^2+vx(2,1)^2+vx(3,1)^2)
vz=cross(vx,vy)
else disp('something went wrong')
end
% the first swingin leg, leg'1'
t1=-pi/6; t2=-pi/40.56; t3=0;
% the intial configuration of the first leg H1 WRT F1
gh1f10=[1 0 0 0;0 1 0 l1;0 0 1 -(l2+l3);0 0 0 1];
% the configuration of the screw axes
w1=[0 0 1];w2=[1 0 0];w3=[1 0 0];
q1=[0 0 0];q2=[0 l1 0];q3=[0 l1 -l2];
% the matrices that expresses the screws of the leg 1
s1=poe(w1,q1);s2=poe(w2,q2);s3=poe(w3,q3);
```

```
% applying the product of exponential to obtain F1 WRT H1
gh1f1=expm(t1*s1)*expm(t2*s2)*expm(t3*s3)*gh1f10
% the relation between the new centroid frame and H1
frame
gcnewh1=[1 0 0 0;0 1 0 r;0 0 1 0;0 0 0 1];
% the relation between the new centroid frame and the
global frame
g0cnew= [1 0 0 cx;0 1 0 cy;0 0 1 cz;0 0 0 1];
% getting the frame F1 wrt global reference frame.
g0f1=g0cnew*gcnewh1*gh1f1;pof1=g0f1(1:3,4)
% getting the position of H1 wrt global reference frame.
g0h1=g0cnew*gcnewh1;p0h1=g0h1(1:3,4);
% the second swingin leg, leg'3'
t1=pi/6; t2=pi/40.56; t3=0;
% the intial configuration of the first leg H3 WRT F3
gh3f30=[1 0 0 0;0 1 0 -l1;0 0 1 -(l2+l3);0 0 0 1];
% the configuration of the screw axes
w1=[0 0 1];w2=[1 0 0];w3=[1 0 0];
q1=[0 0 0];q2=[0 -l1 0];q3=[0 -l1 -l2];
% the matrices that expresses the screws of the leg 3
s1=poe(w1,q1);s2=poe(w2,q2);s3=poe(w3,q3);
% applying the product of exponential to obtain F3 WRT H3
gh3f3=expm(t1*s1)*expm(t2*s2)*expm(t3*s3)*gh3f30
% the relation between the new centroid frame and H3
frame
gcnewh3=[1 0 0 r*cos(pi/6);0 1 0 -r*sin(pi/6);0 0 1 0;0 0
0 1];
% the relation between the new centroid frame and global
frame
g0cnew=[1 0 0 cx;0 1 0 cy;0 0 1 cz;0 0 0 1];
% getting the frame F3 wrt global reference frame.
g0f3=g0cnew*gcnewh3*gh3f3; pof3=g0f3(1:3,4);
% getting the position of H3 wrt global reference frame.
g0h3=g0cnew*gcnewh3;  p0h3=g0h3(1:3,4);
% the third swingin leg, leg'5'
t1=pi/6; t2=pi/40.56; t3=0;
% the intial configuration of the first leg H5 WRT F5
gh5f50=[1 0 0 0;0 1 0 -l1;0 0 1 -l1-l2;0 0 0 1];
% the configuration of the screw axes
w1=[0 0 1];w2=[1 0 0];w3=[1 0 0];
q1=[0 0 0];q2=[0 -l1 0];q3=[0 -l1 -l2];
% the matrices that expresses the screws of the leg 5
s1=poe(w1,q1);s2=poe(w2,q2);s3=poe(w3,q3);
% applying the product of exponential to obtain F5 WRT H5
gh5f5=expm(t1*s1)*expm(t2*s2)*expm(t3*s3)*gh5f50;
% the relation between the centroid frame and H5 frame
gcnewh5=[1 0 0 -r*cos(pi/6);0 1 0 -r*sin(pi/6);0 0 1 0;0
0 0 1];
% getting the frame F5 wrt global reference frame.
g0f5=g0cnew*gcnewh5*gh5f5; pof5=g0f5(1:3,4);
% getting the position of H5 wrt global reference frame.
```

```
g0h5=g0cnew*gcnewh5;p0h5=g0h5(1:3,4);
% drawing the position of H1,H3,H5 WRT global frame
drawpos(p0h1,p0h3,p0h5,4)
% drawing the position of F1,F3,F5 WRT global frame
drawpos(pof1,pof3,pof5,3)
% drawing the position of F2,F4,F6 WRT global frame
drawpos(pof2,pof4,pof6,2)
% drawing the position of H2,H4,H6 WRT global frame
drawpos(poh2,poh4,poh6,1)
% drawing the position CENTER OF MASS WRT global frame
starts=zeros(3,3); ends = [[cx cy cz]; 0 0 0; 0 0 0];
quiver3(starts(:,1), starts(:,1), starts(:,1), ends(:,1),
ends(:,2), ends(:,3), 'black')
% direct velocity analysis for the first moving phase
figure;
%the screw that is reciprocal to all Leg's screws
sr1=[0;0;0;0;1;0];
%the screw that is reciprocal to only the virtual joints
screws
sr2=[1;1;0;0;0;0];
%the velocity of the centroid of the hexapod
delta=[zeros(3) ones(3) ;  ones(3) zeros(3)];
%%%% angular velocity calculation %%%%%
%%%% leg 1 %%%%
w11=(pi/6)/0.5;w12=(pi/40.56)/0.5;w13=0;
%%%% leg 3 %%%%
w31=(-pi/6)/0.5;w32=(-pi/40.56)/0.5;w33=0;
%%%% leg 5 %%%%
w51=(-pi/6)/0.5;w52=(-pi/40.56)/0.5;w53=0;
%leg 1 analysis
%first screw axis s0
s001=[0;0;1]; s0o1=[0;0;0];s01=[s001;cross(s001,s0o1)]
%second screw axis s1
s111=[1;0;0];s1o1=[0;0;0];s11=[s111;cross(s111,s1o1)]
%third screw axis s2
s221=[1;0;0];s2o1=[0;0;l3];s21=[s221;cross(s221,s2o1)]
%fourth screw axis s3
s331=[1;0;0];s3o1=[0;0;l3+l2];s31=[s331;cross(s331,s3o1)]
%fifth screw axis s4
s441=[0;0;1];s4o1=[0;-
l1;l3+l2];s41=[s441;cross(s441,s4o1)]
%leg 3 analysis
% first screw axis s0
s003=[0;0;1];s0o3=[0;0;0];s03=[s003;cross(s003,s0o3)]
% second screw axis s1
s113=[1;0;0];s1o3=[0;0;0];s13=[s113;cross(s113,s1o3)]
% third screw axis s2
s223=[1;0;0];s2o3=[0;0;l3];s23=[s223;cross(s223,s2o3)]
% fourth screw axis s3
s333=[1;0;0];s3o3=[0;0;l3+l2];s33=[s333;cross(s333,s3o3)]
% fifth screw axis s4
```

```
s443=[0;0;1];s4o3=[0;l1;l3+l2];s43=[s443;cross(s443,s4o3)
]
% leg 5 analysis
% first screw axis s0
s005=[0;0;1]; s0o5=[0;0;0];s05=[s005;cross(s005,s0o5)]
% second screw axis s1
s115=[1;0;0];s1o5=[0;0;0];s15=[s115;cross(s115,s1o5)]
% third screw axis s2
s225=[1;0;0];s2o5=[0;0;l3];s25=[s225;cross(s225,s2o5)]
% fourth screw axis s3
s335=[1;0;0];s3o5=[0;0;l3+l2];s35=[s335;cross(s335,s3o5)]
% fifth screw axis s4
s445=[0;0;1];s4o5=[0;l1;l3+l2];s45=[s445;cross(s445,s4o5)
]
%%%%% [transp(sr1);transp(sr2)]*delta*v = Q
Q=[0+0+0
w11*rec(sr2,s41)+w12*rec(sr2,s31)+w13*rec(sr2,s21) +...
w31*rec(sr2,s43)+w32*rec(sr2,s33)+w33*rec(sr2,s23) +...
w51*rec(sr2,s45)+w52*rec(sr2,s35)+w53*rec(sr2,s25) ]
W=[transp(sr1); transp(sr2)]*delta
% drawing the variation of the centroid velocity
time=[0 0.5];wx=[0 0];wy=[0 0];wz=[0 0];
vx=[0 1.7524];vy=[0 0];vz=[0 0.018];
subplot(6,1,1);
line(time,wx,'Color','red','LineStyle','--')
subplot(6,1,2);
line(time,wy,'Color','green','LineStyle','--')
subplot(6,1,3);
line(time,wz,'Color','blue','LineStyle','--')
subplot(6,1,4);
line(time,vx,'Color','red','LineStyle','-')
subplot(6,1,5);
line(time,vy,'Color','green','LineStyle','-')
subplot(6,1,6);
line(time,vz,'Color','blue','LineStyle','-')
hold off;
% drawing the variation of the angle velocity for each
legs
% for first supporting legs
figure;
subplot(9,1,1);
line(time,[0 w11],'Color','red','LineStyle','-')
subplot(9,1,2);
line(time,[0 w12],'Color','green','LineStyle','-')
subplot(9,1,3);
line(time,[0 w13],'Color','blue','LineStyle','-')
% for second supporting legs
subplot(9,1,4);
line(time,[0 w31],'Color','red','LineStyle','-')
subplot(9,1,5);
line(time,[0 w32],'Color','green','LineStyle','-')
```

```
subplot(9,1,6);
line(time,[0 w33],'Color','blue','LineStyle','-')
% for third supporting legs
subplot(9,1,7);
line(time,[0 w51],'Color','red','LineStyle','-')
subplot(9,1,8);
line(time,[0 w52],'Color','green','LineStyle','-')
subplot(9,1,9);
line(time,[0 w53],'Color','blue','LineStyle','-')
end

function reciprocal= rec(v1,v2)
v11=v1(1:3,1);
v1o=v1(4:6,1);
v22=v2(1:3,1);
v2o=v2(4:6,1);
reciprocal=(transp(v11)*v2o) + (transp(v22)*v1o);
end
function pof=poe(w1,q1)
ww1=[0      -w1(3)    w1(2);...
w1(3)    0      -w1(1);...
-w1(2)    w1(1)    0   ];
v1=transp(cross(q1,w1));
pof=[ww1(1:3,1:3) v1(1:3,1);0 0 0 0];
end
function drawpos(p1,p2,p3,colour)
pb1 = [p1(1,1) p1(2,1)  p1(3,1)];
pb2 = [p2(1,1) p2(2,1)  p2(3,1)];
pb3 = [p3(1,1) p3(2,1)  p3(3,1)];
starts = zeros(3,3); ends = [pb1; pb2; pb3];
if colour==1
quiver3(starts(:,1),starts(:,1),starts(:,1),ends(:,1),end
s(:,2),ends(:,3),'yellow')
else if colour==2
quiver3(starts(:,1),starts(:,1),starts(:,1),ends(:,1),end
s(:,2),ends(:,3),'red')
else if colour==3
quiver3(starts(:,1),starts(:,1),starts(:,1),ends(:,1),end
s(:,2),ends(:,3),'blue')
else if colour==4
quiver3(starts(:,1),starts(:,1),
starts(:,1),ends(:,1),ends(:,2),ends(:,3),'green')
hold on;axis equal
    end
    end
    end
end
end
```

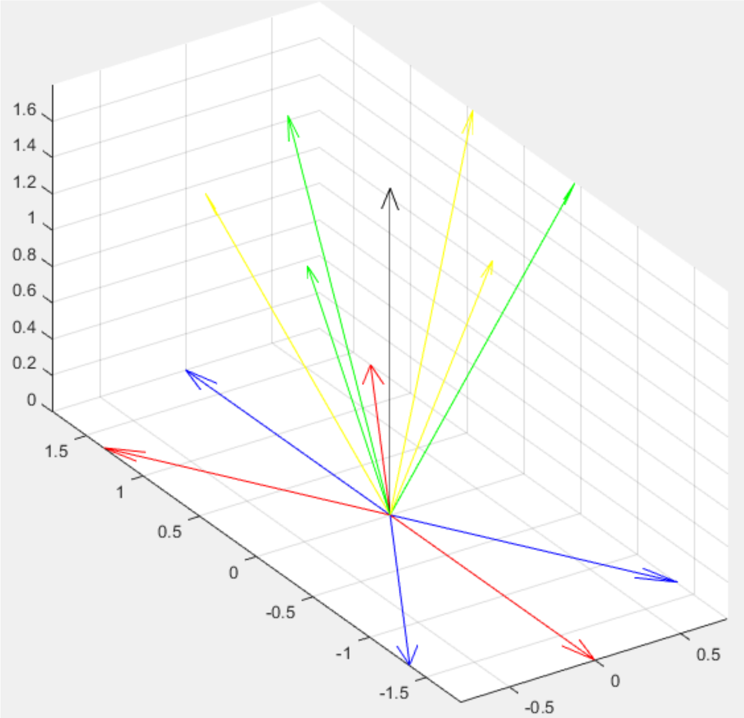

Figure B.1: Position kinematic analysis of the Hexapod robot according to the first switching period of the Insect Locomotion

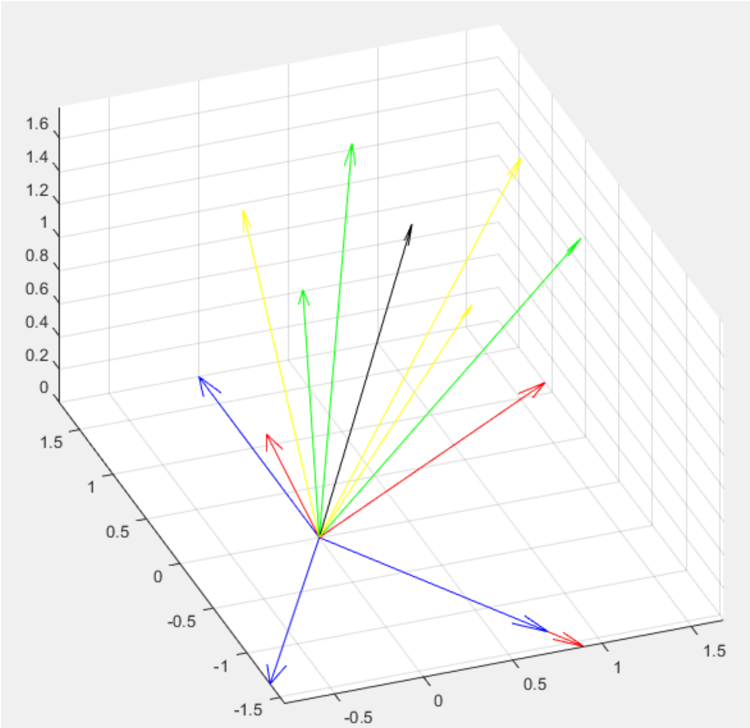

Figure B.2: Position kinematic analysis of the Hexapod robot according to the first moving period of the Insect Locomotion

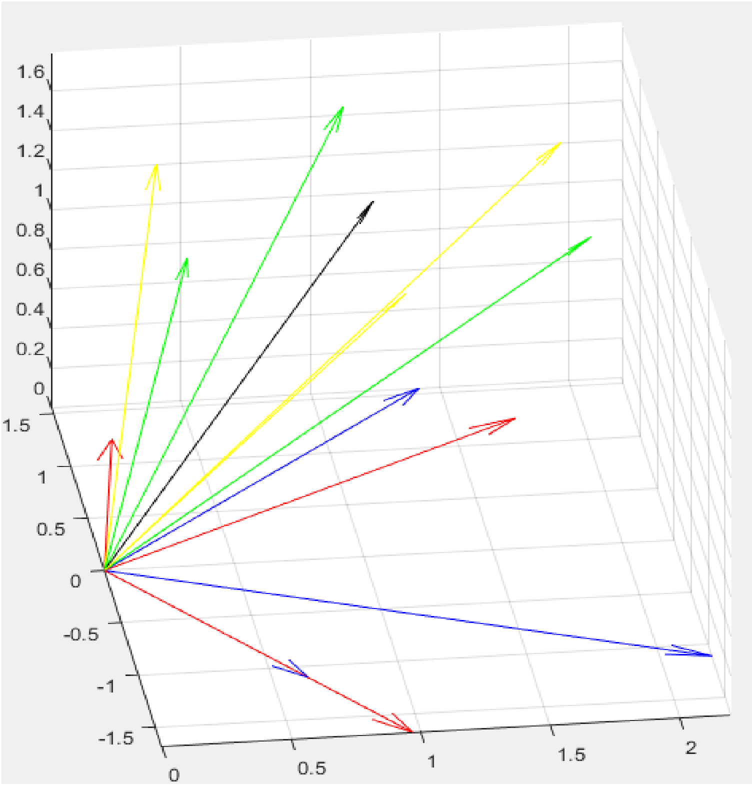

Figure B.3: Position kinematic analysis of the Hexapod robot according to the second moving period of the Insect Locomotion

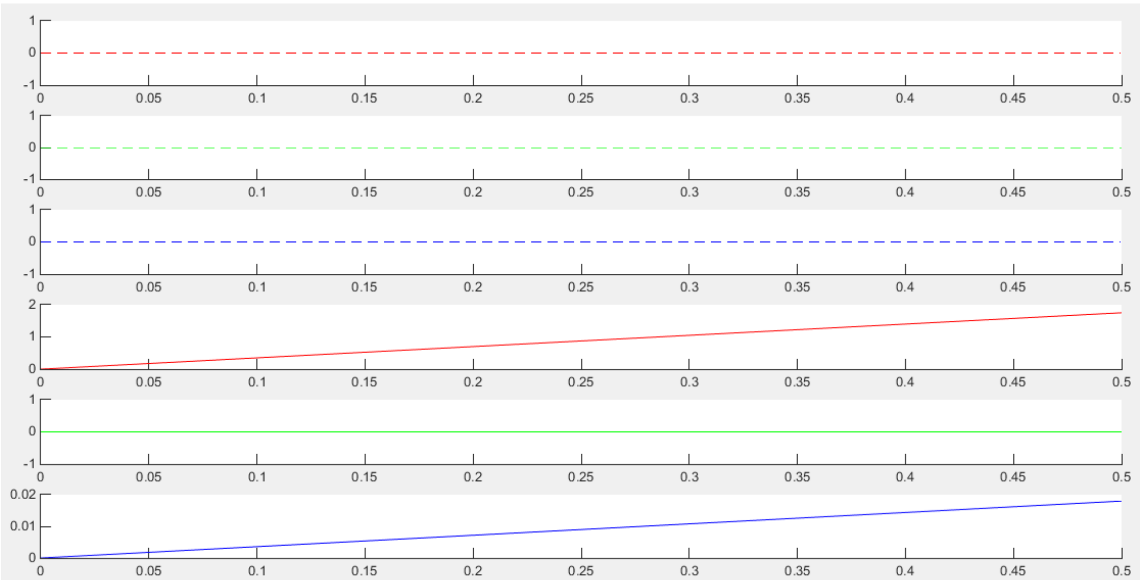

Figure B.4: Forward Velocity analysis of the Hexapod robot through the first moving period of the Insect Locomotion

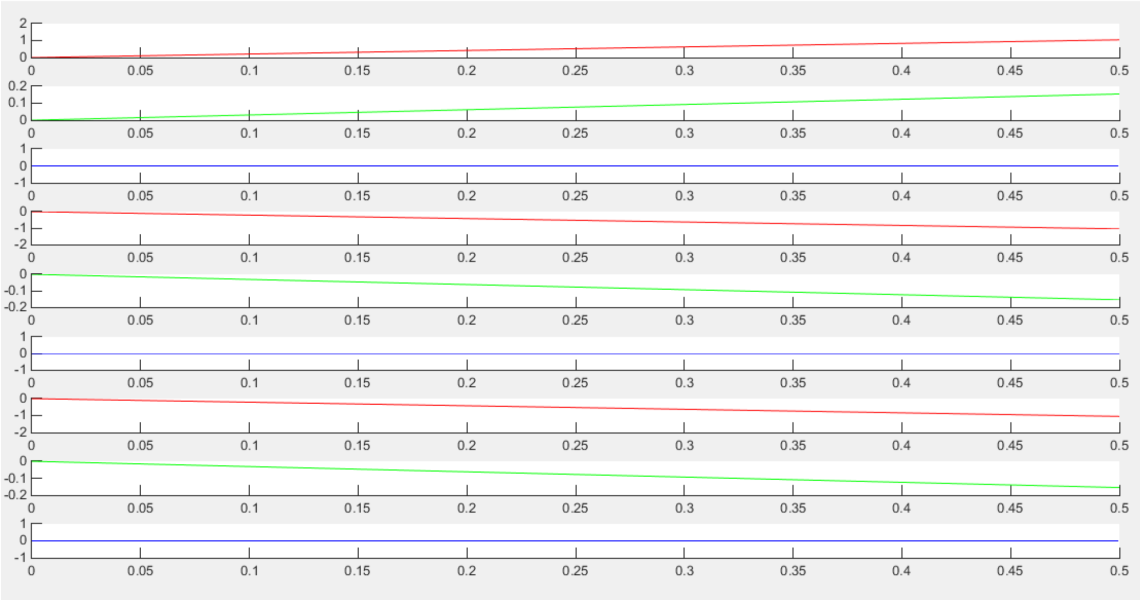

Figure B.5: Velocity analysis of the Leg's active joint of the Hexapod robot through the first moving period of the Insect Locomotion